The Econometrics Journal

Econometrics Journal (2019), volume **00**, pp. 1
doi: 10.1093/ectj/utz002

Quantile coherency: A general measure for dependence between cyclical economic variables

JOZEF BARUNÍK[†] AND TOBIAS KLEY[‡]

[†]*Econometric Department, IITA, The Czech Academy of Sciences and Institute of Economic Studies, Charles University in Prague.*
Email: barunik@fsv.cuni.cz

[‡]*School of Mathematics, University of Bristol.*
Email: tobias.kley@bristol.ac.uk

First version received: 2 October 2018; final version accepted: 28 December 2018.

Summary In this paper, we introduce quantile coherency to measure general dependence structures emerging in the joint distribution in the frequency domain and argue that this type of dependence is natural for economic time series but remains invisible when only the traditional analysis is employed. We define estimators that capture the general dependence structure, provide a detailed analysis of their asymptotic properties, and discuss how to conduct inference for a general class of possibly nonlinear processes. In an empirical illustration we examine the dependence of bivariate stock market returns and shed new light on measurement of tail risk in financial markets. We also provide a modelling exercise to illustrate how applied researchers can benefit from using quantile coherency when assessing time series models.

Keywords: *cross-spectral analysis*, *ranks*, *copula*, *stock market*, *risk*.

JEL codes: *C18*, *C32*, *C10*.

1. DEPENDENCE STRUCTURES BEYOND SECOND-ORDER MOMENTS

One of the fundamental problems faced by a researcher in economics is how to quantify the dependence between economic variables. Although correlated variables are rather commonly observed phenomena in economics, it is often the case that strongly correlated variables under study are truly independent, and that what we measure is mere spurious correlation; see Granger and Newbold (1974). Conversely, but equally deluding, uncorrelated variables may possess dependence in different parts of the joint distribution, and/or at different frequencies. This dependence stays hidden when classical measures based on linear correlation and traditional cross-spectral analysis are used; see Croux et al. (2001), Ning and Chollete (2009), and Fan and Patton (2014). Hence, conventional models derived from averaged quantities, as for example covariance-based measures, may deliver rather misleading results.

In this paper, we introduce a new class of cross-spectral densities that characterize the dependence in quantiles of the joint distribution across frequencies (i.e., with respect to cycles). Subsequently, standardization of the before-mentioned quantile spectra yields a related quantity which we will refer to as quantile coherency. We define and motivate the quantile-based cross-spectral quantities in analogy to their traditional counterparts. But, instead of quantifying dependence in terms of joint moments (i.e., by averaging with respect to the joint distribution), the new measures are defined in terms of the probabilities to exceed quantiles. Hence, they are designed to detect any general type of dependence structure that may arise between the variables under study.

Such complex dynamics may arise naturally in many macroeconomic or financial time series, such as growth rates, inflation, housing markets, or stock market returns. In financial markets, extremely scarce and negative events in one asset can cause irrational outcomes and panics, leading investors to ignore economic fundamentals and cause similarly extreme negative outcomes in other assets. In such situations, markets may be connected more strongly than in calm periods of small or positive returns; cf. Bae et al. (2003). Hence, the co-occurrences of large negative values may be more common across stock markets than co-occurrences of large positive values, reflecting the asymmetric behaviour of economic agents. Moreover, long-term fluctuations in quantiles of the joint distribution may differ from those in the short term owing to the differing risk perception of economic agents over distinct investment horizons. This behaviour produces various degrees of persistence at different parts of the joint distribution, while on average the stock market returns remain impersistent. In univariate macroeconomic variables, researchers document asymmetric adjustment paths (cf. Neftci 1984; Enders and Granger 1998) as firms are more prone to an increase than to a decrease in prices. Asymmetric business cycle dynamics at different quantiles can be caused by positive shocks to output being more persistent than negative shocks. While output fluctuations are known to be persistent, Beaudry and Koop (1993) document less persistence at longer horizons. Such asymmetric dependence at different horizons can be shared by multiple variables. Because classical, covariance-based approaches take only averaged information into account, these types of dependence fail to be identified by traditional means. Revealing such dependence structures, the quantile cross-spectral analysis introduced in this paper can fundamentally change the way we view the dependence between economic time series, and it opens new possibilities for the modelling of interactions between economic and financial variables.

Quantile cross-spectral analysis provides a general, unifying framework for estimating dependence between economic time series. As noted in the early work of Granger (1966), the spectral distribution of an economic variable has a typical shape that distinguishes long-term fluctuations from short-term ones. These fluctuations point to economic activity at different frequencies (after removal of trend in mean, as well as seasonal components). After Granger (1966) had studied the behaviour of single time series, important literature using cross-spectral analysis to identify the dependence between variables quickly emerged [from Granger (1969) to the more recent work by Croux et al. (2001)]. Instead of considering only cross-sectional correlations, researchers started to use coherency (frequency-dependent correlation) to investigate the short-run and long-run dynamic properties of multiple time series, and to identify business cycle synchronization; see Croux et al. (2001). In one of his very last papers, Granger (2010) hypothesized about possible cointegrating relationships in quantiles, leading to the first notion of the general types of dependence that quantile cross-spectral analysis is addressing. The quantile cointegration developed by Xiao (2009) partially addresses the problem, but does not allow a full exploration of the frequency-dependent structure of correlations in different quantiles of the joint distribution.

Three toy examples illustrating the potential offered by quantile cross-spectral analysis are depicted in Figure 1. In each example, one distinct type of dependence is considered: cross-sectional dependence (left), serial dependence (centre), and independence (right). We consider bivariate processes (x_t, y_t) that possess the desired dependence structure, but are indistinguishable in terms of traditional coherency. In the examples, (ϵ_t) is an independent sequence of standard

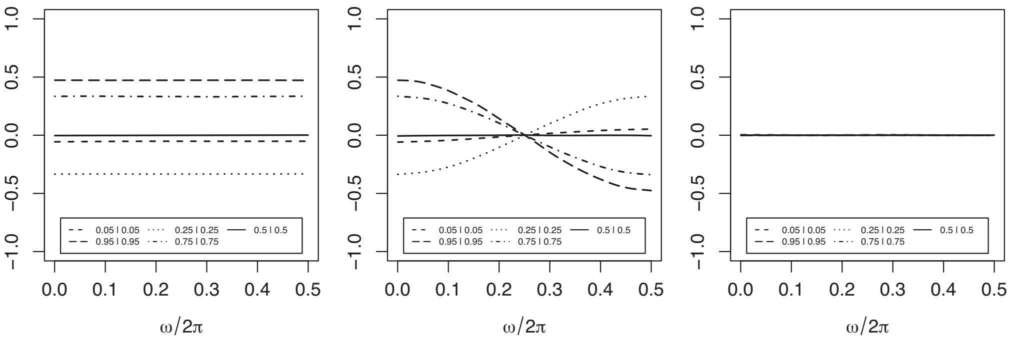

Figure 1. Illustration of dependence between processes x_t and y_t.

normally distributed random variables. In the left column of Figure 1, the dependence emerging between ϵ_t and ϵ_t^2 is depicted. It is important to observe that ϵ_t and ϵ_s^2 are uncorrelated. Therefore, traditional coherency for $(\epsilon_t, \epsilon_t^2)$ would read zero across all frequencies, even though it is obvious that ϵ_t and ϵ_t^2 are dependent. From the newly introduced quantile coherency, this dependence can easily be observed. More precisely, we can distinguish various degrees of dependence for each part of the distribution. For example, there is no dependence in the centre of the distribution (i.e., 0.5|0.5), but when the quantile levels are different from 0.5 the dependence becomes visible.[1] In this example, the quantile coherency is constant across frequencies, which corresponds to the fact that there is no serial dependence. In the centre column of Figure 1, the process $(\epsilon_t, \epsilon_{t-1}^2)$ is studied, where we have introduced a time lag. Intuitively, the dependence in quantiles of this bivariate process will be the same as in the previous example (left column) in the long run, referring to frequencies close to zero. With increasing frequency, dependence will decline or incline gradually to values with opposite signs, as high-frequency movements are in opposition owing to the lag shift. This is clearly captured by quantile coherency, while the dependence structure would stay hidden from traditional coherency, again, as it averages the dependence across quantiles. We can think about these processes as being 'spuriously independent'. To demonstrate the behaviour of the quantile coherency when the processes under consideration are truly independent, we observe in the right column of Figure 1 the quantities for independent bivariate Gaussian white noise, where quantile coherency displays zero dependence at all quantiles and frequencies, as expected. These illustrations strongly support our claim that there is a need for more general measures that can provide a better understanding of the dependence between variables. These very simple, yet illuminating motivating examples focus on uncovering dependence in uncorrelated variables. Later in the paper (Section 6), we further discuss a data-generating process based on quantile vector autoregression (QVAR), which is able to generate even richer dependence structures, revealing once more the limitations of the traditional approach. In Figure 2, the real part of the quantile coherencies of the QVAR(1), QVAR(2), and QVAR(3) example processes are shown. Further, in Section S3, we discuss how to interpret quantile coherency in the special cases of bivariate Gaussian VAR(1).

This paper is organized as follows. In Section 2 we introduce the notation, and define quantile coherency and an estimator for it. In Section 3 we discuss the proposed methodology and related

[1] All plots show real parts of the complex-valued quantities for illustratory purposes. Further discussion on how to interpret the real part and the imaginary part of quantile coherency are deferred to Section 3.

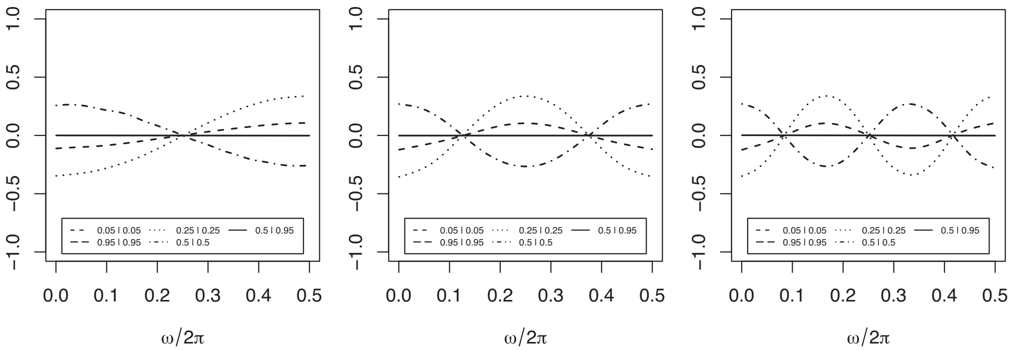

Figure 2. Illustration of dependence between vector quantile autoregressive processes.

literature. In Section 4 we provide a rigorous asymptotic analysis of the estimator's statistical properties. In Section 5, to support our theoretical discussions empirically, we employ the new methodology to inspect bivariate stock market returns, one of the most prominent time series in economics, and reveal dependencies in cycles of quantile-based features. We continue our empirical study in Section 6 by using quantile coherency to compare time series models with respect to their capabilities to capture the revealed dependencies. In the supplementary material to this paper (available from the publisher's homepage), we discuss additional quantile-based cross-spectral quantities (Section S1), discuss quantile vector autoregressive processes as examples with rich dynamics (Section S2), discuss how the new, quantile-based spectral quantities and their traditional counterparts are related (Section S3), state additional theoretical results (Section S4), comment on the construction of the interval estimators (Section S5), and provide rigorous proofs for all theoretical results (Section S6).

2. QUANTILE CROSS-SPECTRAL QUANTITIES AND THEIR ESTIMATORS

Throughout the paper, $(\boldsymbol{X}_t)_{t\in\mathbb{Z}}$ denotes a d-variate, strictly stationary process, with components $X_{t,j}, j = 1, \ldots, d$; i.e., $\boldsymbol{X}_t = (X_{t,1}, \ldots, X_{t,d})'$. The marginal distribution function of $X_{t,j}$ will be denoted by F_j, and by $q_j(\tau) := F_j^{-1}(\tau) := \inf\{q \in \mathbb{R} : \tau \leq F_j(q)\}$, where $\tau \in [0, 1]$, we denote the corresponding quantile function. We use the convention $\inf \emptyset = +\infty$, such that, if $\tau = 0$ or $\tau = 1$, then $-\infty$ and $+\infty$ are possible values for $q_j(\tau)$, respectively. We will write $\overline{z}$ for the complex conjugate, $\Re z$ for the real part, and $\Im z$ for the imaginary part of $z \in \mathbb{C}$. The transpose of a matrix $\boldsymbol{A}$ will be denoted by $\boldsymbol{A}'$, and the inverse of a regular matrix $\boldsymbol{B}$ will be denoted by $\boldsymbol{B}^{-1}$.

As a measure for the serial and cross-dependency structure of $(\boldsymbol{X}_t)_{t\in\mathbb{Z}}$, we define the matrix of quantile cross-covariance kernels, $\Gamma_k(\tau_1, \tau_2) := (\gamma_k^{j_1,j_2}(\tau_1, \tau_2))_{j_1,j_2=1,\ldots,d}$, where

$$\gamma_k^{j_1,j_2}(\tau_1, \tau_2) := \operatorname{Cov}\Big(I\{X_{t+k,j_1} \leq q_{j_1}(\tau_1)\}, I\{X_{t,j_2} \leq q_{j_2}(\tau_2)\}\Big), \tag{2.1}$$

$j_1, j_2 \in \{1, \ldots, d\},\ k \in \mathbb{Z},\ \tau_1, \tau_2 \in [0, 1]$, and $I\{A\}$ denotes the indicator function of the event A. In the frequency domain, this yields (under appropriate mixing conditions) the matrix of quantile cross-spectral density kernels $\mathfrak{f}(\omega; \tau_1, \tau_2) := (\mathfrak{f}^{j_1, j_2}(\omega; \tau_1, \tau_2))_{j_1, j_2=1,\dots,d}$, where

$$\mathfrak{f}^{j_1, j_2}(\omega; \tau_1, \tau_2) := (2\pi)^{-1} \sum_{k=-\infty}^{\infty} \gamma_k^{j_1, j_2}(\tau_1, \tau_2) \mathrm{e}^{-\mathrm{i}k\omega}, \tag{2.2}$$

$j_1, j_2 \in \{1, \dots, d\}$, $\omega \in \mathbb{R}$, $\tau_1, \tau_2 \in [0, 1]$. A closely related quantity that can be used as a measure for the dynamic dependence of the two processes $(X_{t,j_1})_{t\in\mathbb{Z}}$ and $(X_{t,j_2})_{t\in\mathbb{Z}}$ is the quantile coherency kernel of $(X_{t,j_1})_{t\in\mathbb{Z}}$ and $(X_{t,j_2})_{t\in\mathbb{Z}}$, which we define as

$$\mathfrak{R}^{j_1, j_2}(\omega; \tau_1, \tau_2) := \frac{\mathfrak{f}^{j_1, j_2}(\omega; \tau_1, \tau_2)}{\Big(\mathfrak{f}^{j_1, j_1}(\omega; \tau_1, \tau_1)\mathfrak{f}^{j_2, j_2}(\omega; \tau_2, \tau_2)\Big)^{1/2}}, \tag{2.3}$$

$(\tau_1, \tau_2) \in (0, 1)^2$. We define the estimator for the quantile cross-spectral density as the collection

$$I_{n,R}^{j_1, j_2}(\omega; \tau_1, \tau_2) := \frac{1}{2\pi n} d_{n,R}^{j_1}(\omega; \tau_1) d_{n,R}^{j_2}(-\omega; \tau_2), \tag{2.4}$$

$j_1, j_2 = 1, \dots, d$, $\omega \in \mathbb{R}$, $(\tau_1, \tau_2) \in [0, 1]^2$, and call it the rank-based copula cross-periodograms, or, in brief, the CCR-periodograms, where

$$d_{n,R}^{j}(\omega; \tau) := \sum_{t=0}^{n-1} I\{\hat{F}_{n,j}(X_{t,j}) \le \tau\} \mathrm{e}^{-\mathrm{i}\omega t} = \sum_{t=0}^{n-1} I\{R_{n;t,j} \le n\tau\} \mathrm{e}^{-\mathrm{i}\omega t},$$

$j = 1, \dots, d$, $\omega \in \mathbb{R}$, $\tau \in [0, 1]$, and $\hat{F}_{n,j}(x) := n^{-1} \sum_{t=0}^{n-1} I\{X_{t,j} \le x\}$ denotes the empirical distribution function of $X_{t,j}$ and $R_{n;t,j}$ denotes the (maximum) rank of $X_{t,j}$ among $X_{0,j}, \dots, X_{n-1,j}$. We will denote the matrix of CCR-periodograms by

$$\boldsymbol{I}_{n,R}(\omega; \tau_1, \tau_2) := (I_{n,R}^{j_1, j_2}(\omega; \tau_1, \tau_2))_{j_1, j_2=1,\dots,d}. \tag{2.5}$$

From the univariate case, it is already known (cf. Proposition 3.4 in Kley et al. 2016) that the CCR-periodograms fail to estimate $\mathfrak{f}^{j_1, j_2}(\omega; \tau_1, \tau_2)$ consistently. Consistency can be achieved by smoothing $I_{n,R}^{j_1, j_2}(\omega; \tau_1, \tau_2)$ across frequencies. More precisely, we consider

$$\hat{G}_{n,R}^{j_1, j_2}(\omega; \tau_1, \tau_2) := \frac{2\pi}{n} \sum_{s=1}^{n-1} W_n\big(\omega - 2\pi s/n\big) I_{n,R}^{j_1, j_2}(2\pi s/n, \tau_1, \tau_2), \tag{2.6}$$

where W_n denotes a sequence of weight functions, to be defined precisely in Section 4.

We will denote the matrix of smoothed CCR-periodograms by

$$\hat{\boldsymbol{G}}_{n,R}(\omega; \tau_1, \tau_2) := (\hat{G}_{n,R}^{j_1, j_2}(\omega; \tau_1, \tau_2))_{j_1, j_2=1,\dots,d}. \tag{2.7}$$

The estimator for the quantile coherency is then given by

$$\hat{\mathfrak{R}}_{n,R}^{j_1, j_2}(\omega; \tau_1, \tau_2) := \frac{\hat{G}_{n,R}^{j_1, j_2}(\omega; \tau_1, \tau_2)}{\Big(\hat{G}_{n,R}^{j_1, j_1}(\omega; \tau_1, \tau_1)\hat{G}_{n,R}^{j_2, j_2}(\omega; \tau_2, \tau_2)\Big)^{1/2}}. \tag{2.8}$$

In Section 4 we will prove that

$$\hat{\mathfrak{R}}_{n,R}(\omega; \tau_1, \tau_2) := \big(\hat{\mathfrak{R}}_{n,R}^{j_1, j_2}(\omega; \tau_1, \tau_2)\big)_{j_1, j_2=1,\dots,d}$$

is a legitimate estimator for $\mathfrak{R}(\omega; \tau_1, \tau_2) := \big(\mathfrak{R}^{j_1,j_2}(\omega; \tau_1, \tau_2)\big)_{j_1,j_2=1,\dots,d}$, the matrix of quantile coherencies.

3. DISCUSSION OF THE INTRODUCED QUANTITIES AND ESTIMATORS

The quantile-based quantities defined in Section 2 are functions of the two variables τ_1 and τ_2. They are thus richer in information than their traditional counterparts. We have added the term kernel to the name for the quantities to stress this fact, but will frequently omit it in the rest of the paper, for the sake of brevity. For continuous F_{j_1} and F_{j_2}, the quantile cross-covariances defined in (2.1) coincide with the difference of the copula of (X_{t+k,j_1}, X_{t,j_2}) and the independence copula. Thus, they provide important information about both the serial dependence (by letting k vary) and the cross-section dependence (by choosing $j_1 \neq j_2$). For the quantile cross-spectral density we have

$$\int_{-\pi}^{\pi} \mathfrak{f}^{j_1,j_2}(\omega; \tau_1, \tau_2) \mathrm{e}^{\mathrm{i}k\omega} \mathrm{d}\omega + \tau_1\tau_2 = \mathbb{P}\Big(X_{t+k,j_1} \le q_{j_1}(\tau_1), X_{t,j_2} \le q_{j_2}(\tau_2)\Big), \tag{3.1}$$

where the quantity on the right-hand side, as a function of (τ_1, τ_2), is again the copula of the pair (X_{t+k,j_1}, X_{t,j_2}). The equality (3.1) thus shows how any of the pair copulas can be derived from the quantile cross-spectral density kernel defined in (2.2). Thus, the quantile cross-spectral density kernel provides a full description of all copulas of pairs in the process. Comparing these new quantities with their traditional counterparts, it can be observed that covariances and means are essentially replaced by copulas and quantiles. Similar to the regression setting, where this approach provides valuable extra information (cf. Koenker 2005), the quantile-based approach to spectral analysis supplements the traditional L^2-spectral analysis.

Observe that $\mathfrak{R}$ takes values in $\mathbb{C}^{d\times d}$ (the set of all complex-valued $d \times d$ matrices). Further, note that, as a function of ω, but for fixed τ_1, τ_2, it coincides with the traditional coherency of the bivariate, binary process

$$\Big(I\{X_{t,j_1} \le q_{j_1}(\tau_1)\}, I\{X_{t,j_2} \le q_{j_2}(\tau_2)\}\Big)_{t\in\mathbb{Z}}. \tag{3.2}$$

The time series in (3.2) has the bivariate time series $(X_{t,j_1}, X_{t,j_2})_{t\in\mathbb{Z}}$ as a 'latent driver' and indicates whether the values of the components j_1 and j_2 are below the respective marginal distribution's τ_1- and τ_2-quantile.

Note the important fact that $\mathfrak{R}^{j_1,j_2}(\omega; \tau_1, \tau_2)$ is undefined when (τ_1, τ_2) is on the boundary of $[0, 1]^2$. By the Cauchy–Schwarz inequality, we further observe that the range of possible values is limited to $\mathfrak{R}^{j_1,j_2}(\omega; \tau_1, \tau_2) \in \{z \in \mathbb{C} : |z| \le 1\}$. Note that, as (τ_1, τ_2) approaches the border of the unit square, the quantile cross-spectral density vanishes. Therefore, quantile coherency is better suited to measure the dependence of extremes than the quantile cross-spectral density (which is not standardized). Implicitly, we take advantage of the fact that the quantile cross-spectral density and quantile spectral densities vanish at the same rate, and therefore the quotient yields a meaningful quantity when the quantile levels (τ_1, τ_2) approaches the border of the unit square.

The quantile coherency kernel contains very valuable information about the joint dynamics of the time series $(X_{t,j_1})_{t\in\mathbb{Z}}$ and $(X_{t,j_2})_{t\in\mathbb{Z}}$. In contrast to the traditional case, where coherency will always equal one if $j_1 = j_2 =: j$, the quantile-based versions of these quantities are capable of delivering valuable information about one single component of $(\boldsymbol{X}_t)_{t\in\mathbb{Z}}$ as well. Quantile coherency then quantifies the joint dynamics of $(I\{X_{t,j} \le q_j(\tau_1)\})_{t\in\mathbb{Z}}$ and $(I\{X_{t,j} \le q_j(\tau_2)\})_{t\in\mathbb{Z}}$.

Note that quantile coherency is a complex-valued, 2π-periodic function of the variable ω, and Hermitian in the sense that we have

$$\overline{\mathfrak{R}^{j_1,j_2}(\omega;\tau_1,\tau_2)} = \mathfrak{R}^{j_1,j_2}(-\omega;\tau_1,\tau_2) = \mathfrak{R}^{j_2,j_1}(\omega;\tau_2,\tau_1) = \mathfrak{R}^{j_2,j_1}(2\pi+\omega;\tau_2,\tau_1).$$

Following similar arguments to in Section 2.1 of Birr et al. (2018), it can be shown that $\Re\mathfrak{R}^{j_1,j_2}(\omega;\tau_1,\tau_2)$ describes the dynamics of the process switching between the j_1st component being below the τ_1-quantile and the j_2nd component being above the τ_2-quantile. Consequently, for τ_1 close to 0 and for τ_2 close to 1 it describes the dynamics of changing from an extreme in one component to an extreme in another component. Further, it can be shown that $\Im\mathfrak{R}^{j_1,j_2}(\omega;\tau_1,\tau_2)$ contains information about asymmetry.

A discussion of related quantities, of how and how not to interpret them, and of how they are related to their traditional counterparts in the Gaussian case can be found in Sections S1, S2, and S3 of the supplementary material.

Recently, important contributions that aim at accounting for more general dynamics have emerged in the literature. Measures such as, for example, distance correlation (Székely et al. 2007) and martingale difference correlation (Shao and Zhang 2014) go beyond traditional correlation and instead can indicate whether random quantities are independent or martingale differences, respectively. For time series, in the time domain, Zhou (2012) introduced auto distance correlations that are zero if and only if the measured time series components are independent. Linton and Whang (2007), and Davis et al. (2009) introduced the (univariate) concepts of quantilograms and extremograms, respectively. More recently, quantile correlation (Schmitt et al. 2015), and quantile autocorrelation functions (Li et al. 2015) together with cross-quantilograms (Han et al. 2016) have been proposed as a fundamental tool for analysing dependence in quantiles of the distribution.

In the frequency domain, Hong (1999) introduced a generalized spectral density. In the generalized spectral density, covariances are replaced by quantities that are closely related to empirical characteristic functions. In Hong (2000), the Fourier transform of empirical copulas at different lags is considered for testing the hypothesis of pairwise independence. Recently, under the names of Laplace, quantile and copula spectral density and spectral density kernels, various quantile-related spectral concepts have been proposed for the frequency domain. The approaches by Hagemann (2013) and Li (2008, 2012) are designed to consider cyclical dependence in the distribution at user-specified quantiles. Mikosch and Zhao (2014, 2015) define and analyse a periodogram (and its integrated version) of extreme events. As noted by Hagemann (2013), other approaches aim at discovering 'the presence of any type of dependence structure in time series data', referring to work of Dette et al. (2015) and Lee and Rao (2012). This comment also applies to Kley et al. (2016). In the present paper, our aim is to generalize the existing approaches to multivariate time series. The extensions to the terminology that we provide, in particular the introduction of the standardized quantile coherency, is very important for economic applications, because it enables the analyst to perform a more detailed joint analysis of the serial and cross-sectional dependence in multiple time series.

For the univariate case, different approaches to consistent estimation were considered. Li (2008) proposed an estimator for a weighted version of the quantile spectra, based on least absolute deviation regression, for the special case where $\tau_1 = \tau_2 = 0.5$. Li (2012) generalized the estimator, using quantile regression, to the case where $\tau_1 = \tau_2 \in (0, 1)$. The general case, in which the quantities can be related to the copulas of pairs, was first considered by Dette et al. (2015). These authors were also the first to consider a rank-based version of the quantile regression-type estimator, which eliminates the need to estimate the weights in Li (2008, 2012). For the case where $\tau_1 = \tau_2 \in (0, 1)$, Hagemann (2013) proposed a version of the traditional L^2-periodogram where the observations are replaced with $I\{\hat{F}_{n,j}(X_{t,j}) \le \tau\} = I\{R_{n;t,j} \le n\tau\}$. Kley et al. (2016) generalized this estimator, in the spirit of Dette et al. (2015), by considering cross-periodograms for arbitrary couples $(\tau_1, \tau_2) \in [0, 1]^2$, and proved that it converges, as a stochastic process, to a complex-valued Gaussian limit. An estimator defined in analogy to the traditional lag-window estimator was analysed by Birr et al. (2017) in the context of nonstationary time series.

4. ASYMPTOTIC PROPERTIES OF THE PROPOSED ESTIMATORS

To derive the asymptotic properties of the estimators defined in Section 3, some assumptions need to be made. Recall [cf. Brillinger (1975), p. 19] that the rth-order joint cumulant $\mathrm{cum}(Z_1, \dots, Z_r)$ of the random vector $(Z_1, \dots, Z_r)$ is defined as

$$\mathrm{cum}(Z_1, \dots, Z_r) := \sum_{\{\nu_1,\dots,\nu_p\}} (-1)^{p-1}(p-1)!E\Big[\prod_{j\in\nu_1} Z_j\Big]\cdots E\Big[\prod_{j\in\nu_p} Z_j\Big],$$

with summation extending over all partitions $\{\nu_1, \dots, \nu_p\}$, $p = 1, \dots, r$, of $\{1, \dots, r\}$.

Regarding the range of dependence of $(\boldsymbol{X}_t)_{t\in\mathbb{Z}}$ we make the following assumption.

ASSUMPTION 4.1 The process $(\boldsymbol{X}_t)_{t\in\mathbb{Z}}$ is strictly stationary and exponentially α-mixing; that is, there exist constants $K < \infty$ and $\rho \in (0, 1)$, such that

$$\alpha(n) := \sup_{\substack{A\in\sigma(X_0,X_{-1},\dots)\\ B\in\sigma(X_n,X_{n+1},\dots)}} \big|\mathbb{P}(A \cap B) - \mathbb{P}(A)\mathbb{P}(B)\big| \le K\rho^n, \quad n \in \mathbb{N}. \tag{4.1}$$

Further, to establish consistency of the estimates we consider sequences of weights that asymptotically concentrate around multiples of 2π.

ASSUMPTION 4.2 The weights are defined as $W_n(u) := \sum_{j=-\infty}^{\infty} b_n^{-1} W(b_n^{-1}[u + 2\pi j])$, where $b_n > 0$, $n = 1, 2, \dots$, is a sequence of scaling parameters satisfying $b_n \to 0$ and $nb_n \to \infty$, as $n \to \infty$. The weight function W is real-valued, even, has support $[-\pi, \pi]$, bounded variation, and satisfies $\int_{-\pi}^{\pi} W(u)\mathrm{d}u = 1$.

Comments on the assumptions will follow at the end of this section. The main result of this section (Theorem 4.1) will legitimize $\hat{\mathfrak{R}}_{n,R}(\omega; \tau_1, \tau_2)$ as an estimator of the quantile coherency $\mathfrak{R}(\omega; \tau_1, \tau_2)$. Results that legitimize $\boldsymbol{I}_{n,R}(\omega; \tau_1, \tau_2)$ and $\hat{\boldsymbol{G}}_{n,R}(\omega; \tau_1, \tau_2)$ as estimators of the quantile cross-spectral density $\mathfrak{f}(\omega; \tau_1, \tau_2)$ are deferred to the supplementary material so as not to impair the flow of the paper. The legitimacy of the estimates follows from the fact that the estimators converge weakly in the sense of Hoffman–Jørgensen (cf. Chapter 1 of van der Vaart and Wellner 1996). We denote this mode of convergence by $\Rightarrow$. The estimators under consideration take values in the space of (element-wise) bounded functions $[0, 1]^2 \to \mathbb{C}^{d\times d}$, which we denote by $\ell^\infty_{\mathbb{C}^{d\times d}}([0, 1]^2)$. While results in empirical process theory are typically stated for spaces of real-valued, bounded functions, these results transfer immediately by identifying $\ell^\infty_{\mathbb{C}^{d\times d}}([0, 1]^2)$ with the product space $\ell^\infty([0, 1]^2)^{2d^2}$. Note that the space $\ell^\infty_{\mathbb{C}^{d\times d}}([0, 1]^2)$ is constructed along the same lines as the space $\ell^\infty_{\mathbb{C}}([0, 1]^2)$ in Kley et al. (2016).

We are now ready to state the main result of this section.

THEOREM 4.1 *Let Assumptions 4.1 and 4.2 hold. Assume that the marginal distribution functions F_j, $j = 1, \dots, d$ are continuous and that constants $\kappa > 0$ and $k \in \mathbb{N}$ exist, such* *that* $b_n = o(n^{-1/(2k+1)})$ *and* $b_n n^{1-\kappa} \to \infty$. *Assume that for some* $\varepsilon \in (0, 1/2)$ *we have* $\inf_{\tau \in [\varepsilon, 1-\varepsilon]} \mathfrak{f}^{j,j}(\omega; \tau, \tau) > 0$, *for all* $j = 1, \dots, d$. *Then, for any fixed* $\omega \in \mathbb{R}$,

$$\sqrt{nb_n}\Big(\hat{\mathfrak{R}}_{n,R}(\omega;\tau_1,\tau_2) - \mathfrak{R}(\omega;\tau_1,\tau_2) - \mathfrak{B}_n^{(k)}(\omega;\tau_1,\tau_2)\Big)_{(\tau_1,\tau_2)\in[\varepsilon,1-\varepsilon]^2} \Rightarrow \mathbb{L}(\omega;\cdot,\cdot), \tag{4.2}$$

in $\ell^\infty_{\mathbb{C}^{d\times d}}([\varepsilon, 1-\varepsilon]^2)$, *where*

$$\Big\{\mathbb{L}(\omega;\tau_1,\tau_2)\Big\}_{j_1,j_2} := \frac{1}{\sqrt{\mathfrak{f}_{1,1}\mathfrak{f}_{2,2}}}\Big(\mathbb{H}_{1,2} - \frac{1}{2}\frac{\mathfrak{f}_{1,2}}{\mathfrak{f}_{1,1}}\mathbb{H}_{1,1} - \frac{1}{2}\frac{\mathfrak{f}_{1,2}}{\mathfrak{f}_{2,2}}\mathbb{H}_{2,2}\Big), \tag{4.3}$$

$$\Big\{\mathfrak{B}_n^{(k)}(\omega;\tau_1,\tau_2)\Big\}_{j_1,j_2} := \frac{1}{\sqrt{\mathfrak{f}_{1,1}\mathfrak{f}_{2,2}}}\Big(\boldsymbol{B}_{1,2} - \frac{1}{2}\frac{\mathfrak{f}_{1,2}}{\mathfrak{f}_{1,1}}\boldsymbol{B}_{1,1} - \frac{1}{2}\frac{\mathfrak{f}_{1,2}}{\mathfrak{f}_{2,2}}\boldsymbol{B}_{2,2}\Big) \tag{4.4}$$

and we have written $\mathfrak{f}_{a,b}$ *for the quantile cross-spectral density* $\mathfrak{f}^{j_a,j_b}(\omega;\tau_a,\tau_b)$ *as defined in (2.2),* $\boldsymbol{B}_{a,b} := \sum_{\ell=2}^{k} \frac{b_n^\ell}{\ell!}\int_{-\pi}^{\pi} v^\ell W(v)dv \frac{d^\ell}{d\omega^\ell}\mathfrak{f}^{j_a,j_b}(\omega;\tau_a,\tau_b)$, *and* $\mathbb{H}_{a,b}$ *for* $\mathbb{H}^{j_a,j_b}(\omega;\tau_a,\tau_b)$; *a component of* $\mathbb{H}(\omega;\cdot,\cdot) := (\mathbb{H}^{j_1,j_2}(\omega;\cdot,\cdot))_{j_1,j_2=1,\dots,d}$ *defined as a centred,* $\mathbb{C}^{d\times d}$*-valued Gaussian process characterized by*

$$\begin{aligned}\mathrm{Cov}\Big(\mathbb{H}^{j_1,j_2}(\omega;u_1,v_1), \mathbb{H}^{k_1,k_2}(\lambda;u_2,v_2)\Big)\\ = 2\pi\Big(\int_{-\pi}^{\pi} W^2(\alpha)d\alpha\Big)\Big(\mathfrak{f}^{j_1,k_1}(\omega;u_1,u_2)\mathfrak{f}^{j_2,k_2}(-\omega;v_1,v_2)\eta(\omega-\lambda)\\ + \mathfrak{f}^{j_1,k_2}(\omega;u_1,v_2)\mathfrak{f}^{j_2,k_1}(-\omega;v_1,u_2)\eta(\omega+\lambda)\Big),\end{aligned}$$

where $\eta(x) := I\{x = 0 (\mod 2\pi)\}$ *[cf. Brillinger (1975), p. 148] is the* 2π*-periodic extension of Kronecker's delta function. The family* $\{\mathbb{H}(\omega;\cdot,\cdot), \omega \in [0,\pi]\}$ *is a collection of independent processes, and* $\mathbb{H}(\omega;\tau_1,\tau_2) = \overline{\mathbb{H}(-\omega;\tau_1,\tau_2)} = \mathbb{H}(\omega+2\pi;\tau_1,\tau_2)$.

The proof of Theorem 4.1 is lengthy and technical and is therefore deferred to the online supplement (Section S6). Comparing Theorem 4.1 with results for the traditional coherency [see, for example, Theorem 7.6.2 in Brillinger (1975)], we observe that the distribution of $\hat{\mathfrak{R}}_{n,R}(\omega;\tau_1,\tau_2)$ is asymptotically equivalent to that of the traditional estimator [cf. (7.6.14) in Brillinger (1975)] computed from the unobserved time series

$$\big(I\{F_{j_1}(X_{t,j_1}) \le \tau_1\}, I\{F_{j_1}(X_{t,j_2}) \le \tau_2\}\big), \quad t = 0, \dots, n-1. \tag{4.6}$$

The convergence to a Gaussian process in (4.2) can be employed to obtain asymptotically valid pointwise confidence bands. To this end, the covariance kernel of $\mathbb{L}$ can easily be determined from (4.3) and (4.5), yielding an expression similar to (7.6.16) in Brillinger (1975). A more detailed account of how to conduct inference is given in Section S5 of the supplementary material. Note that the bound to the order of the bias given in (7.6.15) in Brillinger (1975) applies to the expansion given in (4.4).

If W is a kernel of order $p \ge 1$, we have that the bias is of order b_n^p. Thus, if we choose the mean square error minimizing bandwidth $b_n \approx n^{-1/(2p+1)}$, the bias will be of order $n^{-p/(2p+1)}$. Regarding the restriction $\varepsilon > 0$, note that the convergence (4.2) cannot hold if (τ_1, τ_2) is on the border of the unit square, as the quantile coherency $\mathfrak{R}(\omega;\tau_1,\tau_2)$ is not defined if $\tau_j \in \{0, 1\}$, as this implies that $\mathrm{Var}(I\{F_j(X_{t,j}) \le \tau_j\}) = 0$.

We now comment on the assumptions. Assumption 4.1 holds for a wide range of popular, linear and nonlinear processes. Examples (possibly, under mild additional assumptions) include the traditional VARMA or vector-ARCH models as well as many others. It is important to observe that Assumption 4.1 does not require the existence of any moments, which is in sharp contrast to the classical assumptions, where moments up to the order of the respective cumulants have to exist. Assumption 4.2 is quite standard in classical time series analysis [cf., for example, Brillinger (1975), p. 147].

5. QUANTILE CROSS-SPECTRAL ANALYSIS OF STOCK MARKET RETURNS: A ROUTE TO MORE ACCURATE RISK MEASURES?

Stock market returns belong to one of the prominent datasets in economics and finance. Although many important stylized facts about their behaviour have been established in the past decades, it remains a very active area of research. Despite these efforts, an important direction that has not been fully addressed is stylized facts about the joint distribution of returns. Especially during the last turbulent decade, an understanding of the behaviour of joint quantiles in return distributions has become particularly important, as this behaviour is essential for understanding systemic risk, namely 'the risk that the intermediation capacity of the entire system can be impaired' (cf. Adrian and Brunnermeier, 2016). Several authors focus on explaining tails of the bivariate market distributions in different ways. Adrian and Brunnermeier (2016) proposed to classify institutions according to the sensitivity of their quantiles to shocks to the market. Most closely related to the notion of how we view the dependence structures is the multivariate regression quantile model of White et al. (2015), which studies the degree of tail interdependence among different random variables directly.

Quantile cross-spectral analysis, as designed in this paper, allows us to analyse the fundamental dependence quantities in the tails (but also in any other part) of the joint distribution and across frequencies. An application to stock market returns may therefore provide deeper insight about dependence in stock markets, and lead to a more powerful analysis, securing us against financial collapses.

One of the important features of stock market returns is time variation in its volatility. Time-varying volatility processes can cross almost every quantile of their distribution (cf. Hagemann, 2013), and create peaks in quantile spectral densities as shown by Li (2014). These notions have recently been documented by Engle and Manganelli (2004) and Žikeš and Baruník (2016), who propose models for the conditional quantiles of the return distribution based on the past volatility. In the multivariate setting, strong common factors in volatility are found by Barigozzi et al. (2014), who conclude that common volatility is an important risk factor. Hence, common volatility should be viewed as a possible source of dependence. Because we aim to find the common structures in the joint distribution of returns, we study returns standardized by its volatility that we estimate by a GARCH(1,1) model; cf. Bollerslev (1986). This first step is commonly taken in the literature of modelling the joint market distribution using copulas; cf. Granger et al. (2006) and Patton (2012). In these approaches, the volatility in the marginal distributions is modelled first, and the common factors are then considered in the second step. Consequently, this will allow us to discover other possible common factors in the joint distribution of market returns across frequencies that result in spurious dependence but that will not be overshadowed by the strong volatility process.

We choose to study the joint distribution of portfolio returns and excess returns on the broad market, hence looking at one of the most commonly studied factor structures in the literature as

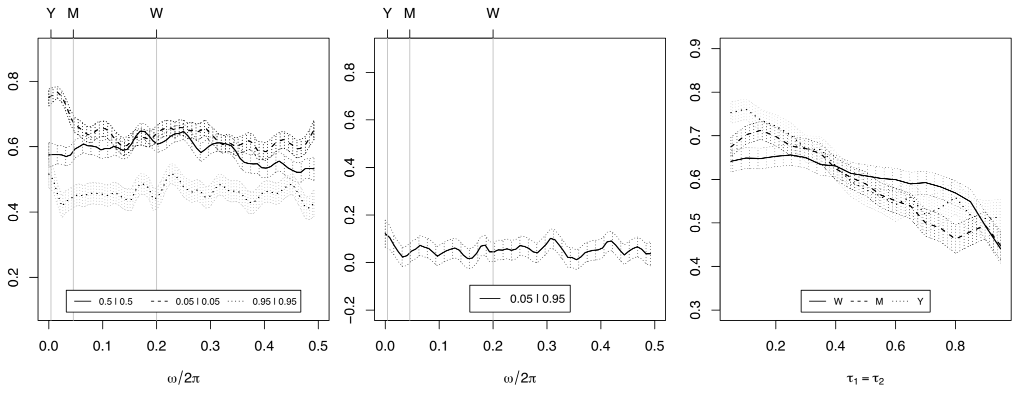

Figure 3. Quantile coherency estimates for the portfolio.

dictated by asset pricing theories; cf. Sharpe (1964) and Lintner (1965). As an excess return on the market, we use value-weighted returns of all firms listed on the NYSE, AMEX, or NASDAQ from the Center for Research in Security Price (CRSP) database. For the benchmark portfolio, we use an industry portfolio formed from consumer non-durables.[2] We used $n = 23{,}385$ daily observations (from July 1, 1926 through to June 30, 2015). The data include several crisis periods and therefore might not be suitable to be viewed as a strictly stationary time series. Nevertheless, we choose to study this long period of data as we believe that longer than yearly cycles might constitute an important possible source of dependence, and that the empirical results are practically interesting. Moreover, by standardizing the returns by their volatility we removed what we believe is the most important source of time-variation in data.[3]

In the left panel of Figure 3, quantile coherency estimates for the 0.05|0.05, 0.5|0.5, and 0.95|0.95 combinations of quantile levels of the joint distribution are shown for the industry portfolio and excess market returns over frequencies. The centre panel in Figure 3, on which we comment later, shows the 0.05|0.95 combination. We have used the Epanechnikov kernel and a bandwidth of $b_n = 0.5n^{1/4}$ for the computation of the estimates (cf. (2.8)). The confidence intervals, shown as dotted regions, are at the 95% level and were constructed according to the procedure described in Section S5 of the supplementary material. For clarity, we plot the x-axis in daily cycles and also indicate the frequencies that correspond to yearly, monthly, and weekly periods. While we use daily data, the highest possible frequency of 0.5 indicates 0.5 cycles per day (i.e., a 2-day period). While precise frequencies do not have an economic meaning, one needs to understand the interpretation with respect to the time domain. For example, a sampling frequency of 0.2 corresponds to 0.2 cycles per day, translating to a 5-day period (equivalent to one week), but a frequency of 0.3 translates to a hardly interpretable $3.\overline{3}$ period. Hence, the upper label of the x-axis is of particular interest to an economist, as one can study how weekly, monthly, or

[2] Note on choice of the data: we use the publicly available data available and maintained by Fama and French at http://mba.tuck.dartmouth.edu/pages/faculty/ken.french/data_library.html. This data set is popular among researchers, and while many types of portfolios can be chosen, we chose consumer non-durables randomly for this application. Although very interesting and attractive, it is far beyond the scope of this work to present and discuss results for wider portfolios formed on distinct criteria.

[3] As a robustness check, we sliced the time series into decades and found that our results on nonoverlapping windows do not materially change.

yearly cycles are connected across quantiles of the joint distribution. For clarity of presentation, we focus on the real part of the quantities, which relates to the dynamics of the process switching between the j_1st component being below the τ_1-quantile and the j_2nd component being above the τ_2-quantile (cf. Section 2).

The real parts of the quantile coherency estimates reveal frequency dynamics in quantiles of the joint distribution of the returns under study. Generally, cycles at the lower quantiles appear to be more strongly dependent than those at the upper quantiles, which is a well-documented stylized fact about stock market returns. It points us to the fact that returns are more dependent during business cycle downturns than during upturns; cf. Erb et al. (1994), Longin and Solnik (2001), Ang and Chen (2002), and Patton (2012). More importantly, lower quantiles are more strongly related in periods longer than one week on average in comparison to shorter than weekly periods, and are even more connected at longer than monthly cycles. This suggests that infrequent clusters of large negative portfolio returns are better explained by excess market returns than small daily fluctuations. Returns in upper quantiles of the joint distribution seem to be connected similarly across all frequencies. The same result holds also for the median. For a better exposure, we also present quantile coherency estimates for three fixed weekly, monthly, and yearly periods (corresponding to $\omega \in 2\pi\{1/5,\ 1/22,\ 1/250\}$, respectively) at all quantile levels $\tau_1 = \tau_2 \in \{0.05, 0.1, \ldots, 0.95\}$ in the right panel of Figure 3. This alternative plot highlights the previous discussion.

We now compare our findings with a corresponding analysis with the cross-quantilogram, a related quantile-based measure for serial dependence in the time domain. Considering a strictly stationary, $\mathbb{R} \times \mathbb{R} \times \mathbb{R}^{d_1} \times \mathbb{R}^{d_2}$-valued time series $(y_{1t}, y_{2t}, x_{1t}, x_{2t})$, with $t \in \mathbb{Z}$ and $d_1, d_2 \in \mathbb{N}$, denoting the conditional distribution of the series y_{it} given x_{it} by $F_{y_i|x_i}(\cdot|x_{it})$, and the quantile function as $q_{i,t}(\tau_i) = \inf\{v : F_{y_i|x_i}(\cdot|x_{it}) \geq \tau_i\}$, $\tau_i \in (0, 1)$, $i = 1, 2$, Han et al. (2016) define the cross-quantilogram as

$$\rho_{(\tau_1,\tau_2)}(k) := \frac{\mathbb{E}\big[(I\{y_{1t} < q_{1,t}(\tau_1)\} - \tau_1)(I\{y_{2,t-k} < q_{2,t-k}(\tau_2)\} - \tau_2)\big]}{\Big(\mathbb{E}\big[(I\{y_{1t} < q_{1,t}(\tau_1)\} - \tau_1)^2\big]\mathbb{E}\big[(I\{y_{2,t-k} < q_{2,t-k}(\tau_2)\} - \tau_2)^2\big]\Big)^{1/2}}.$$

With no covariate information in our data example, this reduces to $x_{1t} = x_{2t} = 1$ and $q_{i,\,t}$ being the quantile of the marginal distribution of y_{it}. It is important to note that the cross-quantilogram is defined as a standardized measure of serial dependencies between the events $\{y_{1t} \leq q_{1,\,t}(\tau_1)\}$ and $\{y_{2t} \leq q_{2,\,t}(\tau_2)\}$ in the time domain, while quantile coherency is defined similarly, but in the frequency domain.

In Figure 4 we present the cross-quantilograms that we estimated from our data example. For the computation we used the estimator and stationary bootstrap procedure defined in Han et al. (2016). More precisely, we used the implementation that is available in the R package quantilogram; cf. Han et al. (2014). Inspecting the plots, it can be seen that there are lags k, typically short, where significant dependence is present. Further, it is possible to guess that there is periodic variation of positive and negative dependence at the 0.05 quantile level, while at the 0.95 quantile level the dependence seems to be largely positive. Yet, taking into account the confidence intervals, it is uncertain if this is a significant pattern. Further, comparing the discussion of these periodic patterns shown by the cross-quantilogram with what we were able to read from quantile coherency in Figure 3, it is difficult to read specific weekly, monthly, and yearly periodic components and whether or not they are significant. Thus, at least in the specific case where a researcher is interested in the dependence of cycles, we believe that quantile coherency can provide a perspective that is unavailable in the time domain analysis.

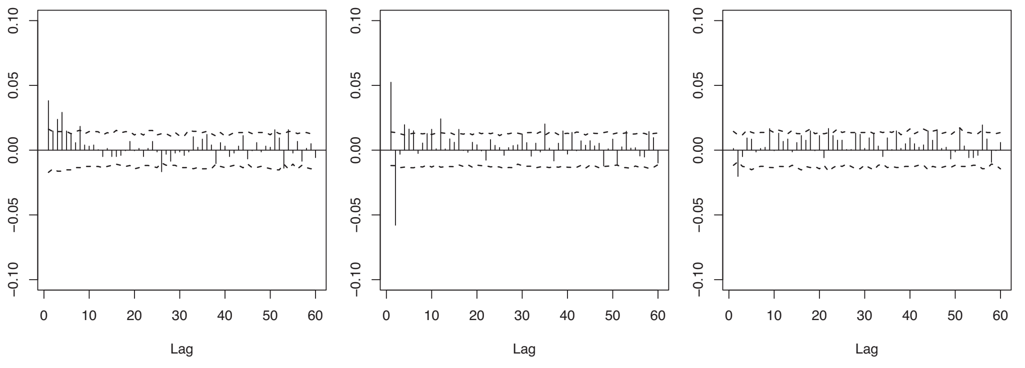

Figure 4. Cross-quantilogram estimates for the portfolio.

To summarize the result of our empirical analysis: while asymmetry is commonly found by researchers, we document the frequency-dependent asymmetry of stock market returns (i.e., asymmetry with respect to cycles in the joint distribution). Were this behaviour to be common across larger classes of assets, our results may have significant implications for one of the cornerstones of asset pricing theory, assuming a normal distribution of returns. It leads us to call for more general models, and more importantly to point to the need to restate asset pricing theory in a way that allows one to distinguish between the short-run and long-run behaviour of investors.

Our results are also crucial for systemic risk measurement, as an investor wishing to optimize a portfolio should focus on stocks that will not be connected at lower quantiles, in a situation of distress, but will be connected at upper quantiles, in a situation of market upturns in a given investment period. We document behaviour that is not favourable to such an investor using traditional pricing theories, as we show that broad stock market returns contain a common factor more frequently during downturns than during upturns. This suggests that the portfolio at hand might be much riskier than would be implied by common measures. Further, our results suggest that this effect becomes even worse for long-run investors.

An important feature of our quantile cross-spectral measures is that they enable us to measure dependence also between $\tau_1 \neq \tau_2$ quantiles of the joint distribution. In the central panel of Figure 3, we document that the dependence between the 0.05|0.95 quantiles of the return distribution is not very strong. Generally speaking, no intense dependence can be seen between large negative returns of the stock market, and large positive returns of the portfolio under study. This kind of analysis may be even more interesting in the case where dependence between individual assets is studied. There, negative news may have a strong opposite impact on the assets under study.

Finally, some words of caution to the reader, about the interpretation of the quantities that we have estimated, are in order. In Section S3 of the supplementary material, we provide a link between quantile coherency and traditional measures of dependence under the assumption of normally distributed data. The quantile-based measures are designed to capture general dependence types without restrictive assumptions on the underlying distribution of the process. Hence, here we have intentionally not related it to traditional correlation, which, ideally, should only be interpreted when the process is known to be Gaussian. The financial returns under study in this section are known to depart from normality. Therefore, quantile coherency is not directly comparable to traditional correlation measures. What we can see is a generally strong dependence between the portfolio returns and excess market returns at all quantiles, confirming the fact that excess returns are a strong common factor for the studied portfolio returns. The details that the quantile-based analysis in this section revealed would have remained hidden in an analysis based on the traditional coherency.

6. QUANTILE COHERENCY IN A MODEL-ASSESSING EXERCISE

In the previous section we demonstrated how quantile coherency can be used by applied researchers to reveal cyclical features of the data that might remain invisible if the data were analysed solely with covariance-based dependency measures. In this section we illustrate how quantile coherency can be used to assess the capability of time series models to capture such cycles documented in the data.

More precisely, we fit several bivariate time series models and then compare the quantile coherencies implied by estimated parameters with those obtained from a nonparametric estimation (cf. Figure 3). The graphical approach of assessing the models is similar to the one proposed in Birr et al. (2018). For the sake of clarity, we focus on two classes of models: (a) vector autoregressive (VAR) models, and (b) vector versions of the quantile autoregressive (QVAR) model introduced by Koenker and Xiao (2006). Classical VAR as used by many applied researchers assumes the same autoregressive structure at all quantiles. To model asymmetry, one can employ more flexible copulas allowing for asymmetric dependence. In addition, QVAR allows a different autoregressive structure at different quantiles. Hence different quantiles can be driven by processes with different cyclical properties.

We discuss the models in order, from simple to more complex, and evaluate if the more complex models are better suited to capture the weekly, monthly, and yearly cycles of the quantile-related features that were discovered in the stock market returns analysis of Section 5.

We begin by fitting a VAR(1) to the stock market returns. The fitted model is

$$\begin{aligned} Y_{t,1} &= 0.0987 + 0.056 Y_{t-1,1} + 0.186 Y_{t-1,2} + \varepsilon_{t,1}, \\ Y_{t,2} &= 0.0369 - 0.056 Y_{t-1,1} + 0.175 Y_{t-1,2} + \varepsilon_{t,2}, \end{aligned} \tag{6.1}$$

where $(\varepsilon_{t,1}, \varepsilon_{t,2})$ is white noise with an estimated $\mathrm{Corr}(\varepsilon_{t,1}, \varepsilon_{t,2}) \approx 0.822$. Adding the common assumption that the $(\varepsilon_{t,1}, \varepsilon_{t,2})$ are independent and jointly Gaussian, the corresponding quantile coherencies can be determined. The quantile coherencies implied by the model (6.1) are depicted in the top row of Figure 5. For easier comparison, we consider the same combinations of frequencies and quantile levels as in Figure 3. In the picture it is clearly visible that dependencies of cycles implied by this Gaussian model are symmetric. For example, the dependences at the 0.05|0.05 and at the 0.95|0.95 level are equally strong for all frequencies. In contrast, the nonparametric estimate obtained from the data (cf. Figure 3) shows strong asymmetry. Further, we can see that for the weekly, monthly, and yearly frequencies, which might be of particular interest for applied researchers, the dependencies at the $\tau|\tau$ and at the $1-\tau|1-\tau$ level coincide as well. If an applied researcher seeks to model dependencies as the ones revealed in Section 5, the Gaussian VAR model might therefore be too restrictive.

Next, we consider non-Gaussian versions of the fitted VAR. To obtain these models, note that the innovations in (6.1) are assumed to be white noise, but are not required to be i.i.d. Gaussian. Another plausible model is therefore obtained by specifying any joint distribution for $(\varepsilon_{t,1}, \varepsilon_{t,2})$ that has first and second moments as implied by the fitted VAR model. For illustration, we now consider the following two cases. In both cases, we assume the marginal distributions to

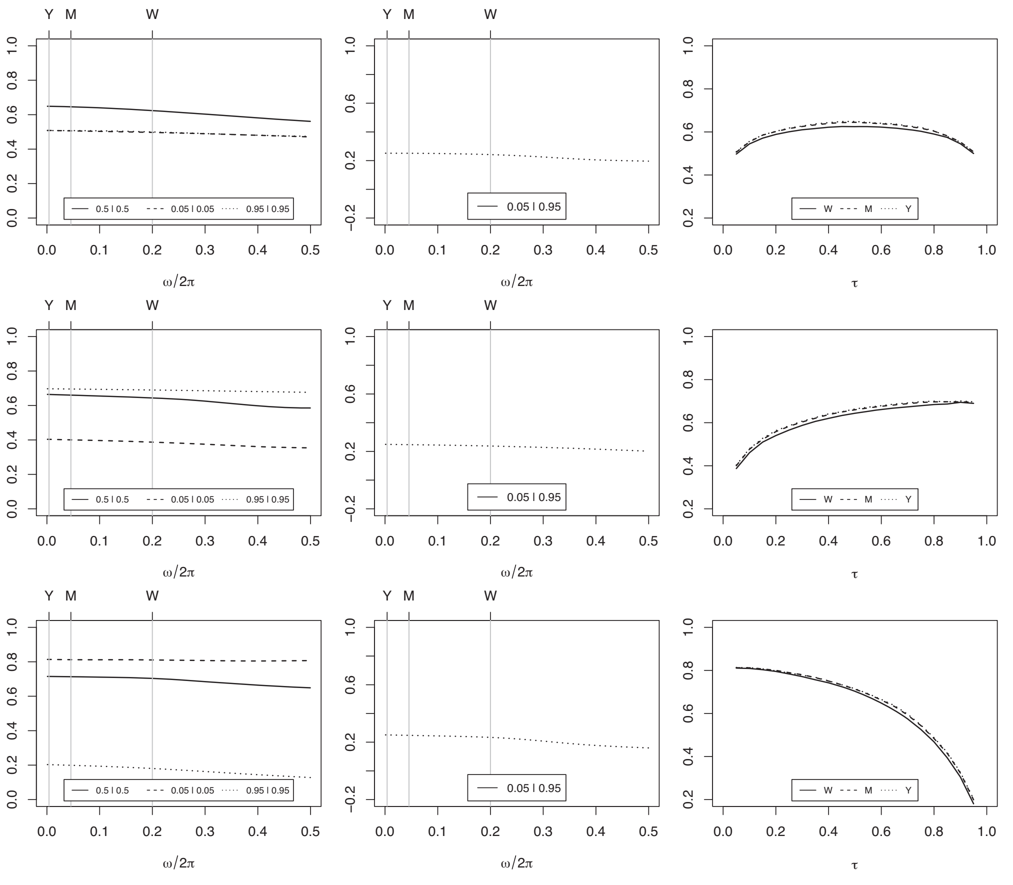

Figure 5. Quantile coherency simulated from the VAR models.

be standard normal. In the first case, we assume that the dependence is according to a Clayton copula with parameter $\theta = 4$. In the second case, we assume that it is according to a Gumbel copula with parameter $\theta = 2.7$. As one might expect, the dependence in the tails of the VAR(1) process is now remarkably different. As can be seen from the middle-left plot in Figure 5, for the case of the Clayton copula there is stronger dependence in the lower tail (0.05|0.05) and weaker dependence in the upper tail (0.95|0.95). The dependence is slightly stronger for low frequencies, which is expected from the temporal dependence in the VAR model. In the bottom-left plot of Figure 5, on the other hand, we see stronger dependence in the upper and weaker dependence in the lower tail. Interestingly, as can be seen from the centre plots, the dependence of cycles in changing from being below the 0.05-quantile in the first component to being below the 0.95-quantile in the second component does not depend much on the choice of the copula. Finally, in the right plots of Figure 5, we see how the dependence changes according to the quantile level when cycles at the weekly, monthly, and yearly frequencies, which we think might be most relevant to some practitioners, are considered. As expected, we see that for the case of the Clayton copula the dependence decreases as the quantile level τ increases, whereas for the case of the

Gumbel copula the dependence increases if τ increases. Although the models with the Gumbel and Clayton copula capture asymmetric dependence better than the one with the Gaussian copula, we can still see that they depart from the data in terms of quantile coherency.

In the discussion above we have seen three versions of a VAR(1) model, none of which was particularly well suited to capture the type of dependence of cycles at quantile level that we observed in Section 5. In the second part of our modelling exercise, we turn our attention to a more flexible class of time series models. Motivated by the quantile autoregression model that was introduced by Koenker and Xiao (2006), we consider quantile vector autoregression, QVAR, a VAR model with random coefficients:

$$Y_{t,j} = \theta_{j0}(U_{t,j}) + \theta_{j1}(U_{t,j})Y_{t-1,1} + \theta_{j2}(U_{t,j})Y_{t-1,2}, \quad j = 1, 2, \tag{6.2}$$

where the θ_{ji} are coefficient functions and the $U_{t,j}$ are assumed to be independent and uniformly distributed on [0, 1]. Zhu et al. (2018) discuss a model similar to (6.2). Our aim here is to assess whether the time series model (6.2) is flexible enough to capture the cyclical features in quantiles that were identified in Section 5. To this end, we choose the parameter functions in a data-driven way and then simulate the corresponding quantile coherency to compare with the nonparameteric estimate. Motivated by the estimation method in Zhu et al. (2018), we compute

$$\hat{\theta}(\tau) = \arg\min_{\theta(\tau)} \sum_{j=1}^{2} \sum_{t=2}^{n} \rho_\tau\big(Y_{t,j} - \theta_{j0}(\tau) - \theta_{j1}(\tau)Y_{t-1,1} - \theta_{j2}(\tau)Y_{t-1,2}\big), \tag{6.3}$$

$\tau \in \mathcal{T} := \{1/50, 2/50, \ldots, 48/50, 49/50\}$, where $\rho_\tau(u) := u(\tau - I\{u < \tau\})$ is the check function; cf. Koenker (2005). For $\tau \notin \mathcal{T}$ we define $\hat{\theta}(\tau) := \hat{\theta}(\eta)$, $\eta := \arg\min_{\eta \in \mathcal{T}} |\tau - \eta|$ (choose the smaller η if there are two). The functions $\hat{\theta}(\tau) = (\hat{\theta}_{ji}(\tau))$, obtained from the stock market returns, are shown in Figure 7. It is interesting to observe that the functions $\hat{\theta}_{j1}$ and $\hat{\theta}_{j2}$ are not constant across quantile levels. This possibly indicates that a VAR model is too simple to capture the complicated dynamics present in the stock market returns. The 'shock' at time t to the jth equation is delivered by $\hat{\theta}_{j0}(U_{tj})$.

Koenker and Xiao (2006) and Zhu et al. (2018) established conditions that ensure that quantile regressions, similar to (6.3), can be used to consistently estimate the parameter functions of the models in their papers. In particular, their model-defining equations [corresponding to (6.2) in our model] are assumed to be monotonically increasing in $U_{t,j}$. The monotonicity condition further implies a particularly convenient form for the conditional quantile function of $Y_{t,j}$ given $Y_{t-1,1}$, $Y_{t-1,2}$. Fan and Fan (2006) argue that the quantile regression estimate considered by Koenker and Xiao (2006) will be a consistent estimate for the argument of the minimum of a population version of the loss function, under some mild conditions. For $\hat{\theta}(\tau)$, defined in (6.3), this corresponds to being a consistent estimator for

$$\theta^*(\tau) = \arg\min_{\theta(\tau)} \sum_{j=1}^{2} \mathbb{E}\rho_\tau\big(Y_{t,j} - \theta_{j0}(\tau) - \theta_{j1}(\tau)Y_{t-1,1} - \theta_{j2}(\tau)Y_{t-1,2}\big).$$

Fan and Fan (2006) point out that additional conditions, such as the monotonicity condition, are necessary for $\theta^*(\tau)$ and $\theta(\tau)$ to coincide. These important arguments have to be taken into account when interpreting $\hat{\theta}(\tau)$ as an estimator for $\theta(\tau)$. Of course, data can always be generated according to equation (6.2), where we substitute $\hat{\theta}(\tau)$ for $\theta(\tau)$. To assess whether the class of QVAR models is rich enough to reflect cyclical features in the quantiles as we have seen in the data in Section 5, it is sufficient to consider individual models from the class. For the purpose of

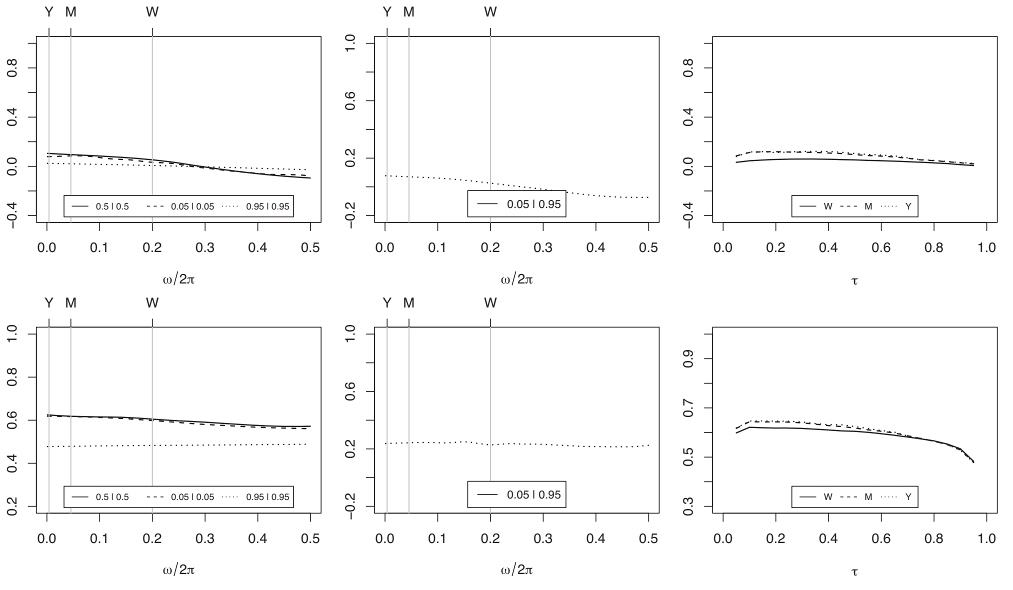

Figure 6. Quantile coherency simulated from several QVAR models.

this section, we select a QVAR model of the kind defined in (6.2), in a data-driven way, to then compare the implied quantile coherency with the one estimated nonparametrically in Section 5.

In the top row of Figure 6, the quantile coherencies associated with model (6.2), where $\hat{\theta}(\tau)$ was substituted for $\theta(\tau)$, are shown. The plots are of the same format as those we considered before. Strikingly, we observe that the quantile coherency of the fitted model is substantially lower than what we see via the nonparametric estimate in Figure 3. Besides this, in the top row of Figure 6, we see that the general shape, decreasing lines with frequency, and ordering (0.95|0.95 shows less dependence than 0.05|0.05) resembles the nonparametric estimate more closely.

Finally, we propose to extend the QVAR(1) stated in (6.2), by adding spatial dependence. More precisely, the model we now consider is

$$\begin{aligned} Y_{t,1} &= \theta_{10}(U_{t,1}) + \theta_{111}(U_{t,1})Y_{t-1,1} + \theta_{121}(U_{t,1})Y_{t-1,2}, \\ Y_{t,2} &= \theta_{20}(U_{t,2}) + \theta_{211}(U_{t,2})Y_{t-1,1} + \theta_{221}(U_{t,2})Y_{t-1,2} + \theta_{210}(U_{t,2})Y_{t,1}. \end{aligned} \tag{6.4}$$

For this model, we compute quantile regression estimates

$$\begin{aligned} \hat{\theta}(\tau) = \arg\min_{\theta(\tau)} \Big(&\sum_{t=2}^{n} \rho_\tau\big(Y_{t,1} - \theta_{10}(\tau) - \theta_{111}(\tau)Y_{t-1,1} - \theta_{121}(\tau)Y_{t-1,2}\big) \\ &+ \sum_{t=2}^{n} \rho_\tau\big(Y_{t,2} - \theta_{20}(\tau) - \theta_{210}(\tau)Y_{t,1} - \theta_{211}(\tau)Y_{t-1,1} - \theta_{221}(\tau)Y_{t-1,2}\big)\Big). \end{aligned}$$

The estimates obtained from the stock returns data, which also should be cautiously interpreted, are depicted in Figure 8. Note that, if we substitute $Y_{1,t}$ in the second equation of (6.4) by the expression given in the first equation, then we see that the 'shocks' in this model are now dependent, as they

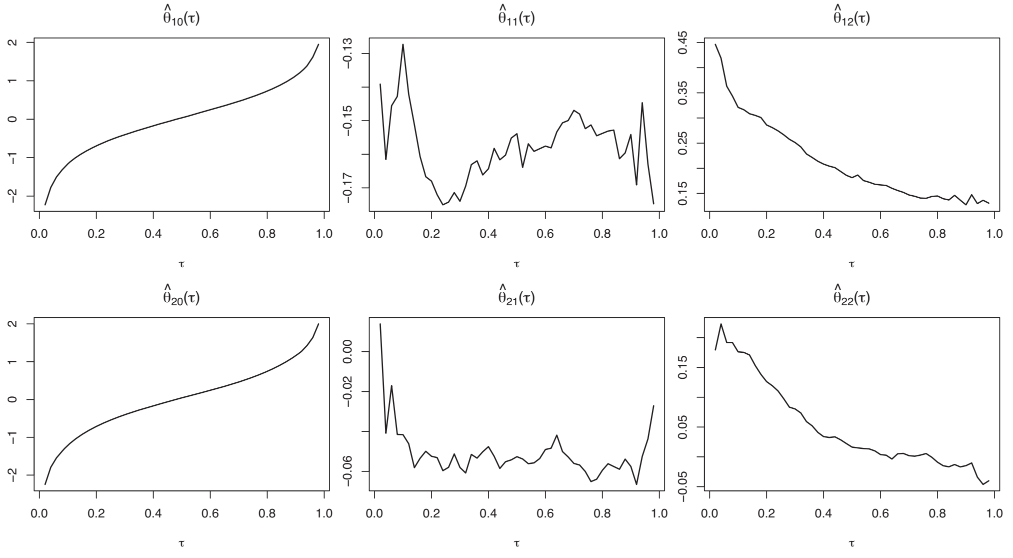

Figure 7. Estimated parameter functions for model (6.2).

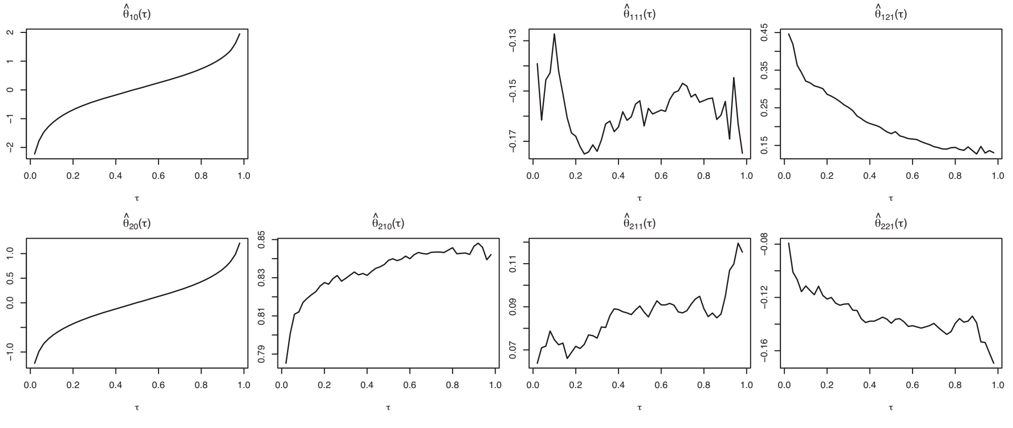

Figure 8. Parameter functions for model (6.4).

are of the form $(\hat{\theta}_{10}(U_{t,1}), \hat{\theta}_{20}(U_{t,2}) + \hat{\theta}_{210}(U_{t,2})\hat{\theta}_{10}(U_{t,1}))$. The parameter function $\hat{\theta}_{210}$ moderates the strength of dependence. We now look again at the quantile coherency, depicted in the bottom row of Figure 6, and see that the quantile coherencies resemble the nonparameter estimates more closely (in shape, order and magnitude). This is true in particular for the right plot, where the frequencies corresponding to the weekly, monthly, and yearly cycles are shown, which could be especially interesting for applied researchers.

In this section we have illustrated how quantile coherency can be used by applied researchers to assess time series models regarding their capabilities to capture dependence between general cycles of stock market returns. We have seen that Gaussian VAR models are completely incapable of capturing asymmetries in the dependence of cycles. Our modelling exercise showed how non-Gaussian VAR models can possibly remedy this by allowing more general copulas for the errors in the model. Going further, we have also inspected bivariate quantile autoregression models and seen that their flexibility does better in capturing the general dependence between cycles that we have discovered using quantile coherency in Section 5.

7. CONCLUSION

In this paper we introduced quantile cross-spectral analysis of economic time series, providing an entirely model-free, nonparametric theory for the estimation of general cross-dependence structures emerging from quantiles of the joint distribution in the frequency domain. We argue that complex dynamics in time series often arise naturally in many macroeconomic and financial time series, as infrequent periods of large negative values (lower quantiles of the joint distribution) may be more dependent than infrequent periods of large positive values (upper quantiles of the joint distribution). Moreover, the dependence may differ in the long-, medium-, or short-run. Quantile cross-spectral analysis hence may fundamentally change the way we view the dependence between economic time series, and may be viewed as a precursor to the subsequent developments in economic research underlying many new modelling strategies.

While connecting two branches of the literature that focus on the dependence between variables in quantiles of their joint distribution and across frequencies separately, the proposed methods may be viewed as an important step in robustifying the traditional cross-spectral analysis as well. Quantile-based spectral quantities are very attractive as they do not require the existence of moments, an important relaxation of the classical assumptions, where moments up to the order of the cumulants involved are typically assumed to exist. The proposed quantities are robust to many common violations of traditional assumptions found in data, including outliers, heavy tails, and changes in higher moments of the distribution. By considering quantiles instead of moments, the proposed methods are able to reveal the dependence that remained invisible to the traditional toolsets. As an essential ingredient for successful applications, we have provided a rigorous analysis of the asymptotic properties of the introduced estimators and shown that for a general class of nonlinear processes, properly centred and smoothed versions of the quantile-based estimators converge to centred Gaussian processes.

In an empirical application, we have shown that classical asset pricing theories may not suit the data well, as commonly documented by researchers, because rich dependence structures exist varying across quantiles and frequencies in the joint distribution of returns. We document strong dependence of the bivariate returns series in periods of large negative returns, while positive returns display less dependence over all frequencies. This result is not favourable for an investor, as exactly the opposite would be desired: choosing to invest in stocks with independent negative returns, but dependent positive returns. Our tool reveals that systematic risk originates more strongly from lower quantiles of the joint distribution in the long-, and medium-run investment horizons in comparison to the upper quantiles. In a modelling exercise, we have illustrated how quantile coherency can be employed in the inspection of time series models and might help to find a model that is capable of capturing the dependencies of cycles of quantile-related features that we had previously revealed in our empirical application.

We believe that our work might open up many exciting new routes for future theoretical as well as empirical research. From the perspective of applications, exploratory analysis based on the quantile cross-spectral estimators can reveal new implications for the improvement or even restating of many economic problems. Dependence in many economic time series is of a non-Gaussian nature, calling for an escape from covariance-based methods and allowing for a detailed analysis of the dependence in the quantiles of the joint distribution.

ACKNOWLEDGEMENTS

Authors are listed in alphabetical order, as they have contributed equally to the project. The authors are grateful to Piotr Fryzlewicz, Roger Koenker, Oliver Linton, Stanislav Volgushev, and participants in various seminars and conferences for their comments. In particular, we would like to thank the editor Dennis Kristensen and two anonymous referees, whose reports helped to improve the paper.

Jozef Baruník gratefully acknowledges support from the Czech Science Foundation under the GA16-14179S project. Tobias Kley is grateful for being partially supported by the EPSRC fellowship 'New challenges in time series analysis' (EP/L014246/1) and by the Collaborative Research Center 'Statistical modelling of non-linear dynamic processes' (SFB 823, Teilprojekt C1) of the German Research Foundation (DFG).

For estimation and inference of the quantile cross-spectral measures introduced in this paper, the `R` package `quantspec` is provided; cf. Kley (2016). The `R` package is available on https://cran.r-project.org/web/packages/quantspec/index.html

REFERENCES

Adrian, T. and M. K. Brunnermeier (2016). CoVaR. *American Economic Review 106*, 1705–41.

Ang, A. and J. Chen (2002). Asymmetric correlations of equity portfolios. *Journal of Financial Economics 63*, 443–94.

Bae, K.-H., G. A. Karolyi and R. M. Stulz (2003). A new approach to measuring financial contagion. *Review of Financial Studies 16*, 717–63.

Barigozzi, M., C. Brownlees, G. M. Gallo and D. Veredas (2014). Disentangling systematic and idiosyncratic dynamics in panels of volatility measures. *Journal of Econometrics 182*, 364–84.

Beaudry, P. and G. Koop (1993). Do recessions permanently change output? *Journal of Monetary Economics 31*, 149–63.

Birr, S., T. Kley and S. Volgushev (2018). Model assessment for time series dynamics using copula spectral densities: A graphical tool. ArXiv e-prints (arxiv:1804.01440).

Birr, S., S. Volgushev, T. Kley, H. Dette and M. Hallin (2017). Quantile spectral analysis for locally stationary time series. *Journal of the Royal Statistical Society: Series B (Statistical Methodology) 79*, 1619–43.

Bollerslev, T. (1986). Generalized autoregressive conditional heteroskedasticity. *Journal of Econometrics 31*, 307–27.

Croux, C., M. Forni and L. Reichlin (2001). A measure of comovement for economic variables: Theory and empirics. *Review of Economics and Statistics 83*, 232–41.

Davis, R. A. and T. Mikosch (2009). The extremogram: A correlogram for extreme events. *Bernoulli 15*, 977–1009.

Dette, H., M. Hallin, T. Kley and S. Volgushev (2015). Of copulas, quantiles, ranks and spectra: An L_1-approach to spectral analysis. *Bernoulli 21*, 781–831.

Enders, W. and C. W. J. Granger (1998). Unit-root tests and asymmetric adjustment with an example using the term structure of interest rates. *Journal of Business and Economic Statistics 16*, 304–11.

Engle, R. F. and S. Manganelli (2004). CAViaR: Conditional autoregressive value at risk by regression quantiles. *Journal of Business and Economic Statistics 22*, 367–81.

Erb, C. B., C. R. Harvey and T. E. Viskanta (1994). Forecasting international equity correlations. *Financial Analysts Journal 50*, 32–45.

Fan, J. and Y. Fan (2006). Comment. *Journal of the American Statistical Association 101*, 991–4.

Fan, Y. and A. J. Patton (2014). Copulas in econometrics. *Annual Review of Economics 6*, 179–200.

Granger, C. W. (2010). Some thoughts on the development of cointegration. *Journal of Econometrics 158*, 3–6.

Granger, C. W. and P. Newbold (1974). Spurious regressions in econometrics. *Journal of Econometrics 2*, 111–20.

Granger, C. W., T. Teräsvirta and A. J. Patton (2006). Common factors in conditional distributions for bivariate time series. *Journal of Econometrics 132*, 43–57.

Granger, C. W. J. (1966). The typical spectral shape of an economic variable. *Econometrica 34*, 150–61.

Granger, C. W. J. (1969). Investigating causal relations by econometric models and cross-spectral methods. *Econometrica 37*, 424–38.

Hagemann, A. (2013). *Robust spectral analysis*.ArXiv e-prints (arxiv:1111.1965v2).

Han, H., O. Linton, T. Oka and Y.-J. Whang (2014). *quantilogram: Quantilogramg*. R package version 0.1, retrieved from https://sites.google.com/site/whangyjhomepage/Rcodes_CrossQuantilogram.zip on 11 Dec. 2018.

Han, H., O. Linton, T. Oka and Y.-J. Whang (2016). The cross-quantilogram: Measuring quantile dependence and testing directional predictability between time series. *Journal of Econometrics 193*, 251–70.

Hong, Y. (1999). Hypothesis testing in time series via the empirical characteristic function: A generalized spectral density approach. *Journal of the American Statistical Association 94*, 1201–20.

Hong, Y. (2000). Generalized spectral tests for serial dependence. *Journal of the Royal Statistical Society: Series B 62*, 557–74.

Kley, T. (2016). Quantile-based spectral analysis in an object-oriented framework and a reference implementation in R: The quantspec package (arxiv:1408.6755), *Journal of Statistical Software 70*, 1–27.

Kley, T., S. Volgushev, H. Dette and M. Hallin (2016). Quantile spectral processes: Asymptotic analysis and inference. *Bernoulli 22*, 1770–807.

Koenker, R. (2005). *Quantile Regression*. Econometric Society Monographs. Cambridge University Press, Cambridge.

Koenker, R. and Z. Xiao (2006). Quantile autoregression. *Journal of the American Statistical Association 101*, 980–90.

Lee, J. and S. S. Rao (2012). The quantile spectral density and comparison based tests for nonlinear time series(arxiv:1112.2759v2). *ArXiv e-prints*.

Li, G., Y. Li and C.-L. Tsai (2015). Quantile correlations and quantile autoregressive modeling. *Journal of the American Statistical Association 110*, 246–61.

Li, T.-H. (2008). Laplace periodogram for time series analysis. *Journal of the American Statistical Association 103*, 757–68.

Li, T.-H. (2012). Quantile periodograms. *Journal of the American Statistical Association 107*, 765–76.

Li, T.-H. (2014). Quantile periodogram and time-dependent variance. *Journal of Time Series Analysis 35*, 322–40.

Lintner, J. (1965). The valuation of risk assets and the selection of risky investments in stock portfolios and capital budgets. *The Review of Economics and Statistics*, 13–37.

Linton, O. and Y.-J. Whang (2007). The quantilogram: With an application to evaluating directional predictability. *Journal of Econometrics 141*, 250–82.

Longin, F. and B. Solnik (2001). Extreme correlation of international equity markets. *Journal of Finance*, 649–76.

Mikosch, T. and Y. Zhao (2014). A Fourier analysis of extreme events. *Bernoulli 20*, 803–45.

Mikosch, T. and Y. Zhao (2015). The integrated periodogram of a dependent extremal event sequence. *Stochastic Processes and their Applications 125*, 3126–69.

Neftci, S. N. (1984). Are economic time series asymmetric over the business cycle? *The Journal of Political Economy*, 307–28.

Ning, C. Q. and L. Chollete (2009). The dependence structure of macroeconomic variables in the US. http://www1.uis.no/ansatt/odegaard/uis_wps_econ_fin/uis_wps_2009_31_chollete_ning.pdf. Technical report.

Patton, A. J. (2012). A review of copula models for economic time series. *Journal of Multivariate Analysis 110*, 4–18.

Schmitt, T. A., R. Schäfer, H. Dette and T. Guhr (2015). Quantile correlations: Uncovering temporal dependencies in financial time series. *Journal of Theoretical and Applied Finance 18*, 16.

Shao, X. and J. Zhang (2014). Martingale difference correlation and its use in high-dimensional variable screening. *Journal of the American Statistical Association 109*, 1302–18.

Sharpe, W. F. (1964). Capital asset prices: A theory of market equilibrium under conditions of risk. *The Journal of Finance 19*, 425–42.

Székely, G. J., M. L. Rizzo and N. K. Bakirov (2007). Measuring and testing dependence by correlation of distances. *Ann. Statist. 35*, 2769–94.

van der Vaart, A. and J. Wellner (1996). *Weak Convergence and Empirical Processes: With Applications to Statistics*. New York: Springer.

White, H., T.-H. Kim and S. Manganelli (2015). VAR for VaR: Measuring tail dependence using multivariate regression quantiles. *Journal of Econometrics 187*, 169–88.

Xiao, Z. (2009). Quantile cointegrating regression. *Journal of Econometrics 150*, 248–60.

Zhou, Z. (2012). Measuring nonlinear dependence in time-series, a distance correlation approach. *Journal of Time Series Analysis 33*, 438–57.

Zhu, X., W. Wang, H. Wang and W. K. Härdle (2018). Network quantile autoregression. Available at SSRN: https://ssrn.com/abstract=3159671or http://dx.doi.org/10.2139/ssrn.3159671.

Žikeš, F. and J. Baruník (2016). Semi-parametric conditional quantile models for financial returns and realized volatility. *Journal of Financial Econometrics 14*, 185–226.

SUPPORTING INFORMATION

Additional Supporting Information may be found in the online version of this article at the publisher's website:

ONLINE SUPPLEMENT
REPLICATION PACKAGE

Co-editor Dennis Kristensen handled this manuscript.

ONLINE SUPPLEMENT: 'QUANTILE COHERENCY: A GENERAL MEASURE FOR DEPENDENCE BETWEEN CYCLICAL ECONOMIC VARIABLES'

S1. FURTHER QUANTITIES RELATED TO THE QUANTILE CROSS-SPECTRAL DENSITY KERNEL

In the situation described in this paper, there exists a right continuous orthogonal increment process $\{Z_j^\tau(\omega) : -\pi \le \omega \le \pi\}$, for every $j \in \{1, \ldots, d\}$ and $\tau \in [0, 1]$, such that the Cramér representation

$$I\{X_{t,j} \le q_j(\tau)\} = \int_{-\pi}^{\pi} \mathrm{e}^{\mathrm{i}t\omega} \mathrm{d}Z_j^\tau(\omega)$$

holds [cf., e. g., Theorem 1.2.15 in Taniguchi and Kakizawa (2000)]. Note the fact that $(X_{t,j})_{t\in\mathbb{Z}}$ is strictly stationary and therefore $(I\{X_{t,j} \le q_j(\tau)\})_{t\in\mathbb{Z}}$ is second-order stationary, as the boundedness of the indicator functions implies existence of their second moments.

The quantile cross-spectral density kernels are closely related to these orthogonal increment processes [cf. Brillinger (1975), p. 101 and Brockwell and Davis (1987), p. 436)]. More specifically, for $-\pi \le \omega_1 \le \omega_2 \le \pi$, the following relation holds:

$$\int_{\omega_1}^{\omega_2} \mathfrak{f}^{j_1,j_2}(\omega; \tau_1, \tau_2)\mathrm{d}\omega = \operatorname{Cov}\left(Z_{j_1}^{\tau_1}(\omega_2) - Z_{j_1}^{\tau_1}(\omega_1), Z_{j_2}^{\tau_2}(\omega_2) - Z_{j_2}^{\tau_2}(\omega_1)\right),$$

or shortly: $\mathfrak{f}^{j_1,j_2}(\omega; \tau_1, \tau_2) = \operatorname{Cov}(\mathrm{d}Z_{j_1}^{\tau_1}(\omega), \mathrm{d}Z_{j_2}^{\tau_2}(\omega))$. It is important to observe that $\mathfrak{f}^{j_1,j_2}(\omega; \tau_1, \tau_2)$ is complex-valued. One way to represent $\mathfrak{f}^{j_1,j_2}(\omega; \tau_1, \tau_2)$ is to decompose it into its real and imaginary parts. The real part is known as the cospectrum [of the processes $(I\{X_{t,j_1} \le q_{j_1}(\tau_1)\})_{t\in\mathbb{Z}}$ and $(I\{X_{t,j_2} \le q_{j_2}(\tau_2)\})_{t\in\mathbb{Z}}$]. The negative of the imaginary part is commonly referred to as the quadrature spectrum. We will refer to these quantities as the quantile cospectrum and quantile quadrature spectrum of $(X_{t,j_1})_{t\in\mathbb{Z}}$ and $(X_{t,j_2})_{t\in\mathbb{Z}}$. Occasionally, to emphasize that these spectra are functions of (τ_1, τ_2), we will refer to them as the quantile cospectrum kernel and quantile quadrature spectrum kernel, respectively. The quantile quadrature spectrum vanishes if $j_1 = j_2$ and $\tau_1 = \tau_2$. More generally, as described in Kley et al. (2016), for any fixed j_1, j_2, the quadrature spectrum will vanish, for all τ_1, τ_2, if and only if (X_{t-k,j_1}, X_{t,j_2}) and (X_{t+k,j_1}, X_{t,j_2}) possess the same copula, for all k.

An alternative way to look at $\mathfrak{f}^{j_1,j_2}(\omega; \tau_1, \tau_2)$ is by representing it in polar coordinates. The radius $|\mathfrak{f}^{j_1,j_2}(\omega; \tau_1, \tau_2)|$ is then referred to as the amplitude spectrum [of the two processes $(I\{X_{t,j_1} \le q_{j_1}(\tau_1)\})_{t\in\mathbb{Z}}$ and $(I\{X_{t,j_2} \le q_{j_2}(\tau_2)\})_{t\in\mathbb{Z}}$], while the angle $\arg(\mathfrak{f}^{j_1,j_2}(\omega; \tau_1, \tau_2))$ is the so-called phase spectrum. We refer to these quantities as the quantile amplitude spectrum and the quantile phase spectrum of $(X_{t,j_1})_{t\in\mathbb{Z}}$ and $(X_{t,j_2})_{t\in\mathbb{Z}}$. We note that the quantile spectral distribution function $\int_0^\omega \mathfrak{f}^{j_1,j_2}(\lambda; \tau_1, \tau_2))\mathrm{d}\lambda$ is clearly another way to represent the quantile-based dependence in the frequency domain. Its properties and estimation procedures are currently investigated in a separate research project and therefore are not further discussed here.

Note that quantile coherency $\mathfrak{R}^{j_1,j_2}(\omega; \tau_1, \tau_2)$, which we defined in Section 2 as a measure for the dynamic dependence of the two processes $(X_{t,j_1})_{t\in\mathbb{Z}}$ and $(X_{t,j_2})_{t\in\mathbb{Z}}$, is the correlation between $\mathrm{d}Z_{j_1}^{\tau_1}(\omega)$ and $\mathrm{d}Z_{j_2}^{\tau_2}(\omega)$. Its modulus squared $|\mathfrak{R}^{j_1,j_2}(\omega; \tau_1, \tau_2)|^2$ is referred to as the quantile coherence kernel of $(X_{t,j_1})_{t\in\mathbb{Z}}$ and $(X_{t,j_2})_{t\in\mathbb{Z}}$. A value of $|\mathfrak{R}^{j_1,j_2}(\omega; \tau_1, \tau_2)|$ close to 1 indicates a strong (linear) relationship between $\mathrm{d}Z_{j_1}^{\tau_1}(\omega)$ and $\mathrm{d}Z_{j_2}^{\tau_2}(\omega)$.

For the readers' convenience, a list of the quantities and symbols introduced in this section is provided in Table S.1.

Table S.1. Spectral quantities related to $\mathfrak{f}^{j_1,j_2}(\omega;\tau_1,\tau_2)$.

Name	Symbol
Quantile cospectrum of $(X_{t,j_1})_{t\in\mathbb{Z}}$ and $(X_{t,j_2})_{t\in\mathbb{Z}}$	$\Re\mathfrak{f}^{j_1,j_2}(\omega;\tau_1,\tau_2)$
Quantile quadrature spectrum of $(X_{t,j_1})_{t\in\mathbb{Z}}$ and $(X_{t,j_2})_{t\in\mathbb{Z}}$	$-\Im\mathfrak{f}^{j_1,j_2}(\omega;\tau_1,\tau_2)$
Quantile amplitude spectrum of $(X_{t,j_1})_{t\in\mathbb{Z}}$ and $(X_{t,j_2})_{t\in\mathbb{Z}}$	$\lvert\mathfrak{f}^{j_1,j_2}(\omega;\tau_1,\tau_2)\rvert$
Quantile phase spectrum of $(X_{t,j_1})_{t\in\mathbb{Z}}$ and $(X_{t,j_2})_{t\in\mathbb{Z}}$	$\arg(\mathfrak{f}^{j_1,j_2}(\omega;\tau_1,\tau_2))$
Quantile coherency of $(X_{t,j_1})_{t\in\mathbb{Z}}$ and $(X_{t,j_2})_{t\in\mathbb{Z}}$	$\mathfrak{R}^{j_1,j_2}(\omega;\tau_1,\tau_2)$
Quantile coherence of $(X_{t,j_1})_{t\in\mathbb{Z}}$ and $(X_{t,j_2})_{t\in\mathbb{Z}}$	$\lvert\mathfrak{R}^{j_1,j_2}(\omega;\tau_1,\tau_2)\rvert^2$

Note: The quantile cross-spectral density kernel $\mathfrak{f}^{j_1,j_2}(\omega;\tau_1,\tau_2)$ of $(X_{t,j_1})_{t\in\mathbb{Z}}$ and $(X_{t,j_2})_{t\in\mathbb{Z}}$ is defined in (2.2).

Estimators for the quantile cospectrum, quantile quadrature spectrum, quantile amplitude spectrum, quantile phase spectrum, and quantile coherence are then naturally given by $\Re\hat{G}_{n,R}^{j_1,j_2}(\omega;\tau_1,\tau_2)$, $-\Im\hat{G}_{n,R}^{j_1,j_2}(\omega;\tau_1,\tau_2)$, $|\hat{G}_{n,R}^{j_1,j_2}(\omega;\tau_1,\tau_2)|$, $\arg(\hat{G}_{n,R}^{j_1,j_2}(\omega;\tau_1,\tau_2))$, and $|\hat{\mathfrak{R}}_{n,R}^{j_1,j_2}(\omega;\tau_1,\tau_2)|^2$, respectively.

S2. AN EXAMPLE OF A PROCESS GENERATING QUANTILE DEPENDENCE ACROSS FREQUENCIES: QVAR(P)

For a better understanding of the dependence structures that we study in this paper, it is illustrative to introduce a process capable of generating them. We focus on generating dependence at different points of the joint distribution, which will vary across frequencies but stays hidden from classical measures. In other words, we illustrate the intuition of spuriously independent variables, a situation when two variables seem to be independent when traditional cross-spectral analysis is used, while they are indeed clearly dependent at different parts of their joint distribution.

We base our example on a multivariate generalization of the popular quantile autoregression process (QAR) introduced by Koenker and Xiao (2006). Inspired by vector autoregression processes (VAR), we link multiple QAR processes through their lag structure and refer to the resulting process as a quantile vector autoregression process (QVAR). This provides a natural way of generating a rich dependence structure between two random variables at points of their joint distribution and over different frequencies. The autocovariance function of a stationary QVAR(p) process is that of a fixed parameter VAR(p) process. This follows from the argument by Knight (2006), who concludes that the exclusive use of autocorrelations may thus 'fail to identify structure in the data that is potentially very informative'. We will show how quantile spectral analysis reveals what otherwise may remain invisible.

Let $\boldsymbol{X}_t = (X_{t,1},\ldots,X_{t,d})'$, $t\in\mathbb{Z}$, be a sequence of random vectors that fulfils

$$\boldsymbol{X}_t = \sum_{j=1}^{p} \boldsymbol{\Theta}^{(j)}(\boldsymbol{U}_t)\boldsymbol{X}_{t-j} + \boldsymbol{\theta}^{(0)}(\boldsymbol{U}_t), \tag{S.1}$$

where $\boldsymbol{\Theta}^{(1)},\ldots,\boldsymbol{\Theta}^{(p)}$ are $d\times d$ matrices of functions, $\boldsymbol{\theta}^{(0)}$ is a $d\times 1$ column vector of functions, and $\boldsymbol{U}_t = (U_{t,1},\ldots,U_{t,d})'$, $t\in\mathbb{Z}$, is a sequence of independent vectors, with components $U_{t,k}$ that are $\mathcal{U}[0,1]$-distributed. We will assume that the elements of the ℓth row $\boldsymbol{\theta}_\ell^{(j)}(u_\ell) = \big(\theta_{\ell,1}^{(j)}(u_\ell),\ldots,\theta_{\ell,d}^{(j)}(u_\ell)\big)$ of $\boldsymbol{\Theta}^{(j)}(u_1,\ldots,u_d) = \big(\boldsymbol{\theta}_1^{(j)}(u_1)',\ldots,\boldsymbol{\theta}_d^{(j)}(u_d)'\big)'$ and that the ℓth element $\theta_\ell^{(0)}(u_\ell)$ of $\boldsymbol{\theta}^{(0)} = \big(\theta_1^{(0)}(u_1),\ldots,\theta_d^{(0)}(u_d)\big)'$ depend only on the ℓth variable, respectively. Under this assumption we can rewrite (S.1) as

$$X_{t,i} = \sum_{j=1}^{p} \boldsymbol{\theta}_i^{(j)}(U_{t,i})\boldsymbol{X}_{t-j} + \theta_i^{(0)}(U_{t,i}), \quad i=1,\ldots,d. \tag{S.2}$$

If the right-hand side of (S.2) is monotonically increasing, then the conditional quantile function of $X_{t,i}$ given $(\boldsymbol{X}_{t-1}, \ldots, \boldsymbol{X}_{t-p})$ can be represented as

$$Q_{X_{t,i}}(\tau|\boldsymbol{X}_{t-1}, \ldots, \boldsymbol{X}_{t-p}) = \sum_{j=1}^{p} \boldsymbol{\theta}_i^{(j)}(\tau)\boldsymbol{X}_{t-j} + \theta_i^{(0)}(\tau).$$

Note that in this design the ℓth component of $\boldsymbol{U}_t$ determines the coefficients for the autoregression equation of the ℓth component of $\boldsymbol{X}_t$. We refer to the process as a quantile vector autoregression process of order p, hence QVAR(p). The class of processes (S.1) without assumptions regarding the parameters $\boldsymbol{\Theta}^{(j)}$ is naturally richer. Yet, the interpretation of the parameters in terms of the conditional quantile functions is possibly lost.

In the bivariate case ($d = 2$) of order $p = 1$, i.e., QVAR(1), (S.1) takes the following form:

$$\begin{pmatrix} X_{t,1} \\ X_{t,2} \end{pmatrix} = \begin{pmatrix} \theta_{11}^{(1)}(U_{t,1}) & \theta_{12}^{(1)}(U_{t,1}) \\ \theta_{21}^{(1)}(U_{t,2}) & \theta_{22}^{(1)}(U_{t,2}) \end{pmatrix} \begin{pmatrix} X_{t-1,1} \\ X_{t-1,2} \end{pmatrix} + \begin{pmatrix} \theta_1^{(0)}(U_{t,1}) \\ \theta_2^{(0)}(U_{t,2}) \end{pmatrix}.$$

For the examples we assume that the components $U_{t,1}$ and $U_{t,2}$ are independent and set the components of $\boldsymbol{\theta}^{(0)}$ to $\theta_1^{(0)}(u) = \theta_2^{(0)}(u) = \Phi^{-1}(u)$, $u \in [0, 1]$, where $\Phi^{-1}(u)$ denotes the u-quantile of the standard normal distribution. Further, we set the diagonal elements of of $\boldsymbol{\Theta}^{(1)}$ to zero (i. e., $\theta_{11}^{(1)}(u) = \theta_{22}^{(1)}(u) = 0$, $u \in [0, 1]$) and the off-diagonal elements to $\theta_{12}^{(1)}(u) = \theta_{21}^{(1)}(u) = 1.2(u - 0.5)$, $u \in [0, 1]$. We thus create cross-dependence by linking the two processes with each other through the other one's lagged contributions. Note that this particular choice of parameter functions leads to the existence of a unique, strictly stationary solution; cf. Bougerol and Picard (1992). $(X_{t,1})_{t\in\mathbb{Z}}$ and $(X_{t,2})_{t\in\mathbb{Z}}$ are uncorrelated. Note that Hafner and Linton (2006) discuss that univariate quantile autoregression nests the popular autoregressive conditional heteroskedasticity (ARCH) models in terms of second-order properties. Analogously, our QVAR(1) can be seen to nest a multivariate versions of ARCH.

In Figure S.1, the dynamics of the described QVAR(1) process are depicted. In terms of traditional coherency there appears to be no dependence across all frequencies. In terms of quantile coherency, on the other hand, rich dynamics are revealed in the different parts of the joint distribution. While, in the centre of the distribution (at the 0.5|0.5 level) the dependence is zero across frequencies, we see that the dependence increases if at least one of the quantile levels (τ_1, τ_2) is chosen closer to 0 or 1. More precisely, we see that the quantile coherency of this QVAR process resembles the shape of a VAR(1) process with coefficient matrix $\boldsymbol{\Theta}^{(1)}(\tau_1, \tau_2)$. The two processes are, for example when $\tau_1 = 0.05$ and $\tau_2 = 0.95$, clearly positively connected at lower frequencies with exactly the opposite value of quantile coherency at high frequencies, where the processes are in opposition. This also resembles the dynamics of the simple motivating examples from the introductory section of this paper, and highlights the importance of the quantile cross-spectral analysis as the dependence structure stays hidden if only the traditional measures are used.

In a second and third example, we consider a similar structure of parameters at the second and third lag. For the QVAR(2) process we let $\theta_{11}^{(j)}(u) = \theta_{22}^{(j)}(u) = 0$, for $j = 1, 2$, $\theta_{12}^{(1)}(u) = \theta_{21}^{(1)}(u) = 0$ and $\theta_{12}^{(2)}(u) = \theta_{21}^{(2)}(u) = 1.2(u - 0.5)$. In other words, here, the processes are connected through the second lag of the other one and, again, not directly through their own lagged contributions. In the QVAR(3) process, all coefficients are again set to zero, except for $\theta_{12}^{(3)}(u) = \theta_{21}^{(3)}(u) = 1.2(u - 0.5)$, such that the processes are connected only through the third lag of the other component and not through their own contributions.

In Figures S.2 and S.3, the dynamics of the described QVAR(2) and QVAR(3) processes are shown. Connecting the quantiles of the two processes through the second and third lag gives us richer dependence structures across frequencies. They, again, resemble the shape of the traditional coherencies of VAR(2) and VAR(3) processes. When traditional coherency is used for the QVAR(2) and QVAR(3) processes, the dependence structure stays completely hidden.

These examples of the general QVAR(p) specified in (S.1) served to show how rich dependence structures can be created across points of the joint distribution and different frequencies. It is obvious how more complicated structures for the coefficient functions would lead to even richer dynamics than in the examples shown.

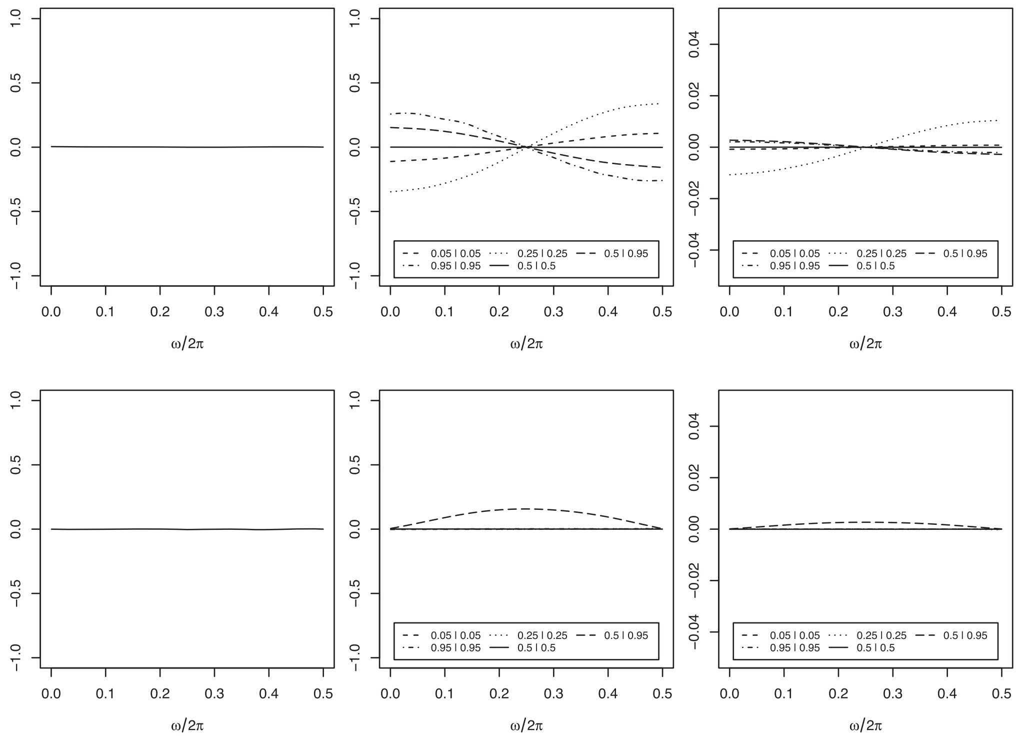

Figure S.1. Example of dependence structures generated by QVAR(1).

S3. RELATION BETWEEN QUANTILE AND TRADITIONAL SPECTRAL QUANTITIES IN THE CASE OF GAUSSIAN PROCESSES

When applying the proposed quantities, it is important to proceed with care when relating them to the traditional correlation and coherency measures. In this section we examine the case of a weakly stationary, multivariate process, where the proposed, quantile-based quantities and their traditional counterparts are directly related. The aim of the discussion is twofold. On the one hand it provides assistance in how to interpret the quantile spectral quantities when the model is known to be Gaussian. On the other hand, and more importantly, it provides additional insight into how the traditional quantities break down when the serial dependency structure is not completely specified by the second moments.

We start with a discussion of the general case, where the process under consideration is assumed to be stationary, but need not be Gaussian. We will state conditions under which the traditional spectra (i. e., the matrix of spectral densities and cross-spectral densities) uniquely determines the quantile spectra (i. e., the matrix of quantile spectral densities and cross-spectral densities). At the end of this section we will discuss three examples of bivariate, stationary Gaussian processes and explain how the traditional coherency and the quantile coherency are related.

Denote by $\boldsymbol{c} := \{c_k^{j_1,j_2} : j_1, j_2 \in \{1, \dots, d\}, k \in \mathbb{Z}\}$. $c_k^{j_1,j_2} := \mathrm{Cov}(X_{t+k,j_1}, X_{t,j_2})$, the family of auto- and cross-covariances. We will also refer to them as the second moment features of the process. We assume that $(|c_k^{j_1,j_2}|)_{k\in\mathbb{Z}}$ is summable, such that the traditional spectra $f^{j_1,j_2}(\omega) := (2\pi)^{-1} \sum_{k\in\mathbb{Z}} c_k^{j_1,j_2} \mathrm{e}^{-\mathrm{i}k\omega}$ exist. Because of the relation $c_k^{j_1,j_2} = \int_{-\pi}^{\pi} f^{j_1,j_2}(\omega)\mathrm{e}^{\mathrm{i}k\omega}\mathrm{d}\omega$ we will equivalently refer to $\boldsymbol{f}(\omega) := (f^{j_1,j_2}(\omega))_{j_1,j_2=1,\dots,d}$ as the second moment features of the process.

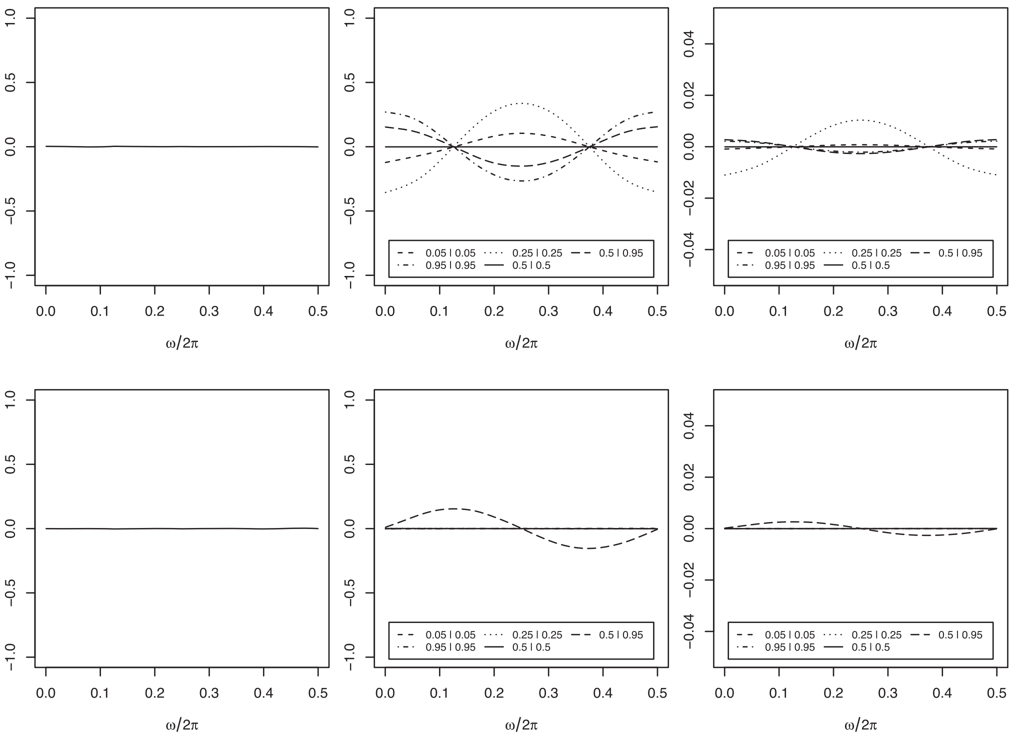

Figure S.2. Example of dependence structures generated by QVAR(2).

We now state conditions under which the traditional spectra uniquely determine the quantile spectra. Assume that the marginal distribution of $X_{t,j}$ ($j \in \{1, \ldots, d\}$), which we denote by F_j, does not depend on t and is continuous. Further, the joint distribution of $\big(F_{j_1}(X_{t+k,j_1}), F_{j_2}(X_{t,j_2})\big)$, $j_1, j_2 \in \{1, \ldots, d\}$, i. e., the copula of the pair (X_{t+k,j_1}, X_{t,j_2}), shall depend only on k, but not on t, and be uniquely specified by the second moment features of the process. More precisely, we assume the existence of functions $C_k^{j_1,j_2}$, such that

$$C_k^{j_1,j_2}\big(\tau_1, \tau_2; \boldsymbol{c}\big) = \mathbb{P}\big(F_{j_1}(X_{t+k,j_1}) \le \tau_1, F_{j_2}(X_{t,j_2}) \le \tau_2\big).$$

Obviously, $\mathfrak{f}^{j_1,j_2}(\omega; \tau_1, \tau_2)$ is then, if it exists, uniquely determined by $\boldsymbol{c}$ [note (2.2) and the fact that $\gamma_k^{j_1,j_2}(\tau_1, \tau_2) = C_k^{j_1,j_2}\big(\tau_1, \tau_2; \boldsymbol{c}\big) - \tau_1\tau_2$].

In the case of stationary Gaussian processes, the assumptions sufficient for the quantile spectra to be uniquely identified by the traditional spectra hold with

$$C_k^{j_1,j_2}\big(\tau_1, \tau_2; \boldsymbol{c}\big) := C^{\text{Gauss}}(\tau_1, \tau_2; c_k^{j_1,j_2}(c_0^{j_1,j_1} c_0^{j_2,j_2})^{-1/2}),$$

where we have denoted the Gaussian copula by $C^{\text{Gauss}}(\tau_1, \tau_2; \rho)$.

The converse can be stated under less restrictive conditions. If the marginal distributions are both known and both possess second moments, then the quantile spectra uniquely determine the traditional spectra.

Assume now the previously described situation in which the second moment features $\boldsymbol{f}$ uniquely determine the quantile spectra, which we denote by $\mathfrak{f}_{\boldsymbol{f}}^{j_1,j_2}(\omega; \tau_1, \tau_2)$ to stress the fact that it is determined by $\boldsymbol{f}$. Thus, the relation between the traditional spectra and the quantile spectra is 1-to-1. Denote the traditional coherency by $R^{j_1,j_2}(\omega) := f^{j_1,j_2}(\omega)/(f^{j_1,j_1}(\omega) f^{j_2,j_2}(\omega))^{1/2}$ and observe that it is also uniquely determined

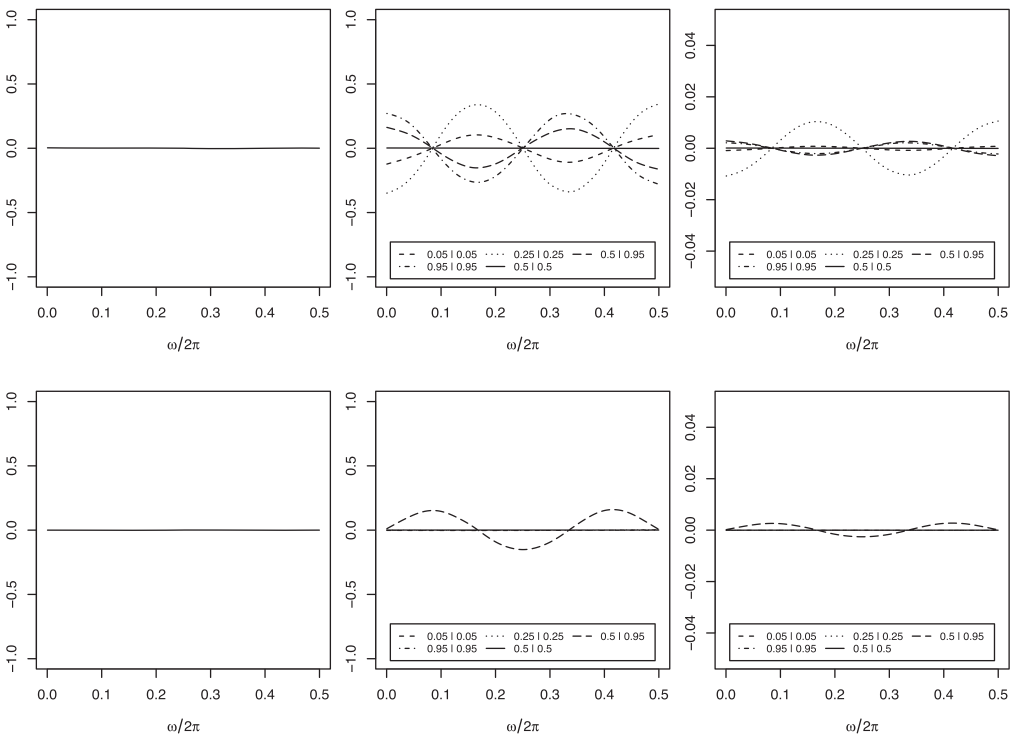

Figure S.3. Example of dependence structures generated by QVAR(3).

by the second moment features $\boldsymbol{f}$. Because the quantile coherency is determined by the quantile spectra, which is related to the second moment features $\boldsymbol{f}$, as previously explained, we have established the relation of the traditional coherency and the quantile coherency. Obviously, this relation is not necessarily 1-to-1 any more.

If the stationary process is from a parametric family of time series models, the second moment features can be determined for each parameter. We now discuss three examples of Gaussian processes. Each example will have a more complex serial dependence than the previous one. Without loss of generality we consider only bivariate examples. The first example is the one of non-degenerate Gaussian white noise. More precisely, we consider a Gaussian process $(X_{t,1}, X_{t,2})_{t\in\mathbb{Z}}$, where $\mathrm{Cov}(X_{t,i}, X_{s,j}) = 0$ and $\mathrm{Var}(X_{t,i}) > 0$, for all $t \neq s$ and $i, j \in \{1, 2\}$.

Observe that, owing to the independence of $(X_{t,1}, X_{t,2})$ and $(X_{s,1}, X_{s,2})$, $t \neq s$, we have $\gamma_k^{1,2}(\tau_1, \tau_2) = 0$ for all $k \neq 0$ and $\tau_1, \tau_2 \in [0, 1]$. It is easy to see that

$$\mathfrak{R}^{1,2}(\omega; \tau_1, \tau_2) = \frac{C^{\mathrm{Gauss}}(\tau_1, \tau_2; R^{1,2}(\omega)) - \tau_1\tau_2}{\sqrt{\tau_1(1-\tau_1)}\sqrt{\tau_2(1-\tau_2))}} \qquad \text{(S.3)}$$

where $R^{1,2}(\omega)$ denotes the traditional coherency, which in this case (a bivariate i. i. d. sequence) equals $c_0^{1,2}(c_0^{1,1}c_0^{2,2})^{-1/2}$ (for all ω).

By employing (S.3), we can thus determine the quantile coherency for any given traditional coherency and fixed combination of $\tau_1, \tau_2 \in (0, 1)$. In the top-centre part of Figure S.4 this conversion is visualized for four pairs of quantile levels and any possible traditional coherency. It is important to observe the limited

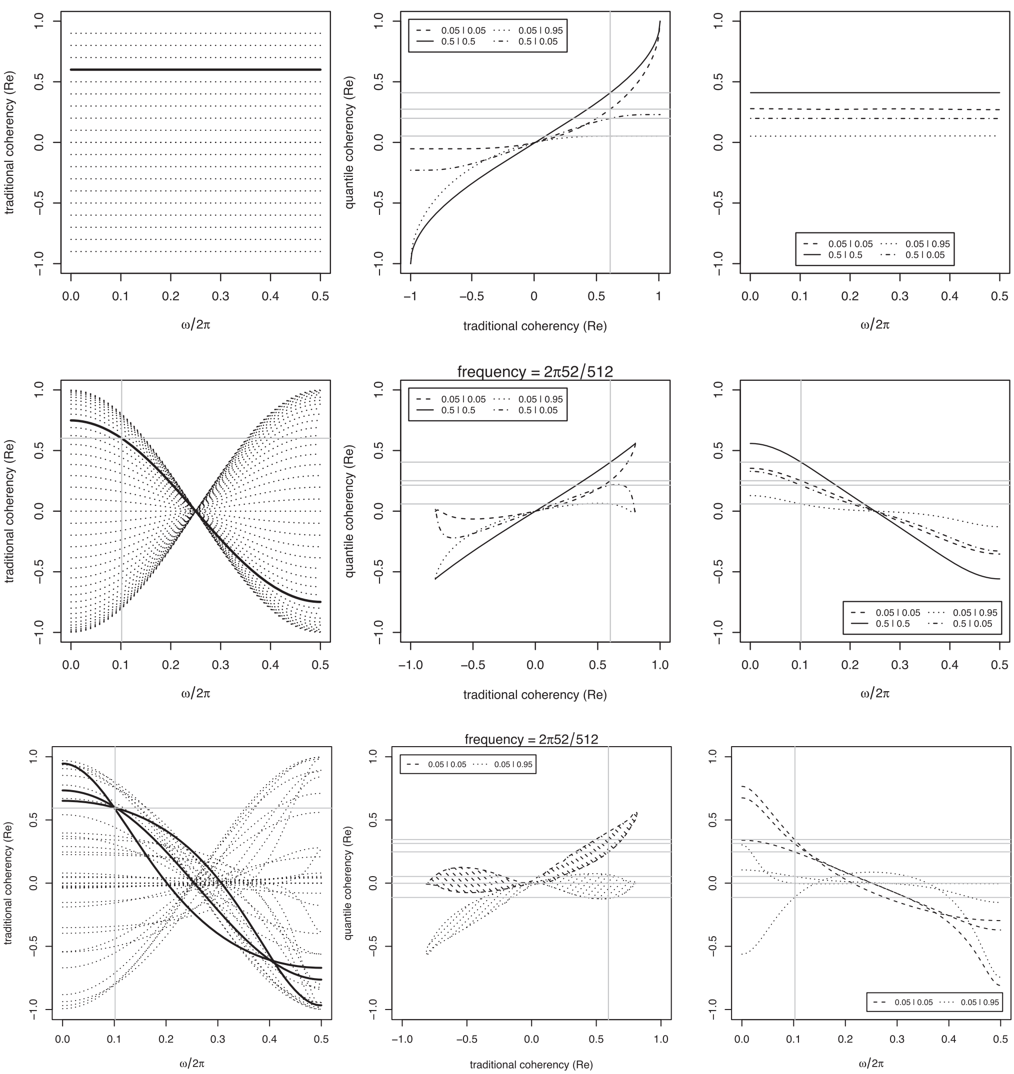

Figure S.4. Quantile and traditional coherency for selected Gaussian processes.

range of the quantile coherency. For example, there never is strong positive dependence between the τ_1-quantile in the first component and the τ_2-quantile in the second component when both τ_1 and τ_2 are close to 0. Similarly, there never is strong negative dependence when one of the quantile levels is chosen close to 0 while the other one is chosen close to 1. This observation is not special for the Gaussian case, but holds for any sequence of pairwise-independent bivariate random variables. Bounds that correspond to the case of perfect positive or perfect negative dependence (at the level of quantiles) can be derived from the Fréchet/Hoeffding bounds for copulas: in the case of serial independence, quantile coherency is bounded by

$$\frac{\max\{\tau_1+\tau_2-1,0\}-\tau_1\tau_2}{\sqrt{\tau_1(1-\tau_1)}\sqrt{\tau_2(1-\tau_2)}} \le \mathfrak{R}^{1,2}(\omega;\tau_1,\tau_2) \le \frac{\min\{\tau_1,\tau_2\}-\tau_1\tau_2}{\sqrt{\tau_1(1-\tau_1)}\sqrt{\tau_2(1-\tau_2)}}.$$

Note that these bounds hold for any joint distribution of $(X_{t,i}, X_{t,j})$. In particular, the bound holds independent of the correlation.

In the top-left part of Figure S.4 traditional coherencies are shown for this example. Because no serial dependence is present, all coherencies are flat lines. Their level is equal to the correlation between the two components. In the top-right part of Figure S.4 the quantile coherency for the example is shown when the correlation is 0.6 (the corresponding coherency is marked with a bold line in the top-left figure). Note that for fixed τ_1 and τ_2, the value of the quantile coherency corresponds to the value in the top-centre figure where the vertical grey line and the corresponding graph intersect. The quantile coherency in the right part does not depend on the frequency, because in this example there is no serial dependence.

In the top-centre part of Figure S.4 it is important to observe that for traditional coherency 0 [i. e., when the components are independent, owing to $(X_{t,1}, X_{t,2})$ being uncorrelated jointly Gaussian] quantile coherency is zero at all quantile levels.

In the next two examples we stay in the Gaussian framework, but introduce serial dependence. Consider a bivariate, stable VAR(1) process $\boldsymbol{X}_t = (X_{t,1}, X_{t,2})'$, $t \in \mathbb{Z}$, fulfilling the difference equation

$$\boldsymbol{X}_t = \boldsymbol{A}\boldsymbol{X}_{t-1} + \boldsymbol{\varepsilon}_t, \tag{S.4}$$

with parameter $\boldsymbol{A} \in \mathbb{R}^{2\times 2}$ and i. i. d., centred, bivariate, jointly normally distributed innovations $\boldsymbol{\varepsilon}_t$ with unit variance $\mathbb{E}(\boldsymbol{\varepsilon}_t\boldsymbol{\varepsilon}_t') = \boldsymbol{I}_2$.

In our second example, serial dependence is introduced by relating each component to the lagged other component in the regression equation. In other words, we consider model (S.4) where the matrix $\boldsymbol{A}$ has diagonal elements equal to 0 and some value a on the off-diagonal. Assuming $|a| < 1$ yields a stable process. As described earlier, the traditional spectral density matrix, which in this example is of the form

$$\boldsymbol{f}(\omega) := (2\pi)^{-1}\left(\boldsymbol{I}_2 - \begin{pmatrix} 0 & a \\ a & 0 \end{pmatrix} \mathrm{e}^{-i\omega}\right)^{-1}\left(\boldsymbol{I}_2 - \begin{pmatrix} 0 & a \\ a & 0 \end{pmatrix} \mathrm{e}^{i\omega}\right)^{-1}, \ |a| < 1,$$

uniquely determines the traditional coherency and, because of the Gaussian innovations, also the quantile coherency.

In the middle-left plot of Figure S.4 the traditional coherencies for this model are shown when a takes different values. If we now fix a frequency [$\neq \pi/4$], then the value of the traditional coherency for this frequency uniquely determines the value of a. In Figure S.4 we have marked the frequency of $\omega = 2\pi 52/512$ and coherency value of 0.6 by grey lines and printed the corresponding coherency (as a function of ω) in bold. Note that of the many pictured coherencies [one for each $a \in (-1, 1)$] only one has the value of 0.6 at this frequency. In the centre plot of the middle row we show the relation between the traditional coherency and quantile coherency for the considered model. For four combinations of quantile levels and all values of $a \in (-1, 1)$ the corresponding traditional coherencies and quantile coherencies are shown. It is important to observe that the relation is shown only for one frequency [$\omega = 2\pi 52/512$]. We observe that the range of values for the quantile coherency is limited and that the range depends on the combination of quantile levels and on the frequency. While this is quite similar to the first example, where quantile coherency had to be bounded owing to the Fréchet/Hoeffding bounds, we here also observe (for this particular model and frequency) that the range of values for the traditional coherency is limited. This fact is also apparent in the middle-left plot. To relate the traditional and quantile coherency at this particular frequency, one can, using the centre-middle plot, proceed as in the first example. For a given frequency, choose a valid traditional coherency (x-axis of the middle-centre plot) and combination of quantile levels (one of the lines in the plot) and then determine the value for the quantile coherency (depicted in the right plot). Note that (in this example), for a given frequency and combination of quantile levels the relation is still a function of the traditional coherency, but fails to be injective.

In our final example we consider the Gaussian VAR(1) model (S.4), where we now allow for an additional degree of freedom by letting the matrix $\boldsymbol{A}$ be of the form where the diagonal elements both are equal to b and keeping the value a on the off-diagonal as before. Thus, compared with the previous example, where $b = 0$ was required, each component now may also depend on its own lagged value. It is easy to see that $|a + b| < 1$ yields a stable process. In this case the traditional spectral density matrix is of the form

$$\boldsymbol{f}(\omega) := (2\pi)^{-1}\left(\boldsymbol{I}_2 - \begin{pmatrix} b & a \\ a & b \end{pmatrix} \mathrm{e}^{-i\omega}\right)^{-1}\left(\boldsymbol{I}_2 - \begin{pmatrix} b & a \\ a & b \end{pmatrix} \mathrm{e}^{i\omega}\right)^{-1}, \; |a + b| < 1.$$

In the bottom-left part of Figure S.4 a collection of traditional coherencies (as functions of ω) is shown. Owing to the extra degree of freedom in the model, the variety of shapes has increased dramatically. In particular, for a given frequency, the value of the traditional coherency does not uniquely specify the model parameter any more. We have marked three coherencies (as functions of ω) that have value 0.6 at $\omega = 2\pi 52/512$ in bold to stress this fact. The corresponding processes have (for a fixed combination of quantile levels) different values of quantile coherency at this frequency. This fact can be seen from the bottom-centre part of Figure S.4, where the relation between traditional and quantile coherency is depicted for the frequency fixed, and two combinations of quantile levels are shown in black and grey. Note the important fact that the relation (for fixed frequency) is not a function of the traditional coherency any more. The bottom-right part of the figure shows the quantile coherency curves (as a function of ω) for the three model parameters (shown in bold in the bottom-left part of the figure) and the two combination of quantile levels. It is clearly visible that even though, for the particular fixed frequency, the traditional coherency coincide, the value and shape of the quantile coherency can be very different depending on the underlying process. This third example illustrates how a frequency-by-frequency comparison of the traditional coherency with its quantile-based counterpart may fail, even when the process is quite simple.

We have seen, from the theoretical discussion at the beginning of this section, that for Gaussian processes, when the marginal distributions are fixed, a relation between the traditional spectra and the quantile spectra exists. This relation is a 1-to-1 relation between the quantities as functions of frequency (and quantile levels). The three examples have illustrated that a comparison on a frequency-by-frequency basis may be possible in special cases but does not hold in general.

In conclusion we therefore advise seeing the quantile cross-spectral density as a measure for dependence on its own, as the quantile-based quantities focus on more general types of dependence. We further point out that quantile coherency may be used in examples where the conditions that make a relation possible are fulfilled, but also, for example, to analyse the dependence in quantile vector autoregressive (QVAR) processes, described in Section S2. The QVAR processes possess more complicated dynamics, which cannot be described only by the second-order moment features.

S4. ASYMPTOTIC PROPERTIES OF THE PROPOSED ESTIMATORS FOR QUANTILE CROSS-SPECTRAL DENSITIES

We are now going to state a result on the asymptotic properties of the CCR-periodogram $\boldsymbol{I}_{n,R}(\omega; \tau_1, \tau_2)$ defined in (2.4) and (2.5).

Proposition S4.1 *Assume that $(\boldsymbol{X}_t)_{t\in\mathbb{Z}}$ is strictly stationary and satisfies Assumption 4.1. Further assume that the marginal distribution functions F_j, $j = 1, \ldots, d$ are continuous. Then, for every fixed $\omega \neq 0 \bmod 2\pi$,*

$$\left(\boldsymbol{I}_{n,R}(\omega; \tau_1, \tau_2)\right)_{(\tau_1,\tau_2)\in[0,1]^2} \Rightarrow \left(\mathbb{I}(\omega; \tau_1, \tau_2)\right)_{(\tau_1,\tau_2)\in[0,1]^2} \quad in\ \ell^\infty_{\mathbb{C}^{d\times d}}([0, 1]^2). \tag{S.5}$$

The $\mathbb{C}^{d\times d}$-valued limiting processes $\mathbb{I}$, indexed by $(\tau_1, \tau_2) \in [0, 1]^2$, is of the form

$$\mathbb{I}(\omega; \tau_1, \tau_2) = \frac{1}{2\pi}\mathbb{D}(\omega; \tau_1)\overline{\mathbb{D}(\omega; \tau_2)'},$$

where $\mathbb{D}(\omega;\tau) = (\mathbb{D}^j(\omega;\tau))_{j=1,\dots,d}$, $\tau \in [0,1]$, $\omega \in \mathbb{R}$ *is a centred,* $\mathbb{C}^d$*-valued Gaussian process with covariance structure of the following form:*

$$\mathrm{Cov}(\mathbb{D}^{j_1}(\omega;\tau_1), \mathbb{D}^{j_2}(\omega;\tau_2)) = 2\pi \mathfrak{f}^{j_1,j_2}(\omega;\tau_1,\tau_2).$$

Moreover, $\mathbb{D}(\omega;\tau) = \overline{\mathbb{D}(-\omega;\tau)} = \mathbb{D}(\omega + 2\pi;\tau)$*, and the family* $\{\mathbb{D}(\omega;\cdot) : \omega \in [0,\pi]\}$ *is a collection of independent processes. In particular, the weak convergence (S.5) holds jointly for any finite fixed collection of frequencies* ω*.*

For $\omega = 0 \mod 2\pi$ the asymptotic behaviour of the CCR-periodogram is as follows: we have $d^j_{n,R}(0;\tau) = n\tau + o_p(n^{1/2})$, where the exact form of the remainder term depends on the number of ties in $X_{j,0},\dots,X_{j,n-1}$. Therefore, under the assumptions of Proposition S4.1, we have $\boldsymbol{I}_{n,R}(0;\tau_1,\tau_2) = n(2\pi)^{-1}\tau_1\tau_2 1_d 1_d' + o_p(1)$, where $1_d := (1,\dots,1)' \in \mathbb{R}^d$.

We now state a result that quantifies the uncertainty in estimating $\mathfrak{f}(\omega;\tau_1,\tau_2)$ by $\boldsymbol{G}_{n,R}(\omega;\tau_1,\tau_2)$ asymptotically.

Theorem S4.1 *Let Assumptions 4.1 and 4.2 hold. Assume that the marginal distribution functions* F_j, $j = 1,\dots,d$ *are continuous and that constants* $\kappa > 0$ *and* $k \in \mathbb{N}$ *exist, such that* $b_n = o(n^{-1/(2k+1)})$ *and* $b_n n^{1-\kappa} \to \infty$*. Then, for any fixed* $\omega \in \mathbb{R}$*, the process*

$$\mathbb{G}_n(\omega;\cdot,\cdot) := \sqrt{nb_n}\Big(\hat{\boldsymbol{G}}_{n,R}(\omega;\tau_1,\tau_2) - \mathfrak{f}(\omega;\tau_1,\tau_2) - \boldsymbol{B}_n^{(k)}(\omega;\tau_1,\tau_2)\Big)_{\tau_1,\tau_2\in[0,1]}$$

satisfies

$$\mathbb{G}_n(\omega;\cdot,\cdot) \Rightarrow \mathbb{H}(\omega;\cdot,\cdot) \text{ in } \ell^\infty_{\mathbb{C}^{d\times d}}([0,1]^2), \tag{S.6}$$

where the elements of the bias matrix $\boldsymbol{B}_n^{(k)}$ *are given by*

$$\Big\{\boldsymbol{B}_n^{(k)}(\omega;\tau_1,\tau_2)\Big\}_{j_1,j_2} := \sum_{\ell=2}^{k} \frac{b_n^\ell}{\ell!}\int_{-\pi}^{\pi} v^\ell W(v)dv \frac{\mathrm{d}^\ell}{\mathrm{d}\omega^\ell}\mathfrak{f}^{j_1,j_2}(\omega;\tau_1,\tau_2) \tag{S.7}$$

and $\mathfrak{f}^{j_1,j_2}(\omega;\tau_1,\tau_2)$ *is defined in (2.2). The process* $\mathbb{H}(\omega;\cdot,\cdot) := (\mathbb{H}^{j_1,j_2}(\omega;\cdot,\cdot))_{j_1,j_2=1,\dots,d}$ *in (S.6) is a centred,* $\mathbb{C}^{d\times d}$*-valued Gaussian process characterized by*

$$\begin{aligned}&\mathrm{Cov}\left(\mathbb{H}^{j_1,j_2}(\omega;u_1,v_1), \mathbb{H}^{k_1,k_2}(\lambda;u_2,v_2)\right)\\ &= 2\pi\Big(\int_{-\pi}^{\pi} W^2(\alpha)\mathrm{d}\alpha\Big)\Big(\mathfrak{f}^{j_1,k_1}(\omega;u_1,u_2)\mathfrak{f}^{j_2,k_2}(-\omega;v_1,v_2)\eta(\omega-\lambda)\\ &+ \mathfrak{f}^{j_1,k_2}(\omega;u_1,v_2)\mathfrak{f}^{j_2,k_1}(-\omega;v_1,u_2)\eta(\omega+\lambda)\Big),\end{aligned} \tag{S.8}$$

where $\eta(x) := I\{x = 0 (\mod 2\pi)\}$ *[cf. Brillinger (1975), p. 148] is the* 2π*-periodic extension of Kronecker's delta function. The family* $\{\mathbb{H}(\omega;\cdot,\cdot), \omega \in [0,\pi]\}$ *is a collection of independent processes and* $\mathbb{H}(\omega;\tau_1,\tau_2) = \overline{\mathbb{H}(-\omega;\tau_1,\tau_2)} = \mathbb{H}(\omega+2\pi;\tau_1,\tau_2)$*.*

A few remarks on the result are in order. In sharp contrast to classical spectral analysis, where higher-order moments are required to obtain smoothness of the spectral density [cf. Brillinger (1975), p. 27], Assumption 4.1 guarantees that the quantile cross-spectral density is an analytical function of ω. Hence, the kth derivative of $\omega \mapsto \mathfrak{f}^{j_1,j_2}(\omega;\tau_1,\tau_2)$ in (S.7) exists without further assumptions.

The case $\omega = 0 \mod 2\pi$ does not require separate treatment as in Proposition S4.1, because $I^{j_1,j_2}_{n,R}(0,\tau_1,\tau_2)$ is excluded in (2.6): the definition of $\hat{G}^{j_1,j_2}_{n,R}(\omega;\tau_1,\tau_2)$.

Assume that W is a kernel of order p; i. e., for some p, it satisfies $\int_{-\pi}^{\pi} v^j W(v)\mathrm{d}v = 0$, for all $j < p$, and $0 < \int_{-\pi}^{\pi} v^p W(v)\mathrm{d}v < \infty$. For example, the Epanechnikov kernel is a kernel of order $p = 2$. Then, the bias is of order b_n^p. As the variance is of order $(nb_n)^{-1}$, the mean squared error is minimal, if $b_n \approx n^{-1/(2p+1)}$. This optimal bandwidth fulfils the assumptions of Theorem S4.1. A detailed discussion of how Theorem S4.1 can be used to construct asymptotically valid confidence intervals is deferred to Section D.

The independence of the limit $\{\mathbb{H}(\omega;\cdot,\cdot),\ \omega \in [0,\pi]\}$ has two important implications. On the one hand, the weak convergence (S.6) holds jointly for any finite fixed collection of frequencies ω. On the other hand, if one were to consider the smoothed CCR-periodogram as a function of the three arguments (ω, τ_1, τ_2), weak convergence cannot hold any more. This limitation of convergence is due to the fact that there exists no tight element in $\ell^{\infty}_{\mathbb{C}^{d\times d}}([0,\pi]\times[0,1]^2)$ that has the right finite-dimensional distributions, which would be required for process convergence in $\ell^{\infty}_{\mathbb{C}^{d\times d}}([0,\pi]\times[0,1]^2)$.

Fixing j_1, j_2 and τ_1, τ_2, the CCR-periodogram $\hat{G}^{j_1,j_2}_{n,R}(\omega;\tau_1,\tau_2)$ and traditional smoothed cross-periodogram determined from the unobservable, bivariate time series

$$\big(I\{F_{j_1}(X_{t,j_1}) \le \tau_1\}, I\{F_{j_1}(X_{t,j_2}) \le \tau_2\}\big), \quad t = 0,\dots,n-1, \tag{S.9}$$

are asymptotically equivalent. Theorem S4.1 thus reveals that, in the context of the estimation of the quantile cross-spectral density, the estimation of the marginal distribution has no impact on the limit distribution [cf. comment after Remark 3.5 in Kley et al. (2016)].

S5. ON THE CONSTRUCTION OF INTERVAL ESTIMATORS

In this section we collect details on how to construct pointwise confidence bands.

Sections 4 and S4 contained asymptotic results on the uncertainty of point estimation of the newly introduced quantile cross-spectral quantities. In this section we describe strategies to estimate the variances (of the real and imaginary parts) that appear in those limit results and describe how asymptotically valid pointwise confidence bands can be constructed.

In all three subsections, the following comment is relevant. Assuming that we have determined the weights W_n form a kernel W that is of order d. We will choose a bandwidth $b_n = o(n^{-1/(2d+1)})$. This choice implies that compared to the variance, the bias (that in some form appears in both limit results) is asymptotically negligible: $\sqrt{nb_n}\boldsymbol{B}^{(k)}_n(\omega;\tau_1,\tau_2) = o(1)$.

S5.1. Pointwise confidence bands for $\mathfrak{f}$

Utilizing Theorem S4.1, we now construct pointwise asymptotic $(1-\alpha)$-level confidence bands for the real and imaginary parts of $\mathfrak{f}^{j_1,j_2}(\omega_{kn};\tau_1,\tau_2)$, $\omega_{kn} := 2\pi k/n$, as follows:

$$C^{(1)}_{\mathrm{r},n}(\omega_{kn};\tau_1,\tau_2) := \Re\tilde{G}^{j_1,j_2}_{n,R}(\omega_{kn};\tau_1,\tau_2) \pm \Re\sigma^{j_1,j_2}_{(1)}(\omega_{kn};\tau_1,\tau_2)\Phi^{-1}(1-\alpha/2),$$

for the real part, and

$$C^{(1)}_{\mathrm{i},n}(\omega_{kn};\tau_1,\tau_2) := \Im\tilde{G}^{j_1,j_2}_{n,R}(\omega_{kn};\tau_1,\tau_2) \pm \Im\sigma^{j_1,j_2}_{(1)}(\omega_{kn};\tau_1,\tau_2)\Phi^{-1}(1-\alpha/2),$$

for the imaginary part of the quantile cross-spectrum. Here,

$$\tilde{G}^{j_1,j_2}_{n,R}(\omega_{kn};\tau_1,\tau_2) := \hat{G}^{j_1,j_2}_{n,R}(\omega_{kn};\tau_1,\tau_2)/W^k_n, \qquad W^k_n := \frac{2\pi}{n}\sum_{s=1}^{n-1} W_n(\omega_{kn}-\omega_{sn}),$$

and Φ denotes the cumulative distribution function of the standard normal distribution,[4]

$$\big(\Re\sigma^{j_1,j_2}(\omega_{kn};\tau_1,\tau_2)\big)^2 := 0 \vee \begin{cases} \mathrm{Cov}(\mathbb{H}_{1,2},\mathbb{H}_{1,2}) & \text{if } j_1 = j_2 \text{ and } \tau_1=\tau_2,\\ \frac{1}{2}\big(\mathrm{Cov}(\mathbb{H}_{1,2},\mathbb{H}_{1,2}) + \Re\,\mathrm{Cov}(\mathbb{H}_{1,2},\mathbb{H}_{2,1})\big) & \text{otherwise,}\end{cases}$$

and

$$\big(\Im\sigma^{j_1,j_2}(\omega_{kn};\tau_1,\tau_2)\big)^2 := 0 \vee \begin{cases} 0 & \text{if } j_1 = j_2 \text{ and } \tau_1=\tau_2,\\ \frac{1}{2}\big(\mathrm{Cov}(\mathbb{H}_{1,2},\mathbb{H}_{1,2}) - \Re\,\mathrm{Cov}(\mathbb{H}_{1,2},\mathbb{H}_{2,1})\big) & \text{otherwise,}\end{cases}$$

[4] Note that for $k = 0,\dots,n-1$ we have $W^k_n := 2\pi/n\sum_{0=s\neq k}^{n-1} W_n(2\pi s/n)$. For $k \in \mathbb{Z}$ with $k<0$ or $k \ge n$ we can define it as the n periodic extension.

where $\mathrm{Cov}(\mathbb{H}_{a,b}, \mathbb{H}_{c,d})$ denotes an estimator of $\mathrm{Cov}\left(\mathbb{H}^{j_a,j_b}(\omega_{kn}; \tau_a, \tau_b), \mathbb{H}^{j_c,j_d}(\omega_{kn}; \tau_c, \tau_d)\right)$. Here, motivated by Theorem 7.4.3 in Brillinger (1975), we use

$$\left(\frac{2\pi}{n \cdot W_n^k}\right) \times \Bigg[\sum_{s=1}^{n-1} W_n\big(2\pi(k-s)/n\big) W_n\big(2\pi(k-s)/n\big) \tilde{G}_{n,R}^{j_a,j_c}(\tau_a, \tau_c; 2\pi s/n) \tilde{G}_{n,R}^{j_b,j_d}(\tau_b, \tau_d; -2\pi s/n) + \sum_{s=1}^{n-1} W_n\big(2\pi(k-s)/n\big) W_n\big(2\pi(k+s)/n\big) \tilde{G}_{n,R}^{j_a,j_d}(\tau_a, \tau_d; 2\pi s/n) \tilde{G}_{n,R}^{j_b,j_c}(\tau_b, \tau_c; -2\pi s/n) \Bigg]. \tag{S.10}$$

The definition of $\sigma_{(1)}^{j_1,j_2}(\omega_{kn}; \tau_1, \tau_2)$ is motivated by the fact that $\Im \hat{G}_{n,R}^{j_1,j_2}(\omega_{kn}; \tau_1, \tau_2) = 0$, if $j_1 = j_2$ and $\tau_1 = \tau_2$. Furthermore, note that, for any complex-valued random variable Z, with complex conjugate $\bar{Z}$,

$$\mathrm{Var}(\Re Z) = \frac{1}{2}\big(\mathrm{Var}(Z) + \Re\,\mathrm{Cov}(Z, \bar{Z})\big); \quad \mathrm{Var}(\Im Z) = \frac{1}{2}\big(\mathrm{Var}(Z) - \Re\,\mathrm{Cov}(Z, \bar{Z})\big), \tag{S.11}$$

and we have $\overline{\mathbb{H}_{1,2}} = \mathbb{H}_{2,1}$.

S5.2. Pointwise confidence bands for $\mathfrak{R}$

We utilize Theorem 4.1 to construct pointwise asymptotic $(1-\alpha)$-level confidence bands for the real and imaginary parts of $\mathfrak{R}^{j_1,j_2}(\omega; \tau_1, \tau_2)$ as follows:

$$C_{\mathrm{r},n}^{(2)}(\omega_{kn}; \tau_1, \tau_2) := \Re \hat{\mathfrak{R}}_{n,R}^{j_1,j_2}(\omega_{kn}; \tau_1, \tau_2) \pm \Re \sigma_{(2)}^{j_1,j_2}(\omega_{kn}; \tau_1, \tau_2) \Phi^{-1}(1-\alpha/2),$$

for the real part, and

$$C_{\mathrm{i},n}^{(2)}(\omega_{kn}; \tau_1, \tau_2) := \Im \hat{\mathfrak{R}}_{n,R}^{j_1,j_2}(\omega_{kn}; \tau_1, \tau_2) \pm \Im \sigma_{(2)}^{j_1,j_2}(\omega_{kn}; \tau_1, \tau_2) \Phi^{-1}(1-\alpha/2),$$

for the imaginary part of the quantile coherency. Here, Φ stands for the cdf of the standard normal distribution,

$$\left(\Re \sigma_{(2)}^{j_1,j_2}(\omega_{kn}; \tau_1, \tau_2)\right)^2 := 0 \vee \begin{cases} 0 & \text{if } j_1 = j_2 \text{ and } \tau_1 = \tau_2, \\ \frac{1}{2}\big(\mathrm{Cov}(\mathbb{L}_{1,2}, \mathbb{L}_{1,2}) + \Re\,\mathrm{Cov}(\mathbb{L}_{1,2}, \mathbb{L}_{2,1})\big) & \text{otherwise,} \end{cases}$$

and

$$\left(\Im \sigma_{(2)}^{j_1,j_2}(\omega_{kn}; \tau_1, \tau_2)\right)^2 := 0 \vee \begin{cases} 0 & \text{if } j_1 = j_2 \text{ and } \tau_1 = \tau_2, \\ \frac{1}{2}\big(\mathrm{Cov}(\mathbb{L}_{1,2}, \mathbb{L}_{1,2}) - \Re\,\mathrm{Cov}(\mathbb{L}_{1,2}, \mathbb{L}_{2,1})\big) & \text{otherwise.} \end{cases}$$

The definition of $\sigma_{(2)}^{j_1,j_2}(\omega_{kn}; \tau_1, \tau_2)$ is motivated by (S.11) and the fact that we have $\overline{\mathbb{L}_{1,2}} = \mathbb{L}_{2,1}$. Furthermore, note that $\hat{\mathfrak{R}}_{n,R}^{j_1,j_2}(\omega_{kn}; \tau_1, \tau_2) = 1$, if $j_1 = j_2$ and $\tau_1 = \tau_2$..

In the definition of $\sigma_{(2)}^{j_1,j_2}(\omega_{kn}; \tau_1, \tau_2)$ we have used $\mathrm{Cov}(\mathbb{L}_{a,b}, \mathbb{L}_{c,d})$ to denote an estimator for

$$\mathrm{Cov}\left(\mathbb{L}^{j_1,j_2}(\omega_{kn}; \tau_1, \tau_2), \mathbb{L}^{j_3,j_4}(\omega_{kn}; \tau_3, \tau_4)\right).$$

Recalling the definition of the limit process in Theorem 4.1 we derive the following expression:

$$\frac{1}{\sqrt{\mathfrak{f}_{1,1}\mathfrak{f}_{2,2}\mathfrak{f}_{3,3}\mathfrak{f}_{4,4}}} \operatorname{Cov}\Big(\mathbb{H}_{1,2} - \frac{1}{2}\frac{\mathfrak{f}_{1,2}}{\mathfrak{f}_{1,1}}\mathbb{H}_{1,1} - \frac{1}{2}\frac{\mathfrak{f}_{1,2}}{\mathfrak{f}_{2,2}}\mathbb{H}_{2,2}, \mathbb{H}_{3,4} - \frac{1}{2}\frac{\mathfrak{f}_{3,4}}{\mathfrak{f}_{3,3}}\mathbb{H}_{3,3} - \frac{1}{2}\frac{\mathfrak{f}_{3,4}}{\mathfrak{f}_{4,4}}\mathbb{H}_{4,4}\Big)$$

$$= \frac{\operatorname{Cov}(\mathbb{H}_{1,2}, \mathbb{H}_{3,4})}{\sqrt{\mathfrak{f}_{1,1}\mathfrak{f}_{2,2}\mathfrak{f}_{3,3}\mathfrak{f}_{4,4}}} - \frac{1}{2}\frac{\overline{\mathfrak{f}_{3,4}}\operatorname{Cov}(\mathbb{H}_{1,2}, \mathbb{H}_{3,3})}{\sqrt{\mathfrak{f}_{1,1}\mathfrak{f}_{2,2}\mathfrak{f}_{3,3}^3\mathfrak{f}_{4,4}}} - \frac{1}{2}\frac{\overline{\mathfrak{f}_{3,4}}\operatorname{Cov}(\mathbb{H}_{1,2}, \mathbb{H}_{4,4})}{\sqrt{\mathfrak{f}_{1,1}\mathfrak{f}_{2,2}\mathfrak{f}_{3,3}\mathfrak{f}_{4,4}^3}}$$

$$- \frac{1}{2}\frac{\mathfrak{f}_{1,2}\operatorname{Cov}(\mathbb{H}_{1,1}, \mathbb{H}_{3,4})}{\sqrt{\mathfrak{f}_{1,1}^3\mathfrak{f}_{2,2}\mathfrak{f}_{3,3}\mathfrak{f}_{4,4}}} + \frac{1}{4}\frac{\mathfrak{f}_{1,2}\overline{\mathfrak{f}_{3,4}}\operatorname{Cov}(\mathbb{H}_{1,1}, \mathbb{H}_{3,3})}{\sqrt{\mathfrak{f}_{1,1}^3\mathfrak{f}_{2,2}\mathfrak{f}_{3,3}^3\mathfrak{f}_{4,4}}} + \frac{1}{4}\frac{\mathfrak{f}_{1,2}\overline{\mathfrak{f}_{3,4}}\operatorname{Cov}(\mathbb{H}_{1,1}, \mathbb{H}_{4,4})}{\sqrt{\mathfrak{f}_{1,1}^3\mathfrak{f}_{2,2}\mathfrak{f}_{3,3}\mathfrak{f}_{4,4}^3}}$$

$$- \frac{1}{2}\frac{\mathfrak{f}_{1,2}\operatorname{Cov}(\mathbb{H}_{2,2}, \mathbb{H}_{3,4})}{\sqrt{\mathfrak{f}_{1,1}\mathfrak{f}_{2,2}^3\mathfrak{f}_{3,3}\mathfrak{f}_{4,4}}} + \frac{1}{4}\frac{\mathfrak{f}_{1,2}\overline{\mathfrak{f}_{3,4}}\operatorname{Cov}(\mathbb{H}_{2,2}, \mathbb{H}_{3,3})}{\sqrt{\mathfrak{f}_{1,1}\mathfrak{f}_{2,2}^3\mathfrak{f}_{3,3}^3\mathfrak{f}_{4,4}}} + \frac{1}{4}\frac{\mathfrak{f}_{1,2}\overline{\mathfrak{f}_{3,4}}\operatorname{Cov}(\mathbb{H}_{2,2}, \mathbb{H}_{4,4})}{\sqrt{\mathfrak{f}_{1,1}\mathfrak{f}_{2,2}^3\mathfrak{f}_{3,3}\mathfrak{f}_{4,4}^3}},$$

where we have written $\mathfrak{f}_{a,b}$ for the quantile spectral density $\mathfrak{f}^{j_a,j_b}(\omega_{kn};\tau_a,\tau_b)$, and $\mathbb{H}_{a,b}$ for the limit distribution $\mathbb{H}^{j_a,j_b}(\omega_{kn};\tau_a,\tau_b)$ for any $a, b = 1, 2, 3, 4$.

Thus, considering the special case where $\tau_3 = \tau_1$ and $\tau_4 = \tau_2$, we have

$$\begin{aligned}
&\operatorname{Cov}(\mathbb{L}_{1,2}, \mathbb{L}_{1,2}) \\
&= \frac{1}{\mathfrak{f}_{1,1}\mathfrak{f}_{2,2}}\Big(\operatorname{Cov}(\mathbb{H}_{1,2}, \mathbb{H}_{1,2}) - \Re\frac{\mathfrak{f}_{1,2}\operatorname{Cov}(\mathbb{H}_{1,1}, \mathbb{H}_{1,2})}{\mathfrak{f}_{1,1}} - \Re\frac{\mathfrak{f}_{1,2}\operatorname{Cov}(\mathbb{H}_{2,2}, \mathbb{H}_{1,2})}{\mathfrak{f}_{2,2}} \\
&\quad + \frac{1}{4}|\mathfrak{f}_{1,2}|^2\Big(\frac{\operatorname{Cov}(\mathbb{H}_{1,1}, \mathbb{H}_{1,1})}{\mathfrak{f}_{1,1}^2} + 2\Re\frac{\operatorname{Cov}(\mathbb{H}_{1,1}, \mathbb{H}_{2,2})}{\mathfrak{f}_{1,1}\mathfrak{f}_{2,2}} + \frac{\operatorname{Cov}(\mathbb{H}_{2,2}, \mathbb{H}_{2,2})}{\mathfrak{f}_{2,2}^2}\Big)\Big)
\end{aligned} \tag{S.12}$$

and for the special case where $\tau_3 = \tau_1$ and $\tau_4 = \tau_2$ we have

$$\begin{aligned}
&\operatorname{Cov}(\mathbb{L}_{1,2}, \mathbb{L}_{2,1}) \\
&= \frac{1}{\mathfrak{f}_{1,1}\mathfrak{f}_{2,2}}\Big(\operatorname{Cov}(\mathbb{H}_{1,2}, \mathbb{H}_{2,1}) - \frac{\mathfrak{f}_{1,2}\operatorname{Cov}(\mathbb{H}_{1,2}, \mathbb{H}_{2,2})}{\mathfrak{f}_{2,2}} - \frac{\mathfrak{f}_{1,2}\operatorname{Cov}(\mathbb{H}_{1,2}, \mathbb{H}_{1,1})}{\mathfrak{f}_{1,1}} \\
&\quad + \frac{1}{4}\mathfrak{f}_{1,2}^2\Big(\frac{\operatorname{Cov}(\mathbb{H}_{1,1}, \mathbb{H}_{1,1})}{\mathfrak{f}_{1,1}^2} + 2\Re\frac{\operatorname{Cov}(\mathbb{H}_{1,1}, \mathbb{H}_{2,2})}{\mathfrak{f}_{1,1}\mathfrak{f}_{2,2}} + \frac{\operatorname{Cov}(\mathbb{H}_{2,2}, \mathbb{H}_{2,2})}{\mathfrak{f}_{2,2}^2}\Big)\Big).
\end{aligned}$$

We substitute consistent estimators for the unknown quantities. To do so, we abuse notation using $\mathfrak{f}_{a,b}$ to denote $\tilde{G}_{n,R}^{j_a,j_b}(\omega_{kn};\tau_a,\tau_b)$ and write $\operatorname{Cov}(\mathbb{H}_{a,b}, \mathbb{H}_{c,d})$ for the quantity defined in (S.10).

S6. PROOFS OF THE RESULTS IN SECTIONS 4 AND S4

In this section the proofs to the results in Sections 4 and S4 are given. Before we begin, note that by a trivial generalization of Proposition 3.1 in Kley et al. (2016) we have that Assumption 4.1 implies that there exist constants $\bar{\rho} \in (0, 1)$ and $K < \infty$ such that, for arbitrary intervals $A_1, \ldots, A_p \subset \mathbb{R}$, arbitrary indices $j_1, \ldots, j_p \in \{1, \ldots, d\}$ and times $t_1, \ldots, t_p \in \mathbb{Z}$,

$$|\operatorname{cum}(I\{X_{t_1,j_1} \in A_1\}, \ldots, I\{X_{t_p,j_p} \in A_p\})| \le K\bar{\rho}^{\max_{i,j}|t_i - t_j|}. \tag{S.13}$$

We will use this fact several times throughout the proofs in this section.

S6.1. Proof of Theorem 4.1

By a Taylor expansion we have, for every $x, x_0 > 0$,

$$\frac{1}{\sqrt{x}} = \frac{1}{\sqrt{x_0}} - \frac{1}{2}\frac{1}{\sqrt{x_0^3}}(x - x_0) + \frac{3}{8}\xi_{x,x_0}^{-5/2}(x - x_0)^2,$$

where ξ_{x,x_0} is between x and x_0. Let $R_n(x, x_0) := \frac{3}{8}\xi_{x,x_0}^{-5/2}(x - x_0)^2$, then

$$\frac{x}{\sqrt{yz}} - \frac{x_0}{\sqrt{y_0 z_0}} = \frac{1}{\sqrt{y_0 z_0}}\Big((x - x_0) - \frac{1}{2}\frac{x_0}{y_0}(y - y_0) - \frac{1}{2}\frac{x_0}{z_0}(z - z_0) + r_n\Big), \tag{S.14}$$

where

$$\begin{aligned} r_n = {} & (x - x_0)\Big(- \frac{1}{2}\frac{1}{y_0}(y - y_0) - \frac{1}{2}\frac{1}{z_0}(z - z_0)\Big) \\ & + x\Big(R_n(y, y_0)\sqrt{y_0}\big(1 - \frac{1}{2}\frac{1}{z_0}(z - z_0)\big) + R_n(z, z_0)\sqrt{z_0}\big(1 - \frac{1}{2}\frac{1}{y_0}(y - y_0)\big) \\ & + \frac{1}{4}\frac{1}{y_0}(y - y_0)\frac{1}{z_0}(z - z_0) + \sqrt{y_0 z_0}R_n(y, y_0)R_n(z, z_0)\Big). \end{aligned}$$

Write $\mathfrak{f}_{a,b}$ for $\mathfrak{f}^{j_a,j_b}(\omega;\tau_a,\tau_b)$, $\mathfrak{G}_{a,b}$ for $\hat{G}^{j_a,j_b}_{n,R}(\omega;\tau_a,\tau_b)$, and $\boldsymbol{B}_{a,b}$ for $\{\boldsymbol{B}_n^{(k)}(\omega;\tau_a,\tau_b)\}_{j_a,j_b}$ $(a, b = 1, 2, 3, 4)$. We want to employ (S.14) and to this end let

$$\begin{aligned} x &:= \mathfrak{G}_{a,b} & y &:= \mathfrak{G}_{a,a} & z &:= \mathfrak{G}_{b,b} \\ x_0 &:= \mathfrak{f}_{a,b} + \boldsymbol{B}_{a,b} & y_0 &:= \mathfrak{f}_{a,a} + \boldsymbol{B}_{a,a} & z_0 &:= \mathfrak{f}_{b,b} + \boldsymbol{B}_{b,b}. \end{aligned}$$

By Theorem S4.1, the differences $x - x_0$, $y - y_0$, and $z - z_0$ are of $O_p((nb_n)^{-1/2})$, uniformly with respect to τ_1, τ_2. Under the assumption that $nb_n \to \infty$, as $n \to \infty$, this entails $\mathfrak{G}_{a,a} - \boldsymbol{B}_{a,a} \to \mathfrak{f}_{a,a}$, in probability. For $\varepsilon \le \tau_1, \tau_2 \le 1 - \varepsilon$, we have $\mathfrak{f}_{a,a} > 0$, such that, by the continuous mapping theorem, we have $(\mathfrak{G}_{a,a} - \boldsymbol{B}_{a,a})^{-5/2} \to \mathfrak{f}_{a,a}^{-5/2}$, in probability. As $\boldsymbol{B}_{a,a} = o(1)$, we have $y^{-5/2} - y_0^{-5/2} = o_p(1)$. Finally, due to

$$\xi_{y,y_0}^{-5/2} \le y_n^{-5/2} \vee y_0^{-5/2} \le (y_n^{-5/2} - y_0^{-5/2}) \vee 0 + y_0^{-5/2} = o_p(1) + O(1) = O_p(1),$$

we have that $R_n(y, y_0) = O_p((nb_n)^{-1})$.

Analogous arguments yield $R_n(z, z_0) = O_p((nb_n)^{-1})$. Thus we have shown that

$$\begin{aligned} & \hat{\mathfrak{R}}^{j_1,j_2}_{n,R}(\omega;\tau_1,\tau_2) - \frac{\mathfrak{f}_{a,b} + \boldsymbol{B}_{a,b}}{\sqrt{\mathfrak{f}_{a,a} + \boldsymbol{B}_{a,a}}\sqrt{\mathfrak{f}_{b,b} + \boldsymbol{B}_{b,b}}} \\ & \quad = \frac{1}{\sqrt{\mathfrak{f}_{1,1}\mathfrak{f}_{2,2}}}\Big([\mathfrak{G}_{1,2} - \mathfrak{f}_{1,2} - \boldsymbol{B}_{1,2}] - \frac{1}{2}\frac{\mathfrak{f}_{1,2}}{\mathfrak{f}_{1,1}}[\mathfrak{G}_{1,1} - \mathfrak{f}_{1,1} - \boldsymbol{B}_{1,1}] - \frac{1}{2}\frac{\mathfrak{f}_{1,2}}{\mathfrak{f}_{2,2}}[\mathfrak{G}_{2,2} - \mathfrak{f}_{2,2} - \boldsymbol{B}_{2,2}]\Big) \\ & \qquad + O_p\big(1/(nb_n)\big), \end{aligned}$$

with the O_p holding uniformly with respect to τ_1, τ_2. Furthermore, note that

$$\begin{aligned} \frac{\mathfrak{f}_{a,b} + \boldsymbol{B}_{a,b}}{\sqrt{\mathfrak{f}_{a,a} + \boldsymbol{B}_{a,a}}\sqrt{\mathfrak{f}_{b,b} + \boldsymbol{B}_{b,b}}} = {} & \frac{\mathfrak{f}_{a,b}}{\sqrt{\mathfrak{f}_{a,a}\mathfrak{f}_{b,b}}} + \frac{1}{\sqrt{\mathfrak{f}_{a,a}\mathfrak{f}_{b,b}}}\Big(\boldsymbol{B}_{a,b} - \frac{1}{2}\frac{\mathfrak{f}_{a,b}}{\mathfrak{f}_{a,a}}\boldsymbol{B}_{a,a} - \frac{1}{2}\frac{\mathfrak{f}_{a,b}}{\mathfrak{f}_{b,b}}\boldsymbol{B}_{b,b}\Big) \\ & + O(|\boldsymbol{B}_{a,b}|(\boldsymbol{B}_{a,a} + \boldsymbol{B}_{b,b}) + \boldsymbol{B}_{a,a}^2 + \boldsymbol{B}_{b,b}^2 + \boldsymbol{B}_{a,a}\boldsymbol{B}_{b,b}), \end{aligned}$$

where we have used (S.14) again. By Lemma 6.5 we have that

$$\sup_{\tau_1,\tau_2 \in [\varepsilon, 1-\varepsilon]} \Big| \frac{\mathrm{d}^\ell}{\mathrm{d}\omega^\ell}\mathfrak{f}^{j_1,j_2}(\omega;\tau_1,\tau_2)\Big| \le C_{\varepsilon,\ell}.$$

Therefore, b_n satisfies

$$\sup_{\tau_1,\tau_2\in[\varepsilon,1-\varepsilon]}\Big|\sum_{\ell=2}^{k}\frac{b_n^\ell}{\ell!}\int_{-\pi}^{\pi}v^\ell W(v)dv\frac{\mathrm{d}^\ell}{\mathrm{d}\omega^\ell}\mathfrak{f}^{j_1,j_2}(\omega;\tau_1,\tau_2)\Big| = o\big((nb_n)^{-1/4}\big),$$

for all $j_1, j_2 = 1, \ldots, d$, which implies that

$$|\boldsymbol{B}_{a,b}|(\boldsymbol{B}_{a,a}+\boldsymbol{B}_{b,b})+\boldsymbol{B}_{a,a}^2+\boldsymbol{B}_{b,b}^2+\boldsymbol{B}_{a,a}\boldsymbol{B}_{b,b} = o\big((nb_n)^{-1/2}\big).$$

Therefore,

$$\sqrt{nb_n}\Big(\hat{\mathfrak{R}}_{n,R}^{j_1,j_2}(\omega;\tau_1,\tau_2)-\mathfrak{R}^{j_1,j_2}(\omega;\tau_1,\tau_2) - \frac{1}{\sqrt{\mathfrak{f}_{a,a}\mathfrak{f}_{b,b}}}\Big(\boldsymbol{B}_{a,b}-\frac{1}{2}\frac{\mathfrak{f}_{a,b}}{\mathfrak{f}_{a,a}}\boldsymbol{B}_{a,a}-\frac{1}{2}\frac{\mathfrak{f}_{a,b}}{\mathfrak{f}_{b,b}}\boldsymbol{B}_{b,b}\Big)\Big)_{\tau_1,\tau_2\in[0,1]}$$

and

$$\frac{\sqrt{nb_n}}{\sqrt{\mathfrak{f}_{1,1}\mathfrak{f}_{2,2}}}\Big([\mathfrak{G}_{1,2}-\mathfrak{f}_{1,2}-\boldsymbol{B}_{1,2}]-\frac{1}{2}\frac{\mathfrak{f}_{1,2}}{\mathfrak{f}_{1,1}}[\mathfrak{G}_{1,1}-\mathfrak{f}_{1,1}-\boldsymbol{B}_{1,1}]-\frac{1}{2}\frac{\mathfrak{f}_{1,2}}{\mathfrak{f}_{2,2}}[\mathfrak{G}_{2,2}-\mathfrak{f}_{2,2}-\boldsymbol{B}_{2,2}]\Big) \tag{S.15}$$

are asymptotically equivalent in the sense that if one of the two converges weakly in $\ell^\infty_{\mathbb{C}^{d\times d}}([0,1]^2)$, then so does the other. The assertion then follows by Theorem S4.1, Slutzky's lemma and the continuous mapping theorem.□

S6.2. Proof of Proposition S4.1

The proof resembles the proof of Proposition 3.4 in Kley et al. (2016), where the univariate case was handled. For $j = 1, \ldots, d$ we have, from the continuity of F_j, that the ranks of the random variables $X_{0,j}$, ..., $X_{n-1,j}$ and $F_j(X_{0,j})$, ..., $F_j(X_{n-1,j})$ coincide almost surely. Thus, without loss of generality, we can assume that the CCR-periodogram is computed from the unobservable data $(F_j(X_{0,j}))_{j=1,\ldots,d}$, ..., $(F_j(X_{n-1,j}))_{j=1,\ldots,d}$. In particular, we can assume the marginals to be uniform.

Applying the continuous mapping theorem afterward, it suffices to prove

$$\Big(n^{-1/2}d_{n,R}^j(\omega;\tau)\Big)_{\tau\in[0,1],\,j=1,\ldots,d} \Rightarrow \Big(\mathbb{D}^j(\omega;\tau)\Big)_{\tau\in[0,1],\,j=1,\ldots,d} \quad \text{in } \ell^\infty_{\mathbb{C}^d}([0,1]), \tag{S.16}$$

where $\ell^\infty_{\mathbb{C}^d}([0,1])$ is the space of bounded functions $[0,1]\to\mathbb{C}^d$ that we identify with the product space $\ell^\infty([0,1])^{2d}$. Let

$$d_{n,U}^j(\omega;\tau) := \sum_{t=0}^{n-1} I\{F_j(X_{t,j})\le\tau\}\mathrm{e}^{-\mathrm{i}\omega t},$$

$j = 1, \ldots, d$, $\omega\in\mathbb{R}$, $\tau\in[0,1]$, and note that for (S.16) to hold, it is sufficient that

$$\big(n^{-1/2}d_{n,U}^j(\omega;\tau)\big)_{\tau\in[0,1],\,j=1,\ldots,d}$$

satisfies the following two conditions:

(i1) convergence of the finite-dimensional distributions, i. e.,

$$\big(n^{-1/2}d_{n,U}^{j_\ell}(\omega_\ell;\tau_\ell)\big)_{\ell=1,\ldots,k} \xrightarrow{d} \big(\mathbb{D}^{j_\ell}(\omega_\ell;\tau_\ell)\big)_{\ell=1,\ldots,k}, \tag{S.17}$$

for any $(j_\ell,\tau_\ell)\in\{1,\ldots,d\}\times[0,1]$, $\omega_\ell\neq 0 \mod 2\pi$, $\ell = 1, \ldots, k$ and $k\in\mathbb{N}$;

(i2) stochastic equicontinuity: for any $x > 0$ and any $\omega \neq 0 \mod 2\pi$,

$$\lim_{\delta\downarrow 0}\limsup_{n\to\infty}\mathbb{P}\Big(\sup_{\substack{\tau_1,\tau_2\in[0,1]\\|\tau_1-\tau_2|\le\delta}}|n^{-1/2}(d^j_{n,U}(\omega;\tau_1)-d^j_{n,U}(\omega;\tau_2))|>x\Big)=0,\quad \forall j=1,\dots,d. \tag{S.18}$$

Under (i1) and (i2), an application of Theorems 1.5.4 and 1.5.7 from van der Vaart and Wellner (1996) then yields

$$\Big(n^{-1/2}d^j_{n,U}(\omega;\tau)\Big)_{\tau\in[0,1],\,j=1,\dots,d}\Rightarrow\Big(\mathbb{D}^j(\omega;\tau)\Big)_{\tau\in[0,1],\,j=1,\dots,d}\quad \text{in } \ell^\infty_{\mathbb{C}^d}([0,1]). \tag{S.19}$$

In combination with

$$\sup_{\tau\in[0,1]}|n^{-1/2}(d^j_{n,R}(\omega;\tau)-d^j_{n,U}(\omega;\tau))|=o_p(1),\quad \text{for } \omega\neq 0 \mod 2\pi,\ j=1,\dots,d, \tag{S.20}$$

which we will prove below, (S.19) yields the desired result: (S.16). For the proof of (S.20), we denote by $\hat F^{-1}_{n,j}(\tau):=\inf\{x:\hat F_{n,j}(x)\ge\tau\}$ the generalized inverse of $\hat F_{n,j}$ and let $\inf\emptyset:=0$. Then, we have, as in (7.25) of Kley et al. (2016), that

$$\sup_{\omega\in\mathbb{R}}\sup_{\tau\in[0,1]}\Big|d^j_{n,R}(\omega;\tau)-d^j_{n,U}(\omega;\hat F^{-1}_{n,j}(\tau))\Big|\le n\sup_{\tau\in[0,1]}|\hat F_{n,j}(\tau)-\hat F_{n,j}(\tau-)|=O_p(n^{1/2k}) \tag{S.21}$$

where $\hat F_{n,j}(\tau-):=\lim_{\xi\uparrow 0}\hat F_{n,j}(\tau-\xi)$. The O_p-bound in (S.21) follows from Lemma S6.7. Therefore, it suffices to bound the terms

$$\sup_{\tau\in[0,1]}n^{-1/2}|d^j_{n,U}(\omega;\hat F^{-1}_{n,j}(\tau))-d^j_{n,U}(\omega,\tau))|,\ \text{for all } j=1,\dots,d.$$

To do so, note that, for any $x>0$ and $\delta_n=o(1)$ satisfying $n^{1/2}\delta_n\to\infty$, we have

$$\begin{aligned}&\mathbb{P}\Big(\sup_{\tau\in[0,1]}n^{-1/2}|d^j_{n,U}(\omega;\hat F^{-1}_{n,j}(\tau))-d^j_{n,U}(\omega;\tau))|>x\Big)\\ &\le\mathbb{P}\Big(\sup_{\tau\in[0,1]}\sup_{|u-\tau|\le\delta_n}|d^j_{n,U}(\omega;u)-d^j_{n,U}(\omega;\tau)|>xn^{1/2},\ \sup_{\tau\in[0,1]}|\hat F^{-1}_{n,j}(\tau)-\tau|\le\delta_n\Big)\\ &\quad+\mathbb{P}\Big(\sup_{\tau\in[0,1]}|\hat F^{-1}_{n,j}(\tau)-\tau|>\delta_n\Big)=o(1)+o(1).\end{aligned}$$

The first $o(1)$ follows from (S.18). The second one is a consequence of Lemma S6.8.

It thus remains to prove (S.17) and (S.18). For any fixed $j=1,\dots,d$ the process $\big(d^j_{n,U}(\omega,\tau)\big)_{\tau\in[0,1]}$ is determined by the univariate time series $X_{0,j},\dots,X_{n-1,j}$. Under the assumptions made here, (S.18) therefore follows from (8.7) in Kley et al. (2016).

Finally, we establish (S.17), by employing Lemma S6.6 in combination with Lemma P4.5 and Theorem 4.3.2 from Brillinger (1975). More precisely, to apply Lemma P4.5 from Brillinger (1975), we have to verify that, for any $j_1,\dots,j_\ell\in\{1,\dots,d\}$, $\tau_1,\dots,\tau_\ell\in[0,1]$, $\ell\in\mathbb{N}$, and $\omega_1,\dots,\omega_\ell\neq 0 \mod 2\pi$, all cumulants of the vector

$$n^{-1/2}\big(d^{j_1}_{n,U}(\omega_1;\tau_1),d^{j_1}_{n,U}(-\omega_1;\tau_1),\dots,d^{j_\ell}_{n,U}(\omega_\ell;\tau_\ell),d^{j_\ell}_{n,U}(-\omega_\ell;\tau_\ell)\big)$$

converge to the corresponding cumulants of the vector

$$\big(\mathbb{D}^{j_1}(\omega_1;\tau_1),\mathbb{D}^{j_1}(-\omega_1;\tau_1),\dots,\mathbb{D}^{j_\ell}(\omega_\ell;\tau_\ell),\mathbb{D}^{j_\ell}(-\omega_\ell;\tau_\ell)\big).$$

For the cumulants of order one, the arguments from the univariate case [cf. the proof of Proposition 3.4 in Kley et al. (2016)] apply: we have $|\mathbb{E}(n^{-1/2}d^j_{n,U}(\omega;\tau))|=o(1)$, for any $j=1,\dots,d$, $\tau\in[0,1]$ and fixed $\omega\neq 0 \mod 2\pi$. Furthermore, for the cumulants of order two, applying Theorem 4.3.1 in Brillinger (1975) to the bivariate process

$$(I\{X_{t,j_1}\le q_{j_1}(\mu_1)\},I\{X_{t,j_2}\le q_{j_2}(\mu_2)\}),$$

we obtain

$$\mathrm{cum}(n^{-1/2}d^{i_1}_{n,U}(\lambda_1;\mu_1), n^{-1/2}d^{i_2}_{n,U}(\lambda_2;\mu_2)) = 2\pi n^{-1}\Delta_n(\lambda_1+\lambda_2)\mathfrak{f}^{i_1,i_2}(\lambda_1;\mu_1,\mu_2)+o(1)$$

for any $(i_1, \lambda_1, \mu_1), (i_2, \lambda_2, \mu_2) \in \bigcup_{\ell=1}^{k}\{(i_\ell, \omega_\ell, \tau_\ell), (j_\ell, -\omega_\ell, \tau_\ell)\}$, which yields the correct second moment structure. The function Δ_n is defined in Lemma S6.6. Finally, the cumulants of order J, with $J \in \mathbb{N}$ and $J \geq 3$, all tend to zero, as in view of Lemma S6.6

$$\begin{aligned}\mathrm{cum}(n^{-1/2}d^{i_1}_{n,U}\ &(\lambda_1;\mu_1), \ldots, n^{-1/2}d^{i_J}_{n,U}(\lambda_J;\mu_J))\\ &\leq Cn^{-J/2}(|\Delta_n(\sum_{j=1}^{J}\lambda_j)|+1)\varepsilon(|\log\varepsilon|+1)^d = O(n^{-(J-2)/2}) = o(1),\end{aligned}$$

for $(i_1, \lambda_1, \mu_1), \ldots, (i_J, \lambda_J, \mu_J) \in \bigcup_{\ell=1}^{k}\{(i_\ell, \omega_\ell, \tau_\ell), (i_\ell, -\omega_\ell, \tau_\ell)\}$, where $\varepsilon := \min_{j=1}^{J}\mu_j$. This implies that the limit $\mathbb{D}^j(\tau;\omega)$ is Gaussian, and completes the proof of (S.17). Proposition S4.1 follows. □

S6.3. Proof of Theorem S4.1

We proceed in a similar fashion as in the proof of the univariate estimator, which was analysed in Kley et al. (2016). First, we state an asymptotic representation result by which the estimator $\hat{\boldsymbol{G}}_{n,R}$ can be approximated, in a suitable uniform sense, by another process $\hat{\boldsymbol{G}}_{n,U}$ which is not defined as a function of the standardized ranks $\hat{F}_{n,j}(X_{t,j})$, but as a function of the unobservable quantities $F_j(X_{t,j})$, $t = 0, \ldots, n-1$, $j = 1, \ldots, d$. More precisely, this process is defined as

$$\hat{\boldsymbol{G}}_{n,U}(\omega;\tau_1,\tau_2) := (\hat{G}^{j_1,j_2}_{n,U}(\omega;\tau_1,\tau_2))_{j_1,j_2=1,\ldots,d},$$

where

$$\begin{aligned}\hat{G}^{j_1,j_2}_{n,U}(\omega;\tau_1,\tau_2) &:= \tfrac{2\pi}{n}\textstyle\sum_{s=1}^{n-1} W_n\big(\omega-2\pi s/n\big)I^{j_1,j_2}_{n,U}(2\pi s/n,\tau_1,\tau_2)\\ I^{j_1,j_2}_{n,U}(\omega;\tau_1,\tau_2) &:= \tfrac{1}{2\pi n}d^{j_1}_{n,U}(\omega;\tau_1)d^{j_2}_{n,U}(-\omega;\tau_2)\\ d^{j}_{n,U}(\omega;\tau) &:= \textstyle\sum_{t=0}^{n-1} I\{F_j(X_{t,j})\leq\tau\}\mathrm{e}^{-\mathrm{i}\omega t}.\end{aligned} \tag{S.22}$$

Theorem S4.1 then follows from the asymptotic representation of $\hat{\boldsymbol{G}}_{n,R}$ by $\hat{\boldsymbol{G}}_{n,U}$ [i. e., Theorem S6.1(iii)] and the asymptotic properties of $\hat{\boldsymbol{G}}_{n,U}$ [i. e., Theorem S6.1(i)–(ii)], which we now state:

THEOREM S6.1. *Let Condition (S.13) and Assumption 4.2 hold, and assume that the distribution functions F_j of $X_{0,j}$ are continuous for all $j = 1, \ldots, d$. Let b_n satisfy the assumptions of Theorem S4.1. Then,*

(i) for any fixed $\omega \in \mathbb{R}$, as $n \to \infty$,

$$\sqrt{nb_n}\big(\hat{\boldsymbol{G}}_{n,U}(\omega;\tau_1,\tau_2) - \mathbb{E}\hat{\boldsymbol{G}}_{n,U}(\omega;\tau_1,\tau_2)\big)_{\tau_1,\tau_2\in[0,1]} \Rightarrow \mathbb{H}(\omega;\cdot,\cdot)$$

in $\ell^{\infty}_{\mathbb{C}^{d\times d}}([0,1]^2)$, where the process $\mathbb{H}(\omega;\cdot,\cdot)$ is defined in Theorem S4.1;

(ii) still as $n \to \infty$,

$$\sup_{\substack{j_1,j_2\in\{1,\ldots,d\}\\ \tau_1,\tau_2\in[0,1]\\ \omega\in\mathbb{R}}}\left|\mathbb{E}\hat{G}^{j_1,j_2}_{n,U}(\tau_1,\tau_2;\omega) - \mathfrak{f}^{j_1,j_2}(\omega;\tau_1,\tau_2) - \big\{\boldsymbol{B}^{(k)}_n(\omega;\tau_1,\tau_2)\big\}_{j_1,j_2}\right| = O((nb_n)^{-1}) + o(b_n^k),$$

where $\big\{\boldsymbol{B}^{(k)}_n(\omega;\tau_1,\tau_2)\big\}_{j_1,j_2}$ is defined in (S.7);

(iii) for any fixed $\omega \in \mathbb{R}$,

$$\sup_{\substack{j_1,j_2\in\{1,\ldots,d\}\\ \tau_1,\tau_2\in[0,1]}} |\hat{G}^{j_1,j_2}_{n,R}(\tau_1,\tau_2;\omega) - \hat{G}^{j_1,j_2}_{n,U}(\tau_1,\tau_2;\omega)| = o_p\big((nb_n)^{-1/2} + b_n^k\big);$$

if moreover the kernel W is uniformly Lipschitz-continuous, this bound is uniform with respect to $\omega \in \mathbb{R}$.

The proof of Theorem S6.1 is lengthy, technical and in many places similar to the proof of Theorem 3.6 in Kley et al. (2016). We provide the proof in Sections S6.3.1–S6.3.3, with technical details deferred to Section S6.4. For the reader's convenience we first give a brief description of the necessary steps.

Part (ii) of Theorem S6.1 can be proved along the lines of classical results from Brillinger (1975), but uniformly with respect to the arguments τ_1 and τ_2. Parts (i) and (iii) require additional arguments that are different from the classical theory. These additional arguments are due to the fact that the estimator is a stochastic process and stochastic equicontinuity of

$$\big(\hat{H}^{j_1,j_2}_n(a;\omega)\big)_{a\in[0,1]^2} := \sqrt{nb_n}\big(\hat{G}^{j_1,j_2}_{n,U}(\omega;\tau_1,\tau_2) - \mathbb{E}\hat{G}^{j_1,j_2}_{n,U}(\omega;\tau_1,\tau_2)\big)_{\tau_1,\tau_2\in[0,1]} \tag{S.23}$$

for all $j_1, j_2 = 1, \ldots, d$ has to be proven to ensure that the convergence holds not only pointwise, but also uniformly. The key to the proof of (i) and (iii) is a uniform bound on the increments $\hat{H}^{j_1,j_2}_n(a;\omega) - \hat{H}^{j_1,j_2}_n(b;\omega)$ of the process $\hat{H}^{j_1,j_2}_n$. This bound is needed to show the stochastic equicontinuity of the process. To employ a restricted chaining technique (cf. Lemma S6.3), we require two different bounds. First, we prove a general bound, uniform in a and b, on the moments of the increments $\hat{H}^{j_1,j_2}_n(a;\omega) - \hat{H}^{j_1,j_2}_n(b;\omega)$ (cf. Lemma S6.4). Second, we prove a sharper bound on the increments $\hat{H}^{j_1,j_2}_n(a;\omega) - \hat{H}^{j_1,j_2}_n(b;\omega)$ when a and b are 'sufficiently close' (cf. Lemma S6.10).

Condition (S.28), which we will require for Lemma S6.4 to hold, is rather general. In Lemma S6.6 we prove that condition (S.13), which is implied by Assumption 4.1, implies (S.28).

S6.3.1. Proof of Theorem S6.1(i). It is sufficient to prove the following two claims:

(i1) convergence of the finite-dimensional distributions of the process (S.23), that is,

$$\Big(\hat{H}^{j_{1\ell},j_{2\ell}}_n\big((a_{1\ell},a_{2\ell});\omega_j\big)\Big)_{j=1,\ldots,k} \xrightarrow{d} \Big(\mathbb{H}^{j_{1\ell},j_{2\ell}}\big((a_{1\ell},a_{2\ell});\omega_j\big)\Big)_{j=1,\ldots,k} \tag{S.24}$$

for any $(j_{1\ell}, j_{2\ell}, a_{1\ell}, a_{2\ell}, \omega_\ell) \in \{1,\ldots,d\} \times [0,1]^2 \times \mathbb{R}$, $\ell = 1,\ldots,k$ and $k \in \mathbb{N}$;

(i2) stochastic equicontinuity: for any $x > 0$, any $\omega \in \mathbb{R}$, and any $j_1, j_2 = 1, \ldots, d$,

$$\lim_{\delta\downarrow 0}\limsup_{n\to\infty} \mathbb{P}\Big(\sup_{\substack{a,b\in[0,1]^2\\ \|a-b\|_1\le\delta}} |\hat{H}^{j_1,j_2}_n(a;\omega) - \hat{H}^{j_1,j_2}_n(b;\omega)| > x\Big) = 0. \tag{S.25}$$

By (S.25) we have stochastic equicontinuity of all real parts $\Re\hat{H}^{j_1,j_2}_n(\cdot;\omega)$ and imaginary parts $\Im\hat{H}^{j_1,j_2}_n(\cdot;\omega)$. Therefore, in view of Theorems 1.5.4 and 1.5.7 in van der Vaart and Wellner (1996), we will have proved part (i).

First we prove (i1). For fixed τ_1, τ_2, $\hat{G}^{j_1,j_2}_{n,U}(\omega;\tau_1,\tau_2)$ is the traditional smoothed periodogram estimator of the cross-spectrum of the clipped processes $(I\{F_{j_1}(X_{t,j_1}) \le \tau_1\})_{t\in\mathbb{Z}}$ and $(I\{F_{j_2}(X_{t,j_2}) \le \tau_2\})_{t\in\mathbb{Z}}$ [see Chapter 7.1 in Brillinger (1975)]. Thus, (S.24) follows from Theorem 7.4.4 in Brillinger (1975), by which these estimators are asymptotically jointly Gaussian. The first and second moment structures of the limit are given by Theorem 7.4.1 and Corollary 7.4.3 in Brillinger (1975). The joint convergence (S.24) follows. Note that condition (S.13), which is implied by Assumption 4.1, implies the summability condition [i. e., Assumption 2.6.2(ℓ) in Brillinger (1975), for every ℓ] required for the three theorems in Brillinger (1975) to be applied.

Now to the proof of (i2). The Orlicz norm $\|X\|_\Psi = \inf\{C > 0 : \mathbb{E}\Psi(|X|/C) \le 1\}$ with $\Psi(x) := x^6$ coincides with the L_6 norm $\|X\|_6 = (\mathbb{E}|X|^6)^{1/6}$. Therefore, for any $\kappa > 0$ and sufficiently small $\|a-b\|_1$, we have by Lemma S6.4 and Lemma S6.6 that

$$\|\hat{H}_n^{j_1,j_2}(a;\omega) - \hat{H}_n^{j_1,j_2}(b;\omega)\|_\Psi \leq K\Big(\frac{\|a-b\|_1^{\kappa}}{(nb_n)^2} + \frac{\|a-b\|_1^{2\kappa}}{nb_n} + \|a-b\|_1^{3\kappa}\Big)^{1/6}.$$

Consequently, for all a, b with $\|a-b\|_1$ sufficiently small and $\|a-b\|_1 \geq (nb_n)^{-1/\gamma}$ and all $\gamma \in (0, 1)$ such that $\gamma < \kappa$,

$$\|\hat{H}_n^{j_1,j_2}(a;\omega) - \hat{H}_n^{j_1,j_2}(b;\omega)\|_\Psi \leq \bar{K}\|a-b\|_1^{\gamma/2}.$$

Note that $\|a-b\|_1 \geq (nb_n)^{-1/\gamma}$ if and only if $d(a,b) := \|a-b\|_1^{\gamma/2} \geq (nb_n)^{-1/2} =: \bar{\eta}_n/2$. The packing number [van der Vaart and Wellner (1996), p. 98] $D(\varepsilon, d)$ of $([0, 1]^2, d)$ satisfies $D(\varepsilon, d) \approx \varepsilon^{-4/\gamma}$. By Lemma S6.3, we therefore have, for all $x, \delta > 0$ and $\eta \geq \bar{\eta}_n$,

$$\begin{aligned}
&\mathbb{P}\Big(\sup_{\|a-b\|_1 \leq \delta^{2/\gamma}} |\hat{H}_n^{j_1,j_2}(a;\omega) - \hat{H}_n^{j_1,j_2}(b;\omega)| > x\Big)\\
&= \mathbb{P}\Big(\sup_{d(a,b)\leq\delta} |\hat{H}_n^{j_1,j_2}(a;\omega) - \hat{H}_n^{j_1,j_2}(b;\omega)| > x\Big)\\
&\leq \Big[\frac{8\tilde{K}}{x}\Big(\int_{\bar{\eta}_n/2}^{\eta} \epsilon^{-2/(3\gamma)}\mathrm{d}\epsilon + (\delta + 2\bar{\eta}_n)\eta^{-4/(3\gamma)}\Big)\Big]^6\\
&\quad + \mathbb{P}\Big(\sup_{d(a,b)\leq\bar{\eta}_n} |\hat{H}_n^{j_1,j_2}(a;\omega) - \hat{H}_n^{j_1,j_2}(b;\omega)| > x/4\Big).
\end{aligned}$$

Now, choosing $2/3 < \gamma < 1$ and letting n tend to infinity, the second term tends to zero by Lemma S6.10, because, by construction, $1/\gamma > 1$ and $d(a, b) \leq \bar{\eta}_n$ if and only if $\|a-b\|_1 \leq 2^{2/\gamma}(nb_n)^{-1/\gamma}$. All together, this yields

$$\lim_{\delta\downarrow 0}\limsup_{n\to\infty}\mathbb{P}\Big(\sup_{d(a,b)\leq\delta} |\hat{H}_n(a;\omega) - \hat{H}_n(b;\omega)| > x\Big) \leq \Big[\frac{8\tilde{K}}{x}\int_0^{\eta} \epsilon^{-2/(3\gamma)}\mathrm{d}\epsilon\Big]^6,$$

for every $x, \eta > 0$. The claim then follows, as the integral on the right-hand side may be arbitrarily small by choosing η accordingly.□

S6.3.2. Proof of Theorem S6.1(ii). Following the arguments that were applied in Section 8.1 of Kley et al. (2016), we can derive asymptotic expansions for $\mathbb{E}[I_{n,U}^{j_1,j_2}(\omega;\tau_1,\tau_2)]$ and $\mathbb{E}[\hat{G}_{n,U}^{j_1,j_2}(\omega;\tau_1,\tau_2)]$. In fact, it is easy to see that the proofs can still be applied when the Laplace cumulants

$$\mathrm{cum}\big(I\{X_{k_1} \leq x_1\}, I\{X_{k_2} \leq x_2\}, \ldots, I\{X_0 \leq x_p\}\big)$$

that were considered in Kley et al. (2016) are replaced by their multivariate counterparts

$$\mathrm{cum}\big(I\{X_{k_1,j_1} \leq x_1\}, I\{X_{k_2,j_2} \leq x_2\}, \ldots, I\{X_{0,j_p} \leq x_p\}\big).$$

More precisely, we now state Lemmas S6.1 and S6.2 (without proof) that are multivariate counterparts to Lemmas 8.4 and 8.5 in Kley et al. (2016), for which we assume

ASSUMPTION S6.1 Let $p \geq 2$, $\delta > 0$. There exists a non-increasing function $a_p : \mathbb{N} \to \mathbb{R}^+$ such that $\sum_{k\in\mathbb{N}} k^\delta a_p(k) < \infty$ and

$$\sup_{x_1,\ldots,x_p} |\mathrm{cum}\big(I\{X_{k_1,j_1} \leq x_1\}, I\{X_{k_2,j_2} \leq x_2\}, \ldots, I\{X_{0,j_p} \leq x_p\}\big)| \leq a_p\big(\max_j |k_j|\big),$$

for all $j_1, \ldots, j_p = 1, \ldots, d$.

Note that Assumption S6.1 follows from condition (S.13), which is in turn implied by Assumption 4.1, but that it is in fact somewhat weaker. We now state the first of the two lemmas. It is a generalization of Theorem 5.2.2 in Brillinger (1975).

LEMMA S6.1 *Under Assumption S6.1 with $K = 2$, $\delta > 3$,*

$$\mathbb{E}I_{n,U}^{j_1,j_2}(\omega;\tau_1,\tau_2) = \begin{cases} \mathfrak{f}^{j_1,j_2}(\omega;\tau_1,\tau_2) + \frac{1}{2\pi n}\left[\frac{\sin(n\omega/2)}{\sin(\omega/2)}\right]^2 \tau_1\tau_2 + \varepsilon_n^{\tau_1,\tau_2}(\omega) & \omega \neq 0 \mod 2\pi \\ \mathfrak{f}^{j_1,j_2}(\omega;\tau_1,\tau_2) + \frac{n}{2\pi}\tau_1\tau_2 + \varepsilon_n^{\tau_1,\tau_2}(\omega) & \omega = 0 \mod 2\pi \end{cases} \tag{S.26}$$

with $\sup_{\tau_1,\tau_2\in[0,1],\omega\in\mathbb{R}} |\varepsilon_n^{\tau_1,\tau_2}(\omega)| = O(1/n)$.

The second of the two lemmas is a generalization of Theorem 5.6.1 in Brillinger (1975).

LEMMA S6.2 *Assume that Assumption S6.1, with $p = 2$ and $\delta > k + 1$, and Assumption 4.2 hold. Then, with the notation of Theorem S4.1,*

$$\sup_{\tau_1,\tau_2\in[0,1],\omega\in\mathbb{R}} \left|\mathbb{E}\hat{G}_n^{j_1,j_2}(\omega;\tau_1,\tau_2) - \mathfrak{f}^{j_1,j_2}(\omega;\tau_1,\tau_2) - \left\{\boldsymbol{B}_n^{(k)}(\omega;\tau_1,\tau_2)\right\}_{j_1,j_2}\right|$$
$$= O((nb_n)^{-1}) + o(b_n^k).$$

Because condition (S.13), which is implied by Assumption 4.1, implies Assumption S6.1, Lemma S6.2 implies Theorem S6.1(ii).□

S6.3.3. Proof of Theorem S6.1(iii). Using (S.20) and argument similar to those in the proof of Lemma S6.10, it follows that

$$\sup_{\omega\in\mathbb{R}}\sup_{\tau_1,\tau_2\in[0,1]} |\hat{G}_{n,R}^{j_1,j_2}(\omega;\tau_1,\tau_2) - \hat{G}_{n,U}^{j_1,j_2}(\omega;\hat{F}_{n,j_1}^{-1}(\tau_1),\hat{F}_{n,j_2}^{-1}(\tau_2))| = o_p(1).$$

It therefore suffices to bound the differences

$$\sup_{\tau_1,\tau_2\in[0,1]} |\hat{G}_{n,U}^{j_1,j_2}(\omega;\tau_1,\tau_2) - \hat{G}_{n,U}^{j_1,j_2}(\omega;\hat{F}_{n,j_1}^{-1}(\tau_1),\hat{F}_{n,j_2}^{-1}(\tau_2))|$$

for $j_1, j_2 = 1, \ldots, d$, pointwise and uniformly in ω.

We first prove the statement for fixed $\omega \in \mathbb{R}$ in full detail and will later sketch the additional arguments needed for the proof of the uniform result. For any $x > 0$ and sequence δ_n we have,

$$\begin{aligned}
&P^n(\omega) := \\
&\mathbb{P}\Big(\sup_{\tau_1,\tau_2\in[0,1]} |\hat{G}_{n,U}^{j_1,j_2}(\omega;\hat{F}_{n,j_1}^{-1}(\tau_1),\hat{F}_{n,j_2}^{-1}(\tau_2)) - \hat{G}_{n,U}^{j_1,j_2}(\omega;\tau_1,\tau_2)| > x((nb_n)^{-1/2} + b_n^k)\Big) \\
&\leq \mathbb{P}\Big(\sup_{\tau_1,\tau_2\in[0,1]} \sup_{\substack{\|(u,v)-(\tau_1,\tau_2)\|_\infty \\ \leq \sup_{i=1,2;\tau\in[0,1]}|\hat{F}_{n,j_i}^{-1}(\tau)-\tau|}} |\hat{G}_{n,U}^{j_1,j_2}(\omega;u,v) - \hat{G}_{n,U}^{j_1,j_2}(\omega;\tau_1,\tau_2)| > x((nb_n)^{-1/2} + b_n^k)\Big) \\
&\qquad \leq \mathbb{P}\Big(\sup_{\tau_1,\tau_2\in[0,1]} \sup_{\substack{|u-\tau_1|\leq\delta_n \\ |v-\tau_2|\leq\delta_n}} |\hat{G}_{n,U}^{j_1,j_2}(\omega;u,v) - \hat{G}_{n,U}^{j_1,j_2}(\omega;\tau_1,\tau_2)| > x((nb_n)^{-1/2} + b_n^k), \\
&\qquad\qquad \sup_{i=1,2;\tau\in[0,1]} |\hat{F}_{n,j_i}^{-1}(\tau) - \tau| \leq \delta_n\Big) + \sum_{i=1}^{2} \mathbb{P}\Big(\sup_{\tau\in[0,1]} |\hat{F}_{n,j_i}^{-1}(\tau) - \tau| > \delta_n\Big) \\
&\qquad = P_1^n + P_2^n, \quad \text{say.}
\end{aligned}$$

We choose δ_n such that $n^{-1/2} \ll \delta_n = o(n^{-1/2}b_n^{-1/2}(\log n)^{-D})$, where D denotes the constant from Lemma S6.5. It then follows from Lemma S6.8 that P_2^n is $o(1)$. For P_1^n, on the other hand, we have the following bound:

$$\mathbb{P}\Big(\sup_{\tau_1,\tau_2\in[0,1]}\sup_{\substack{|u-\tau_1|\le\delta_n\\|v-\tau_2|\le\delta_n}}|\hat{H}^{j_1,j_2}_{n,U}(\omega;u,v)-\hat{H}^{j_1,j_2}_{n,U}(\omega;\tau_1,\tau_2)|>(1+(nb_n)^{1/2}b_n^k)x/2\Big)$$

$$+I\Big\{\sup_{\tau_1,\tau_2\in[0,1]}\sup_{\substack{|u-\tau_1|\le\delta_n\\|v-\tau_2|\le\delta_n}}|\mathbb{E}\hat{G}^{j_1,j_2}_{n,U}(\omega;u,v)-\mathbb{E}\hat{G}^{j_1,j_2}_{n,U}(\omega;\tau_1,\tau_2)|>((nb_n)^{-1/2}+b_n^k)x/2\Big\}.$$

The first term tends to zero because of (S.25). The indicator vanishes for n large enough, because we have

$$\sup_{\tau_1,\tau_2\in[0,1]}\sup_{\substack{|u-\tau_1|\le\delta_n\\|v-\tau_2|\le\delta_n}}|\mathbb{E}\hat{G}^{j_1,j_2}_{n,U}(\omega;u,v)-\mathbb{E}\hat{G}^{j_1,j_2}_{n,U}(\omega;\tau_1,\tau_2)|$$

$$\le\sup_{\tau_1,\tau_2\in[0,1]}\sup_{\substack{|u-\tau_1|\le\delta_n\\|v-\tau_2|\le\delta_n}}|\mathbb{E}\hat{G}^{j_1,j_2}_{n,U}(\omega;u,v)-\mathfrak{f}^{j_1,j_2}(\omega;u,v)-\big\{B_n^{(k)}(\omega;u,v)\big\}_{j_1,j_2}|$$

$$+\sup_{\tau_1,\tau_2\in[0,1]}\sup_{\substack{|u-\tau_1|\le\delta_n\\|v-\tau_2|\le\delta_n}}|\big\{B_n^{(k)}(\omega;\tau_1,\tau_2)\big\}_{j_1,j_2}+\mathfrak{f}^{j_1,j_2}(\omega;\tau_1,\tau_2)-\mathbb{E}\hat{G}^{j_1,j_2}_{n,U}(\omega;\tau_1,\tau_2)|$$

$$+\sup_{\tau_1,\tau_2\in[0,1]}\sup_{\substack{|u-\tau_1|\le\delta_n\\|v-\tau_2|\le\delta_n}}|\mathfrak{f}^{j_1,j_2}(\omega;u,v)+\big\{B_n^{(k)}(\omega;u,v)\big\}_{j_1,j_2}$$

$$-\mathfrak{f}^{j_1,j_2}(\omega;\tau_1,\tau_2)-\big\{B_n^{(k)}(\omega;\tau_1,\tau_2)\big\}_{j_1,j_2}|$$

$$=o(n^{-1/2}b_n^{-1/2}+b_n^k)+O(\delta_n(1+|\log\delta_n|)^D),$$

where D is still the constant from Lemma S6.5. We have applied part (ii) of Theorem S6.1 to bound the first two terms, and Lemma S6.5 for the third one. Thus, for any fixed ω, we have shown $P^n(\omega)=o(1)$, which is the pointwise version of the claim.

Next, we outline the proof of the uniform (with respect to ω) convergence. For any $y_n>0$, by similar arguments to above, using the same δ_n, we have

$$\mathbb{P}\Big(\sup_{\omega\in\mathbb{R}}\sup_{\tau_1,\tau_2\in[0,1]}|\hat{G}^{j_1,j_2}_{n,R}(\omega;\tau_1,\tau_2)-\hat{G}^{j_1,j_2}_{n,U}(\omega;\tau_1,\tau_2)|>y_n\Big)$$

$$\le\mathbb{P}\Big(\sup_{\omega\in\mathbb{R}}\sup_{\tau_1,\tau_2\in[0,1]}\sup_{\substack{|u-\tau_1|\le\delta_n\\|v-\tau_2|\le\delta_n}}|\hat{H}^{j_1,j_2}_{n,U}(\omega;u,v)-\hat{H}^{j_1,j_2}_{n,U}(\omega;\tau_1,\tau_2)|>(nb_n)^{1/2}y_n/2\Big)$$

$$+I\Big\{\sup_{\omega\in\mathbb{R}}\sup_{\tau_1,\tau_2\in[0,1]}\sup_{\substack{|u-\tau_1|\le\delta_n\\|v-\tau_2|\le\delta_n}}|\mathbb{E}\hat{G}^{j_1,j_2}_{n,U}(\omega;u,v)-\mathbb{E}\hat{G}^{j_1,j_2}_{n,U}(\omega;\tau_1,\tau_2)|>y_n/2\Big\}+o(1).$$

The indicator in the latter expression is $o(1)$ by the same arguments as above [note that Lemma S6.5 and the statement of part (ii) both hold uniformly with respect to $\omega\in\mathbb{R}$]. For the bound of the probability, note that by Lemma S6.9,

$$\sup_{\tau_1,\tau_2}\sup_{k=1,\ldots,n}|I^{j_1,j_2}_{n,U}(2\pi k/n;\tau_1,\tau_2)|=O_p(n^{2/K}),\ \text{for any } K>0.$$

Moreover, by the uniform Lipschitz continuity of W, the function W_n is also uniformly Lipschitz-continuous with constant of order $O(b_n^{-2})$. Combining those facts with Lemma S6.5 and the assumptions on b_n, we obtain

$$\sup_{\substack{\omega_1,\omega_2\in\mathbb{R}\\|\omega_1-\omega_2|\le n^{-3}}}\sup_{\tau_1,\tau_2\in[0,1]}|\hat{H}^{j_1,j_2}_{n,U}(\omega_1;\tau_1,\tau_2)-\hat{H}^{j_1,j_2}_{n,U}(\omega_2;\tau_1,\tau_2)|=o_p(1).$$

By the periodicity of $\hat{H}^{j_1,j_2}_{n,U}$ (with respect to ω), it suffices to show that

$$\max_{\omega=0,2\pi n^{-3},\dots,2\pi}\ \sup_{\tau_1,\tau_2\in[0,1]}\ \sup_{\substack{|u-\tau_1|\le\delta_n\\|v-\tau_2|\le\delta_n}} |\hat{H}^{j_1,j_2}_{n,U}(\omega;u,v)-\hat{H}^{j_1,j_2}_{n,U}(\omega;\tau_1,\tau_2)| = o_p(1).$$

By Lemmas S6.3 and S6.10 there exists a random variable $S(\omega)$ such that

$$\sup_{\tau_1,\tau_2\in[0,1]}\ \sup_{\substack{|u-\tau_1|\le\delta_n\\|v-\tau_2|\le\delta_n}} |\hat{H}^{j_1,j_2}_{n,U}(\omega;u,v)-\hat{H}^{j_1,j_2}_{n,U}(\omega;\tau_1,\tau_2)| \le |S(\omega)| + R_n(\omega),$$

for any fixed $\omega\in\mathbb{R}$, with $\sup_{\omega\in\mathbb{R}}|R_n(\omega)| = o_p(1)$ and

$$\max_{\omega=0,2\pi n^{-3}\dots,2\pi} \mathbb{E}[|S^{2L}(\omega)|] \le K_L^{2L}\bigg(\int_0^\eta \epsilon^{-4/(2L\gamma)}\mathrm{d}\epsilon + (\delta_n^{\gamma/2}+2(nb_n)^{-1/2})\eta^{-8/(2L\gamma)}\bigg)^{2L}$$

for any $0<\gamma<1$, $L\in\mathbb{N}$, $0<\eta<\delta_n$, and a constant K_L depending on L only. For appropriately chosen L and γ, this latter bound is $o(n^{-3})$. Note that the maximum is with respect to a set of cardinality $O(n^3)$, which completes the proof of part (iii). □

S6.4. Auxiliary lemmas

In this section we state multivariate versions of the auxiliary lemmas from Section 7.4 in Kley et al. (2016). Note that Lemma S6.3 is unaltered and therefore stated without proof. The remaining lemmas are adapted to the multivariate quantities and proofs or directions on how to adapt the proofs in Kley et al. (2016) are collected at the end of this section.

For the statement of Lemma S6.3, we define the Orlicz norm [see e.g. van der Vaart and Wellner (1996), Chapter 2.2] of a real-valued random variable Z as

$$\|Z\|_\Psi = \inf\Big\{C>0 : \mathbb{E}\Psi\Big(|Z|/C\Big)\le 1\Big\},$$

where $\Psi:\mathbb{R}^+\to\mathbb{R}^+$ may be any non-decreasing, convex function with $\Psi(0)=0$.

For the statement of Lemmas S6.4, S6.6, and S6.9 we define, for any Borel set A,

$$d_n^j(\omega;A) := \sum_{t=0}^{n-1} I\{X_{t,j}\in A\}\mathrm{e}^{-\mathrm{i}t\omega}. \tag{S.27}$$

LEMMA S6.3. *Let $\{\mathbb{G}_t : t\in T\}$ be a separable stochastic process with $\|\mathbb{G}_s-\mathbb{G}_t\|_\Psi \le Cd(s,t)$ for all s, t with $d(s,t)\ge\bar\eta/2\ge 0$. Denote by $D(\epsilon, d)$ the packing number of the metric space (T, d). Then, for any $\delta>0$, $\eta\ge\bar\eta$, there exists a random variable S_1 and a constant $K<\infty$ such that*

$$\sup_{d(s,t)\le\delta}|\mathbb{G}_s-\mathbb{G}_t| \le S_1 + 2\sup_{d(s,t)\le\bar\eta,t\in\tilde T}|\mathbb{G}_s-\mathbb{G}_t| \quad \textit{and}$$

$$\|S_1\|_\Psi \le K\Big[\int_{\bar\eta/2}^{\eta}\Psi^{-1}\big(D(\epsilon,d)\big)d\epsilon + (\delta+2\bar\eta)\Psi^{-1}\big(D^2(\eta,d)\big)\Big],$$

where the set $\tilde T$ contains at most $D(\bar\eta,d)$ points. In particular, by Markov's inequality [cf. van der Vaart and Wellner (1996), p. 96],

$$\mathbb{P}\Big(|S_1|>x\Big) \le \bigg(\Psi\Big(x\big[8K\big(\int_{\bar\eta/2}^{\eta}\Psi^{-1}\big(D(\epsilon,d)\big)d\epsilon + (\delta+2\bar\eta)\Psi^{-1}\big(D^2(\eta,d)\big)\big)\big]^{-1}\Big)\bigg)^{-1}.$$

for any $x>0$.

LEMMA S6.4. *Let $\boldsymbol{X}_0,\dots,\boldsymbol{X}_{n-1}$, where $\boldsymbol{X}_t=(X_{t,1},\dots,X_{t,d})$, be the finite realization of a strictly stationary process with $X_{0,j}\sim U[0,1]$, $j=1,\dots,d$. Let Assumption 4.2 hold. For $x=(x_1,x_2)$*

let $\hat{H}_n^{j_1,j_2}(x;\omega) := \sqrt{nb_n}(\hat{G}_n^{j_1,j_2}(x_1,x_2;\omega) - \mathbb{E}[\hat{G}_n^{j_1,j_2}(x_1,x_2;\omega)])$. *Let* $d_n^j(\omega; A)$ *be defined as in (S.27). Assume that, for* $p = 1, \dots, P$, *there exist a constant C and a function* $g : \mathbb{R}^+ \to \mathbb{R}^+$, *both independent of* $\omega_1, \dots, \omega_p \in \mathbb{R}$, *n and* $A_1, \dots, A_p$, *such that*

$$\left|\mathrm{cum}(d_n^{j_1}(\omega_1;A_1),\dots,d_n^{j_p}(\omega_p;A_p))\right| \le C\Big(\Big|\Delta_n\Big(\sum_{i=1}^{p}\omega_i\Big)\Big|+1\Big)g(\varepsilon) \tag{S.28}$$

for any indices $j_1, \dots, j_p \in \{1, \dots, d\}$ *and intervals* $A_1, \dots, A_p$ *with* $\min_k \mathbb{P}(X_{0,j_k} \in A_k) \le \varepsilon$. *Then, there exists a constant K (depending on C, L, g only) such that*

$$\sup_{\omega\in\mathbb{R}}\sup_{\|a-b\|_1\le\varepsilon}\mathbb{E}|\hat{H}_n^{j_1,j_2}(a;\omega)-\hat{H}_n^{j_1,j_2}(b;\omega)|^{2L} \le K\sum_{\ell=0}^{L-1}\frac{g^{L-\ell}(\varepsilon)}{(nb_n)^{\ell}}$$

for all ε *with* $g(\varepsilon) < 1$ *and all* $L = 1, \dots, P$.

LEMMA S6.5. *Under the assumptions of Theorem S4.1, the derivative*

$$(\tau_1,\tau_2)\mapsto\frac{\mathrm{d}^k}{\mathrm{d}\omega^k}\mathfrak{f}^{j_1,j_2}(\omega;\tau_1,\tau_2)$$

exists and satisfies, for any $k \in \mathbb{N}_0$ *and some constants C, d that are independent of* $a = (a_1, a_2)$, $b = (b_1, b_2)$, *but may depend on k,*

$$\sup_{\omega\in\mathbb{R}}\left|\frac{\mathrm{d}^k}{\mathrm{d}\omega^k}\mathfrak{f}^{j_1,j_2}(\omega;a_1,a_2)-\frac{\mathrm{d}^k}{\mathrm{d}\omega^k}\mathfrak{f}^{j_1,j_2}(\omega;b_1,b_2)\right| \le C\|a-b\|_1(1+|\log\|a-b\|_1|)^D.$$

LEMMA S6.6. *Let the strictly stationary process* $(\boldsymbol{X}_t)_{t\in\mathbb{Z}}$ *satisfy condition (S.13). Let* $d_n^j(\omega; A)$ *be defined as in (S.27). Let* $A_1, \dots, A_p \subset [0, 1]$ *be intervals, and let*

$$\varepsilon := \min_{k=1,\dots,p}\mathbb{P}(X_{0,j_k}\in A_k).$$

Then, for any p-tuple $\omega_1, \dots, \omega_p \in \mathbb{R}$ *and* $j_1, \dots, j_p \in \{1, \dots, d\}$,

$$\left|\mathrm{cum}(d_n^{j_1}(\omega_1;A_1),\dots,d_n^{j_p}(\omega_p;A_p))\right| \le C\Big(\Big|\Delta_n\Big(\sum_{i=1}^{p}\omega_i\Big)\Big|+1\Big)\varepsilon(|\log\varepsilon|+1)^D,$$

where $\Delta_n(\lambda) := \sum_{t=0}^{n-1} e^{\mathrm{i}t\lambda}$ *and the constants C, D depend only on K, p, and* ρ *[with* ρ *from condition (S.13)].*

LEMMA S6.7. *Let the strictly stationary process* $(\boldsymbol{X}_t)_{t\in\mathbb{Z}}$ *satisfy condition (S.13) and* $X_{0,j} \sim U[0, 1]$. *Denote the empirical distribution function of* $X_{0,j}, \dots, X_{n-1,j}$ *by* $\hat{F}_{n,j}$. *Then, for any* $k \in \mathbb{N}$, *there exists a constant* d_k *depending only on k, such that*

$$\sup_{x,y\in[0,1],|x-y|\le\delta_n}\sqrt{n}|\hat{F}_{n,j}(x)-\hat{F}_{n,j}(y)-(x-y)| = O_p\Big((n^2\delta_n+n)^{1/2k}(\delta_n|\log\delta_n|^{d_k}+n^{-1})^{1/2}\Big),$$

as $\delta_n \to 0$.

LEMMA S6.8. *Let* $\boldsymbol{X}_0, \dots, \boldsymbol{X}_{n-1}$, *where* $\boldsymbol{X}_t = (X_{t,1}, \dots, X_{t,d})$, *be the finite realization of a strictly stationary process satisfying condition (S.13) and* $X_{0,j} \sim U[0, 1]$, $j = 1, \dots, d$. *Then,*

$$\sup_{j=1,\dots,d}\sup_{\tau\in[0,1]}|\hat{F}_{n,j}^{-1}(\tau)-\tau| = O_p(n^{-1/2}).$$

LEMMA S6.9. *Let the strictly stationary process* $(\boldsymbol{X}_t)_{t\in\mathbb{Z}}$ *satisfy condition (S.13) and* $X_{0,j} \sim U[0, 1]$. *Let* $d_n^j(\omega; A)$ *be defined as in (S.27). Then, for any* $k \in \mathbb{N}$,

$$\sup_{j=1,\dots,d}\sup_{\omega\in\mathcal{F}_n}\sup_{y\in[0,1]}|d_n^j(\omega;[0,y])| = O_p(n^{1/2+1/k}).$$

LEMMA S6.10. *Under the assumptions of Theorem S6.1, let δ_n be a sequence of non-negative real numbers. Assume that there exists $\gamma \in (0, 1)$, such that $\delta_n = O((nb_n)^{-1/\gamma})$. Then,*

$$\sup_{j_1,j_2,\in\{1,\dots,d\}} \sup_{\omega\in\mathbb{R}} \sup_{\substack{u,v\in[0,1]^2\\ \|u-v\|_1\le\delta_n}} |\hat{H}_n^{j_1,j_2}(u;\omega) - \hat{H}_n^{j_1,j_2}(v;\omega)| = o_p(1).$$

Proof of Lemma S6.3. The lemma is stated unaltered as in Kley et al. (2016). The proof can be found in Section 8.3.1 of the Online Appendix of Kley et al. (2016).

Proof of Lemma S6.4. Along the same lines as the proof of the univariate version [Section 8.3.2 in Kley et al. (2016)] we can prove

$$\mathbb{E}|\hat{H}_n^{j_1,j_2}(a;\omega) - \hat{H}_n^{j_1,j_2}(b;\omega)|^{2L} = \sum_{\substack{\{\nu_1,\dots,\nu_R\}\\ |\nu_j|\ge 2,\ j=1,\dots,R}} \prod_{r=1}^{R} \mathcal{D}_{a,b}(\nu_r) \tag{S.29}$$

with the summation running over all partitions $\{\nu_1, \dots, \nu_R\}$ of $\{1, \dots, 2L\}$ such that each set ν_j contains at least two elements, and

$$\mathcal{D}_{a,b}(\xi) := \sum_{\ell_{\xi_1},\dots,\ell_{\xi_q}\in\{1,2\}} n^{-3q/2} b_n^{q/2} \Big(\prod_{m\in\xi} \sigma_{\ell_m}\Big)$$

$$\times \sum_{s_{\xi_1},\dots,s_{\xi_q}=1}^{n-1} \Big(\prod_{m\in\xi} W_n(\omega - 2\pi s_m/n)\Big) \operatorname{cum}(D_{\ell_m,(-1)^{m-1}s_m} : m \in \xi),$$

for any set $\xi := \{\xi_1, \dots, \xi_q\} \subset \{1, \dots, 2L\}$, $q := |\xi|$, and

$$D_{\ell,s} := d_n^{j_1}(2\pi s/n; M_1(\ell)) d_n^{j_2}(-2\pi s/n; M_2(\ell)), \quad \ell = 1, 2, \quad s = 1, \dots, n-1,$$

with the sets $M_1(1)$, $M_2(2)$, $M_2(1)$, $M_1(2)$ and the signs $\sigma_\ell \in \{-1, 1\}$ defined as

$$\begin{aligned} \sigma_1 &:= 2I\{a_1 > b_1\} - 1, & \sigma_2 &:= 2I\{a_2 > b_2\} - 1,\\ M_1(1) &:= (a_1 \wedge b_1, a_1 \vee b_1], & M_2(2) &:= (a_2 \wedge b_2, a_2 \vee b_2],\\ M_2(1) &:= \begin{cases} [0, a_2] & b_2 \ge a_2 b_2 > b_2 \\ & a_2 > b_2, \end{cases} & M_1(2) &:= \begin{cases} [0, b_1] & b_2 \ge a_2 a_1 > a_1 \\ & a_2 > b_2. \end{cases} \end{aligned} \tag{S.30}$$

Employing assumption (S.28), we can further prove, by following the arguments of the univariate version, that

$$\sup_{\substack{\xi\subset\{1,\dots,2L\}\\ |\xi|=q}} \sup_{\|a-b\|_1\le\varepsilon} |\mathcal{D}_{a,b}(\xi)| \le C(nb_n)^{1-q/2} g(\varepsilon), \quad 2 \le q \le 2L.$$

The lemma then follows, by observing that

$$\Big|\prod_{r=1}^{R} \mathcal{D}_{a,b}(\nu_r)\Big| \le C g^R(\varepsilon)(nb_n)^{R-L}$$

for any partition in (S.29) [note that $\sum_{r=1}^{R} |\nu_r| = 2L$].□

Proof of Lemma S6.5. Note that

$$\begin{aligned} &\operatorname{cum}(I\{X_{0,j_1} \le q_{j_1}(a_1)\}, I\{X_{k,j_2} \le q_{j_2}(a_2)\})\\ &\quad - \operatorname{cum}(I\{X_{0,j_1} \le q_{j_1}(b_1)\}, I\{X_{k,j_2} \le q_{j_2}(b_2)\})\\ &= \sigma_1 \operatorname{cum}(I\{F_{j_1}(X_{0,j_1}) \in M_1(1)\}, I\{F_{j_2}(X_{k,j_2}) \in M_2(1)\})\\ &\qquad + \sigma_2 \operatorname{cum}(I\{F_{j_1}(X_{0,j_1}) \in M_1(2)\}, I\{F_{j_2}(X_{k,j_2}) \in M_2(2)\}), \end{aligned}$$

with the sets $M_1(1)$, $M_2(2)$, $M_2(1)$, $M_1(2)$ and the signs $\sigma_\ell \in \{-1, 1\}$ defined in (S.30).

From the fact that $\lambda(M_j(j)) \leq \|a-b\|_1$ for $j = 1, 2$, we conclude that

$$\Big|\frac{\mathrm{d}^\ell}{\mathrm{d}\omega^\ell}\mathfrak{f}^{j_1,j_2}(\omega; a_1, a_2) - \frac{\mathrm{d}^\ell}{\mathrm{d}\omega^\ell}\mathfrak{f}^{j_1,j_2}(\omega; b_1, b_2)\Big|$$

$$\leq \sum_{k\in\mathbb{Z}} |k|^\ell |\operatorname{cum}(I\{F_{j_1}(X_{0,j_1}) \in M_1(1)\}, I\{F_{j_2}(X_{k,j_2}) \in M_2(1)\})|$$

$$+ \sum_{k\in\mathbb{Z}} |k|^\ell |\operatorname{cum}(I\{F_{j_1}(X_{0,j_1}) \in M_1(2)\}, I\{F_{j_2}(X_{k,j_2}) \in M_2(2)\})|$$

$$\leq 4\sum_{k=0}^{\infty} k^\ell \Big((K\rho^\ell) \wedge \|a-b\|_1\Big).$$

The assertion then follows after some algebraic manipulations.□

Proof of Lemma S6.6. Similar to (8.27) in Kley et al. (2016) we have, by the definition of cumulants and strict stationarity,

$$\operatorname{cum}\,(d_n^{j_1}(\omega_1; A_1), \ldots, d_n^{j_p}(\omega_p; A_p))$$

$$= \sum_{u_2,\ldots,u_p=-n}^{n} \operatorname{cum}(I\{X_{0,j_1} \in A_1\}, I\{X_{u_2,j_2} \in A_2\} \ldots, I\{X_{u_p,j_p} \in A_p\}) \exp\Big(-\mathrm{i}\sum_{j=2}^{p}\omega_j u_j\Big)$$

$$\times \sum_{t_1=0}^{n-1} \exp\Big(-\mathrm{i}t_1\sum_{j=1}^{p}\omega_j\Big) I_{\{0\leq t_1+u_2<n\}} \cdots I_{\{0\leq t_1+u_p<n\}}. \tag{S.31}$$

By Lemma 8.1 in Kley et al. (2016),

$$\Big|\Delta_n(\sum_{j=1}^{p}\omega_j) - \sum_{t_1=0}^{n-1}\exp\Big(-\mathrm{i}t_1\sum_{j=1}^{p}\omega_j\Big) I\{0\leq t_1+u_2<n\}\cdots I\{0\leq t_1+u_p<n\}\Big|$$

$$\leq 2\sum_{j=2}^{p}|u_j|. \tag{S.32}$$

Following the arguments for the proof of (8.29) in Kley et al. (2016), we further have, for any $p+1$ intervals $A_0, \ldots, A_p \subset \mathbb{R}$, any indices $j_0, \ldots, j_p \in \{1, \ldots, d\}$, and any p-tuple $\kappa := (\kappa_1, ..., \kappa_p) \in \mathbb{R}_+^p$, $p \geq 2$, that

$$\sum_{k_1,\ldots,k_p=-\infty}^{\infty}\Big(1+\sum_{\ell=1}^{p}|k_\ell|^{\kappa_\ell}\Big)\Big|\operatorname{cum}\Big(I\{X_{k_1,j_1}\in A_1\}, \ldots, I\{X_{k_p,j_p}\in A_p\}, I\{X_{0,j_0}\in A_0\}\Big)\Big|$$

$$\leq C\varepsilon(|\log\varepsilon|+1)^d. \tag{S.33}$$

To this end, define $k_0 = 0$, consider the set

$$T_m := \Big\{(k_1, ..., k_p) \in \mathbb{Z}^p \,|\, \max_{i,j=0,\ldots,p}|k_i - k_j| = m\Big\},$$

and note that $|T_m| \leq c_p m^{p-1}$ for some constant c_p. From the definition of cumulants and some simple algebra we get the bound

$$|\operatorname{cum}(I\{X_{t_1,j_1}\in A_1\}, ..., I\{X_{t_p,j_p}\in A_p\})| \leq C\min_{i=1,\ldots,p} P(X_{0,j_i}\in A_i).$$

With this bound and condition (S.13), which is implied by Assumption 4.1, we obtain, employing the above notation, that

$$\sum_{k_1,\dots,k_p=-\infty}^{\infty}\Big(1+\sum_{j=1}^{p}|k_\ell|^{\kappa_\ell}\Big)\big|\operatorname{cum}\big(I\{X_{k_1,j_1}\in A_1\},\dots,I\{X_{k_p,j_p}\in A_p\},I_{\{X_{0,j_0}\in A_0\}}\big)\big|$$
$$=\sum_{m=0}^{\infty}\sum_{(k_1,\dots,k_p)\in T_m}\Big(1+\sum_{\ell=1}^{p}|k_\ell|^{\kappa_\ell}\Big)\big|\operatorname{cum}\big(I\{X_{k_1,j_1}\in A_1\},\dots,I\{X_{k_p,j_p}\in A_p\},I\{X_{0,j_0}\in A_0\}\big)\big|$$
$$\le\sum_{m=0}^{\infty}\sum_{(k_1,\dots,k_p)\in T_m}\Big(1+pm^{\max_j\kappa_j}\Big)\Big(\rho^m\wedge\varepsilon\Big)K_p\le C_p\sum_{m=0}^{\infty}\Big(\rho^m\wedge\varepsilon\Big)|T_m|m^{\max_j\kappa_j}.$$

For $\varepsilon\ge\rho$, (S.33) then follows trivially. For $\varepsilon<\rho$, set $m_\varepsilon:=\log\varepsilon/\log\rho$ and note that $\rho^m\le\varepsilon$ if and only if $m\ge m_\varepsilon$. Thus,

$$\sum_{m=0}^{\infty}\Big(\rho^m\wedge\varepsilon\Big)m^u\le\sum_{m\le m_\varepsilon}m^u\varepsilon+\sum_{m>m_\varepsilon}m^u\rho^m\le C\Big(\varepsilon m_\varepsilon^{u+1}+\rho^{m_\varepsilon}\sum_{m=0}^{\infty}(m+m_\varepsilon)^u\rho^m\Big).$$

The fact that $\rho^{m_\varepsilon}=\varepsilon$ completes the proof of the desired inequality (S.33). The assertion follows from (S.31), (S.32), (S.33), and the triangle inequality. □

Proofs of Lemmas S6.7, S6.8, and S6.9. Note that the component processes $(X_{t,j})$ are stationary and fulfil Assumption (C) in Kley et al. (2016), for every $j=1,\dots,d$. The assertion then follows from the univariate versions [i.e., Lemma 8.6, 7.5, and 7.6 in Kley et al. (2016), respectively], as the dimension d does not depend on n.□

Proof of Lemma S6.10. Assume, without loss of generality, that $n^{-1}=o(\delta_n)$ [otherwise, enlarge the supremum by considering $\tilde\delta_n:=\max(n^{-1},\delta_n)$]. With the notation $a=(a_1,a_2)$ and $b=(b_1,b_2)$, we have

$$\hat H_n^{j_1,j_2}(a;\omega)-\hat H_n^{j_1,j_2}(b;\omega)=b_n^{1/2}n^{-1/2}\sum_{s=1}^{n-1}W_n(\omega-2\pi s/n)(K_{s,n}(u,v)-\mathbb{E}K_{s,n}(u,v))$$

where, with $d_{n,U}^{j}$ defined in (S.22),

$$K_{s,n}(a,b):=n^{-1}\big(d_{n,U}^{j_1}(2\pi s/n;u_1)d_{n,U}^{j_2}(-2\pi s/n;u_2)-d_{n,U}^{j_1}(2\pi s/n;v_1)d_{n,U}^{j_2}(-2\pi s/n;v_2)\big)$$
$$=d_{n,U}^{j_1}(2\pi s/n;u_1)n^{-1}\big[d_{n,U}^{j_2}(-2\pi s/n;u_2)-d_{n,U}^{j_2}(-2\pi s/n;v_2)\big]$$
$$+d_{n,U}^{j_2}(-2\pi s/n;v_2)n^{-1}\big[d_{n,U}^{j_1}(2\pi s/n;u_1)-d_{n,U}^{j_1}(2\pi s/n;v_1)\big].$$

By Lemma S6.9, we have, for any $k\in\mathbb{N}$,

$$\sup_{y\in[0,1]}\sup_{\omega\in\mathcal{F}_n}|d_{n,U}^{j}(\omega;y)|=O_p\Big(n^{1/2+1/k}\Big).\tag{S.34}$$

Employing Lemma S6.7, we have, for any $\ell \in \mathbb{N}$ and $j = 1, \ldots, d$,

$$\begin{aligned}
&\sup_{\omega\in\mathbb{R}} \sup_{y\in[0,1]} \sup_{x:|x-y|\le\delta_n} n^{-1}|d^j_{n,U}(\omega; x) - d^j_{n,U}(\omega; y)| \\
&\le \sup_{y\in[0,1]} \sup_{x:|x-y|\le\delta_n} n^{-1} \sum_{t=0}^{n-1} |I\{F_j(X_{t,j}) \le x\} - I\{F_j(X_{t,j}) \le y\}| \\
&\le \sup_{y\in[0,1]} \sup_{x:|x-y|\le\delta_n} |\hat{F}_{n,j}(x \vee y) - \hat{F}_{n,j}(x \wedge y) - x \vee y + x \wedge y| + C\delta_n \\
&= O_p\big(\rho_n(\delta_n, \ell) + \delta_n\big),
\end{aligned}$$

with $\rho_n(\delta_n, \ell) := n^{-1/2}(n^2\delta_n + n)^{1/2\ell}(\delta_n|\log\delta_n|^{D_\ell} + n^{-1})^{1/2}$, $\hat{F}_{n,j}$ denoting the empirical distribution function of $F_j(X_{0,j}), \ldots, F_j(X_{n-1,j})$, and d_ℓ being a constant depending only on ℓ. Combining these arguments and observing that

$$\sup_{\omega\in\mathbb{R}} \sum_{s=1}^{n-1} \Big|W_n(\omega - 2\pi s/n)\Big| = O(n) \tag{S.35}$$

yields

$$\sup_{\omega\in\mathbb{R}} \sup_{\substack{u,v\in[0,1]^2 \\ \|u-v\|_1\le\delta_n}} \Big|\sum_{s=1}^{n-1} W_n(\omega - 2\pi s/n)K_{s,n}(u, v)\Big| = O_p\big(n^{3/2+1/k}(\rho(\delta_n, \ell) + \delta_n)\big). \tag{S.36}$$

With $M_i(j)$, $i, j = 1, 2$, as defined in (S.30), we have

$$\begin{aligned}
&\sup_{\|a-b\|_1\le\delta_n} \sup_{s=1,\ldots,n-1} |\mathbb{E}K_{s,n}(a, b)| \\
&\le n^{-1} \sup_{\|a-b\|_1\le\delta_n} \sup_{s=1,\ldots,n-1} \Big|\operatorname{cum}(d^{j_1}_{n,U}(2\pi s/n; M_1(1)), d^{j_2}_{n,U}(-2\pi s/n; M_2(1)))\Big| \\
&+ n^{-1} \sup_{\|a-b\|_1\le\delta_n} \sup_{s=1,\ldots,n-1} \Big|\operatorname{cum}(d^{j_1}_{n,U}(2\pi s/n; M_1(2)), d^{j_2}_{n,U}(-2\pi s/n; M_2(2)))\Big|
\end{aligned} \tag{S.37}$$

where we have used $\mathbb{E}d^j_{n,U}(2\pi s/n; M) = 0$. Lemma S6.6 and $\lambda(M_j(j)) \le \delta_n$, for $j = 1, 2$ (with λ denoting the Lebesgue measure over $\mathbb{R}$) yield

$$\sup_{\|a-b\|_1\le\delta_n} \sup_{s=1,\ldots,n-1} |\operatorname{cum}(d^{j_1}_n(2\pi s/n; M_1(j)), d^{j_2}_n(-2\pi s/n; M_2(j)))| \le C(n+1)\delta_n(1 + |\log\delta_n|)^D.$$

It follows that the right-hand side in (S.37) is $O(\delta_n|\log\delta_n|^D)$. Therefore, by (S.35), we obtain

$$\sup_{\omega\in\mathbb{R}} \sup_{\|a-b\|_1\le\delta_n} \Big|b_n^{1/2}n^{-1/2}\sum_{s=1}^{n-1} W_n(\omega - 2\pi s/n)\mathbb{E}K_{s,n}(a, b)\Big| = O\big((nb_n)^{1/2}\delta_n|\log n|^D\big).$$

In view of the assumption that $n^{-1} = o(\delta_n)$, we have $\delta_n = O(n^{1/2}\rho_n(\delta_n, \ell))$, which, in combination with (S.36), yields

$$\begin{aligned}
&\sup_{\omega\in\mathbb{R}} \sup_{\|a-b\|_1\le\delta_n} |\hat{H}^{j_1,j_2}_n(a; \omega) - \hat{H}^{j_1,j_2}_n(b; \omega)| \\
&= O_p\Big((nb_n)^{1/2}[n^{1/2+1/k}(\rho_n(\delta_n, \ell) + \delta_n) + \delta_n|\log\delta_n|^D]\Big) \\
&= O_p\Big((nb_n)^{1/2}n^{1/2+1/k}\rho_n(\delta_n, \ell)\Big) \\
&= O_p\Big((nb_n)^{1/2}n^{1/k+1/\ell}(n^{-1} \vee \delta_n(\log n)^{D_\ell})^{1/2}\Big) = o_p(1).
\end{aligned}$$

The $o_p(1)$ holds, as we have, for arbitrary k and ℓ,

$$O((nb_n)^{1/2}n^{1/k+1/\ell}\delta_n^{1/2}(\log n)^{D_\ell/2}) = O((nb_n)^{1/2-1/2\gamma}n^{1/k+1/\ell}(\log n)^{D_\ell/2}).$$

The assumptions on b_n imply $(nb_n)^{1/2 - 1/2\gamma} = o(n^{-\kappa})$ for some $\kappa > 0$, such that this latter quantity is $o(1)$ for k, ℓ sufficiently large. The term $(nb_n)^{1/2} n^{1/k + 1/\ell} n^{-1/2}$ is handled in a similar fashion. This concludes the proof. □

REFERENCES -Appendix

Bougero,l P. and N. Picard (1992). Strict stationarity of generalized autoregressive processes. *The Annals of Probability 20*, 1714–30.

Brillinger, D. R. (1975). *Time Series: Data Analysis and Theory*. New York, NY: Holt, Rinehart and Winston, Inc.

Brockwell, P. J. and R. A. Davis (1987). *Time Series: Theory and Methods*. Springer Series in Statistics. New York, NY: Springer.

Hafner, C. M. and O. B. Linton (2006). Comment. *Journal of the American Statistical Association 101*, 998–1001.

Kley, T., S. Volgushev, H. Dette and M. Hallin (2016). Quantile spectral processes: Asymptotic analysis and inference. *Bernoulli 22*, 1770–807.

Knight, K. (2006). Comment on "Quantile autoregression". *Journal of the American Statistical Association 101*, 994–6.

Koenker, R. and Z. Xiao (2006). Quantile autoregression. *Journal of the American Statistical Association 101*, 980–90.

Taniguchi, M. and Y. Kakizawa (2000). *Asymptotic Theory of Statistical Inference for Time Series*. New York, NY: Springer.

van der Vaart, A. and J. Wellner (1996). *Weak Convergence and Empirical Processes: With Applications to Statistics*. New York, NY: Springer.